In silico mining of a system wide transcriptional profiling database for clinically relevant gene modulation by FDA approved or FDA ready agents; validation of a novel translational approach

Luke Witherspoon

Thesis submitted on Monday, June 06, 2011 to the Faculty of Medicine in partial fulfillment of the requirements for the M.Sc. in Cellular and Molecular Medicine

Cellular and Molecular Medicine

Faculty of Medicine

University of Ottawa

Abstract

It has been recognized that small molecules can affect a substantial proportion of the human transcriptome in ways that are currently unknown and difficult to predict. Working with the Broad Institute, using their Connectivity Map database, we have worked to identify compounds anticipated to modulate two diseases; myotonic dystrophy (DM1) and Duchenne muscular dystrophy (DMD). DM1 stems from an expanded CTG repeat found in the *DMPK* gene. The down regulation of DMPK mRNA represents a valid therapeutic avenue. DMD is characterized by degeneration of muscle, caused by mutations in the dystrophin gene. One therapeutic strategy for DMD is to increase the dystrophin homologue utrophin. We have identified a number of compounds capable of decreasing DMPK mRNA and others which increase utrophin mRNA and protein. We hope our success in compound identification not only leads to potential therapeutics for these diseases, but highlights the usefulness of using *in silico* screens.

Table of Contents

Chapter 1

Chapter 2

Chapter 3

Chapter 4

List of Figures and Tables

List of Abbreviations

AA – Amino acid

ADME – Absorption, distribution, metabolism, excretion

AONS – Anti–sense oligonucleotides

ARE – AU rich elements

BMD – Becker Muscular Dystrophy

cDNA – Complementary DNA

ClC–1 – Chloride channel 1

cTNT – Cardiac troponin

CUBGP1 – CUG binding protein 1

DM1 – Myotonic Dystrophy Type 1

DMD – Duchenne Muscular Dystrophy

DMPK – Dystrophia Myotonica Protein Kinase

DMSO – Dimethyl sulfide

DNA – Deoxyribonucleic acid

DPC – Dystrophin–associated protein complex

ER – Endoplasmic reticulum

ERK – Extracellular signal–related kinase

FCS – Fetal calf serum

GABP – GA–binding protein

Gastroc – Gastrocnemius

I.P. – Intraperitoneal injection

IC_{50}– Half maximal inhibitory concentration

IR – Insulin receptor

MBNL1 – Muscle blind–like protein 1

MIT – Massachusetts Institute of Technology

mRNA – Messenger RNA

NFAT – Nuclear factor of activated T cells

NMJ – Neuromuscular junction

nNOS – Nitric oxide synthase

PBS – Phosphate buffered saline

PKC – Protein Kinase C

PMSF – Phenylmethylsulfonyl fluoride

PPAR – Peroxisome proliferator receptor

PPRE – PPAR responsive element

qPCR – Quantitative polymerase chain reaction

RNA – Ribonucleic acid

SEM – Standard error of the mean

SMA – Spinal muscular atrophy

SMN1 – Survival of motor neuron 1, telomeric

SMN2 – Survival of motor neuron 2, centromeric

SP1 – Specific protein 1

STATs – Signal transducers and activators of transcription

TTX – Tetrodotoxin

ZNF9 – Zinc finger nine

Acknowledgements

I would like to thank my supervisor Dr. Alex MacKenzie for his support and humour throughout my studies. I would also like to thank Faraz Farooq for the time he took from his own work to teach me so many of the techniques used in this project. My honours student Sean O'Reilly deserves special mention for his dedication, initiative, and enthusiasm. His ability to both identify and address problems in an efficient and timely manner was invaluable. My fellow masters student Jeremiah Hadwen served as a valuable resource by developing techniques and protocols to optimize aspects of our Duchenne Muscular Dystrophy research. A special thanks is extended to Kristen Timusk for helping me navigate the CMM master's program and keeping me on track with requirements and deadlines.

I would like to thank the administrative staff at the Apoptosis Research Centre, particularly Lynn Kelly, whose dedication to research at ARC is unrivaled and whose contribution to this project represents many hours of hard work. I would also like to recognize my committee members Dr. Bernard Jasmin and Dr. Bob Korneluk for input and expertise throughout the course of this project.

There are many who helped this project progress outside of the laboratory. Caroline, I would like to thank you for all of the support you have given me along the way, and especially for spending many hours reviewing this thesis. Last but not least I would like to thank my parents, as without them this project, and I, would not have been possible.

Contributors

Sean O'Reilly worked on the utrophin inducers screen and aided in all mice trials for this project.

Jeremiah Hadwin aided in optimization of our utrophin western protocol and in verification of utrophin protein induction by identified compounds.

Chapter 1

1. Introduction

1.1 Pharmacologic transcript modulation; a translational opportunity for rare genetic diseases?

Although disorders caused by single gene defects are individually rare, in aggregate their frequency approximates or even surpasses more common disorders; collectively they impose a formidable clinical, psychological and fiscal burden on society. Of the 22,000 protein coding human genes approximately 10% (~2,500) have been linked to human disease (McKusick-Nathans Institute of Genetic Medicine, Johns Hopkins University (Baltimore, MD) and National Center for Biotechnology Information, National Library of Medicine (Bethesda, MD), 2011) with an additional 3,500 for which the molecular basis is not known. Moreover, there are believed to be as many disorders which are currently unreported as are now known. These disorders pose an enormous clinical challenge not only from a diagnostic point of view, but ultimately therapeutically as well.

In this regard, it has been recognized in recent years that small molecules can affect a substantial proportion of the human transcriptome in ways that are currently unknown and impossible to predict. With the enormous costs and time required to develop new compounds and investigate their efficacy and safety, the prospect of finding new uses for approved drugs is appealing. Finding new uses for FDA approved compounds benefits developers, by decreasing the investments required for drug

discovery. More importantly, patients benefit by increased speed of delivery and pre-existing knowledge of safe dosage and treatment regimens. Monogenic disorders, where mutations in a single gene result in the disease phenotype, stand to benefit significantly from this type of drug discovery.

Dramatic advances in our understanding of the molecular pathophysiology of monogenic disorders have resulted in the identification of hundreds of transcripts and proteins that either cause or impact these conditions. Given the number of genes involved in human disease and the substantial subset of the transcriptome modulated by drugs, it is a virtual certainty that genes exist that both act as modifiers of human disease and are responsive to pharmacologic modulation. The modulation of these transcripts and proteins may serve a therapeutic purpose. In the case of monogenic disorders, this might occur through the up regulation of genes that encode sequentially and functionally similar proteins that can effectively replace the recessive disease gene, or by down regulation of the mutated autosomal dominant genes that confer the pathology. In this thesis we outline piloting of this approach for two monogenic disorders, Myotonic dystrophy type 1 (DM1) and Duchenne muscular dystrophy (DMD).

1.2 Myotonic Dystrophy

1.2.1 DM1 incidence and disease background

Myotonic dystrophy is an example of a monogenic disorder that may benefit from pharmacological transcript modulation. It is an autosomal dominant disease and one of

the most common forms of muscular dystrophy with an estimated incidence of 1 in 8000 (Vignaud et al., 2010). Myotonic dystrophy is one of more than 20 conditions characterized as repeat expansion diseases (Brouwer et al., 2009). These diseases are caused by repetitive series of usually trinucleotide repeats in the genome of affected individuals which when expanded can be deleterious to the patient. There are two types of Myotonic dystrophy; DM1 caused by a trinucleotide CTG repeat in the 3' untranslated region of the dystrophia myotonica protein kinase (*DMPK*) gene mapping to chromosome 19 in humans (Lee and Cooper, 2009). The second form of myotonic dystrophy, DM2, is characterized by tetranucleotide (CCTG) repeats localized in intron 1 of the zinc finger nine (ZNF9) gene (Liquori et al., 2001). Although previously thought the least common of the two forms of myotonic dystrophy it now appears that DM2 is comparatively common, possibly more common than DM1, albeit less severe (Amack et al., 2002; Suominen et al., 2011).

The pathological CTG expansion in the 3' untranslated region (exon 15) was identified in 1992. Subsequent analyses demonstrated the correlation between disease severity and the number of trinucleotide repeats (Brook et al., 1992; Harper, 2001; Hunter et al., 1992). This disease manifests with somatic instability during weeks 13-16 of gestation (possibly leading to CTG repeat expansion) while symptoms progress into adulthood (Jansen et al., 1994). While unaffected individuals typically have between 5-38 repeats (Lee and Cooper, 2009), repeat numbers have been reported as high as 4000, resulting in the congenital form of the disease and repeats in the range of 50 are associated with the adult-onset form of DM1 (Lee and Cooper, 2009). The length of the

CTG repeat tract usually expands between generations; thus one generation can have few or no symptoms, and the next generation can develop the disease (Harley et al., 1992). The multisystemic expression of the *DMPK* gene combined with the wide range of DMPK CTG trinucleotide repeat number observed in DM1 leads to a large number of physical signs and symptoms as well as a varying severity. These include myotonia (i.e. failure of muscle relaxation following contraction), muscle wasting, insulin resistance, cardiac conduction defects (mainly arrhythmias), cataracts, testicular atrophy, cognitive dysfunction and mental retardation (Lee and Cooper, 2009; Harper, 2001). Those symptoms relating to the musculature appear to affect distal muscles more severely than proximal muscles (Kaliman and Llagostera, 2008).

1.2.2 DM1 pathogenesis: *DMPK* haploinsufficiency or pathogenic RNA?

The diverse range of symptoms and physical signs associated with DM1 initially made a clear mechanistic pathogenic formulation difficult; how did *DMPK* CTG repeat expansion affect so many systems so variably? Due to studies that identified decreases in the amount of DMPK mRNA and protein in patients with DM1, it was initially thought that the loss of DMPK protein might be a key pathogenic mechanism (Fu et al., 1993). The subsequent generation of a *DMPK*-knockout mouse which showed only mild cardiac conduction defects, no myotonia, and normal longevity appeared to disprove this hypothesis (Berul et al., 1999). This led to the generation of a second hypothesis, suggesting the expanded CTG repeats had a pathogenic role in the disease and caused the multitude of symptoms observed in patients. Significant evidence was lent to this theory when a mouse model was developed containing 250 CTG repeats in the 3' UTR of the α-

actin gene (Mankodi et al., 2000). Unlike the *DMPK*-knockout mouse, these mice developed myotonia and histological analysis of muscle samples revealed centrally located nuclei and ring fibers, longstanding criteria used to diagnose DM1 (Mankodi et al., 2000). Interestingly, the RNA gain-of-function mechanism of disease does not appear to hold up across different species, as repeat length is not a primary determinant of pathology in drosophila (Le Mee et al., 2008). Six years after the discovery of DM1, the identification of a second repeat expansion underlying the clinically milder but similar DM2 lent strong support to the pathogenic RNA hypothesis (Ranum et al., 1998).

1.2.3 DMPK protein structure, function, and localization

The original hypothesis that DM1 was caused by a decrease in DMPK levels was impeded by the lack of knowledge of the function of DMPK protein itself. Although its exact function(s) has/have yet to be elucidated, the fact that *DMPK*-knockout mice have a mild phenotype (Berul et al., 1999) indicates that *DMPK* is not vital to the function of living organisms. Although DMPK mRNA has been detected in a range of tissues (skeletal muscle, heart, smooth muscle, bone, testis, pituitary, brain, eye, skin, thymus, lung, intestinal epithelium, cartilage, and liver), significant levels of DMPK protein are found only in skeletal muscle and heart, with comparatively lower expression in smooth muscle (Lam et al., 2000). Its structure can be broken down into three distinct regions; a catalytic domain, followed by a coiled-coil domain, and a hydrophobic C-terminal domain (Lam et al., 2000). This protein is homologous to the p21-activated kinases MRCK and ROCK/rho-kinase/ROK with a similar serine/threonine structure (Kaliman

and Llagostera, 2008). Although as many as six different isoforms **(Fig. 1)** have been described and grouped across a range of sizes (67-74kDa) (Groenen et al., 2000; Wansink et al., 2003; Oude Ophuis et al., 2009), other studies suggest that there is only one form of DMPK protein with a size of approximately 80kDa (Lam et al., 2000). Further studies have shown that the isoforms differ in the presence or absence of a 5-amino-acid VSGGG motif and the structure of the C-terminus (Wansink et al., 2003); the latter differences appear to play a role in DMPK subcellular localization, and may also modulate substrate specificity (Kaliman and Llagostera, 2008; Wansink et al., 2003). Those isoforms with a hydrophobic C terminus (A, B) localize at the endoplasmic reticulum (ER) while presence of the hydrophilic C terminus (C,D), results in localization to the mitochondrial outer membrane and isoforms with a very short C-terminal tail (E, F) are cytosolic (Kaliman and Llagostera, 2008; Wansink et al., 2003). DMPK isoforms containing a tail (99-100AA long) are expressed in skeletal/cardiac tissue, those without are localized to smooth muscle, although the precise function of the carboxy terminus domains in localization are unclear (van Herpen et al., 2005). The activity of the serine/threonine kinase domain has been analyzed through experiments whereby the predicted ATP binding site is mutated, resulting in a kinase deficient DMPK protein (Kaliman and Llagostera, 2008; Wansink et al., 2003; Jin et al., 2000). While the function of the protein was not elucidated in this study, a loss of the ability to induce apoptosis by overexpression of the mutated DMPK protein was observed (Jin et al., 2000). Using an antibody specific for phosphorylated DMPK, hyperphosphorylation of a C-terminal truncated form of the protein was observed, suggesting the DMPK C-terminus may have

an auto inhibitory role similar to that observed with the homologous Rho-kinases (Kaliman and Llagostera, 2008; Wansink et al., 2003; Jin et al., 2000).

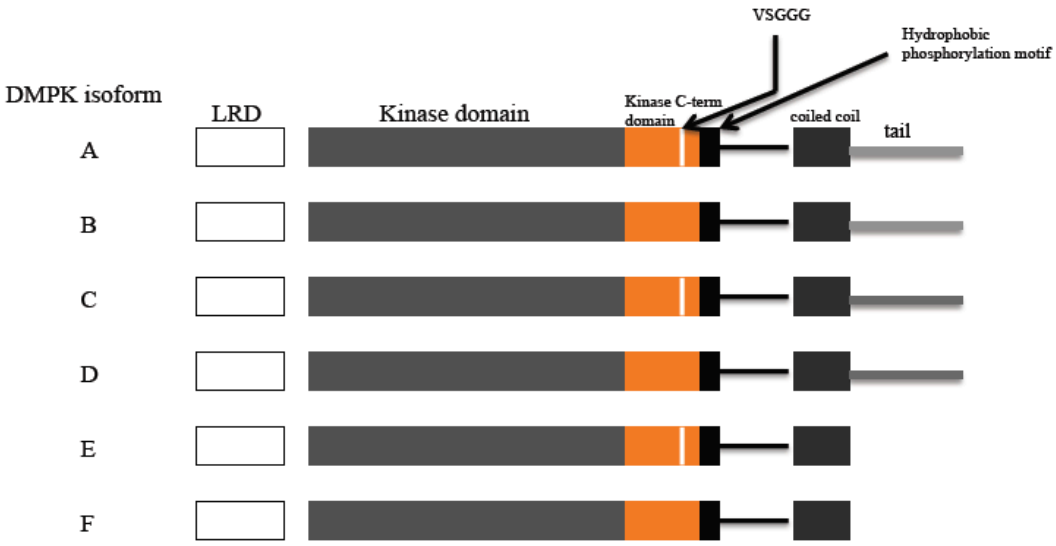

Figure 1 – Schematic presentation of DMPK isoforms

DMPK isoforms have a N-terminal leucine rich domain (LRD), a serine/threonine kinase domain, a protein kinase C-terminal domain which contains the hydrophobic phosphorylation motif, the presence/absence of a VSGGG sequence, and a coiled coil domain. Isoforms A, C, and E contain the VSGGG motif. Isoforms differ in the presence of two types of C-terminal tails (A, B), (C, D) or absence (E, F) of a tail (Groenen et al., 2000).

DMPK protein expression has been found to be up regulated through the canonical myogenic pathway (phosphatidyl inositol 3-kinase, nuclear factor-B, nitric oxide synthase, p38 mitogenic-activated protein kinase) in C2C12 muscle cells suggesting a role for DMPK in the maintenance and/or generation of muscle (Kaliman and Llagostera, 2008; Canicio et al., 2001; Carrasco et al., 2002). Overexpression of DMPK, however, appears to impede normal muscle maturation, inhibiting C2C12 myoblast differentiation into myotubes (Okoli et al., 1998). A lack of DMPK similarly impedes myotube differentiation, potentially through repressing myogenin and MyoD expression (Amack et al., 2002; Harmon et al., 2008). DMPK may also modulate ion channel activity, as DMPK -/- myotubes have higher resting Ca^{2+} than controls due to increased open voltage-dependent calcium and sodium channels (Benders et al., 1997). Conversely however, *DMPK*-knockout mice have decreased sodium channel activity, suggesting a potential role in sodium channel activation (Lee et al., 2003; Mounsey et al., 2000).

1.2.4 Pathogenic RNA modulates disease symptoms

While the exact functions of DMPK remain to be elucidated, the mechanisms by which the pathogenic DMPK trinucleotide repeat interferes with normal cell function, and results in many of the DM1 symptoms, have been better characterized. Although it has become clear that mutated DMPK mRNA is the chief DM1 pathogenic mediator, at the level of the genome the increased number of repeats in the *DMPK* gene also appear to alter expression of adjacent genes. For example, the *SIX5* gene which maps to a region of

condensed chromatin downstream of amplified CTG repeats demonstrates transcriptional repression in DM1 patients (Otten and Tapscott, 1995). Interestingly, *SIX5* null mice develop cataracts, one of the many reported DM1 physical signs (Thornton et al., 1997; Klesert et al., 2000). The expanded DMPK mRNA may itself also decrease the expression of other genes as it has been found to bind and sequester the transcription factors SP1 (specific protein 1) and the STATs (signal transducers and activators of transcription) 1 and 3 (Ebralidze et al., 2004).

1.2.4.1 MBNL1 Sequestration

The central pathogenic DM1 mechanism is increasingly being recognized as devolving from the distinct nuclear foci formed by the expanded DMPK mRNA (Davis et al., 1997). A number of RNA-binding proteins localize to these foci, suggesting that the expanded mRNA is interacting with these proteins potentially interfering with their normal function. It was discovered that RNA CUG expansions comprised of as few as 11 repeats form hairpin-like structures with C-G base pairs interrupted by u-u mismatches (Napierala and Krzyzosiak, 1997). Shortly thereafter, muscle blind-like protein 1 (MBNL1) was identified as a potential CUG hairpin binder (Miller et al., 2000). Upon further investigation, MBNL1 was found to preferentially localize to DMPK RNA foci decreasing its presence elsewhere in the nucleoplasm **(Fig. 2)** (Jiang et al., 2004; Lin et al., 2006). Furthermore, the binding of MBNL1 to the pathogenic RNA may result in its entrapment in the nucleus given that MBNL1 down regulation restores cytosolic levels of the pathogenic mRNA, where it is ultimately degraded (Smith et al., 2007). MBNL1

itself was implicated in DM1 pathogenesis with the observation that MBNL1 knockout mice developed myotonia and cataracts (Kanadia et al., 2003). The pathogenic DMPK mRNA complexing of MBNL1 results in a reduction of the alternative RNA splicing normally mediated by this protein. Over two dozen alternative mRNA splicing events that are either impeded or in some other fashion altered have been identified in DM1 (Ranum and Cooper, 2006). Experiments in both mice and cell lines have shown that loss of MBNL1 results in the improper splicing of, among other genes, cTNT (cardiac troponin), IR (Insulin receptor), and ClC-1 (Chloride channel 1) (Kanadia et al., 2006; Ho et al., 2004). Interestingly, the majority of these inappropriate splicing events result in persistence of fetal forms of the proteins (Lee and Cooper, 2009). This suggests that the disease may, to some degree, be the result of differentiated cells expressing predominantly fetal (and inappropriate) isoforms of a number of critical proteins.

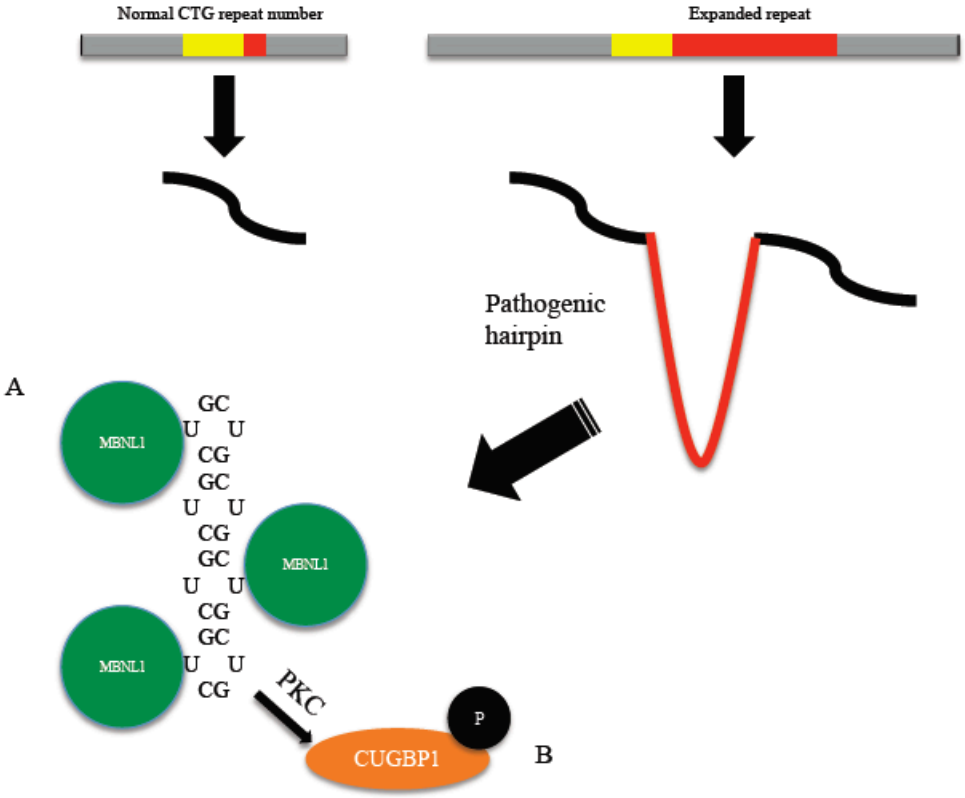

Figure 2 – Schematic presentation of pathogenic expanded RNA's interaction with MBNL1 and CUGBP1.

A) The expanded repeat forms a hairpin which binds MBNL1, sequestering it and depleting it from the nucleoplasm. B) Through an unknown mechanism the expanded repeat activates the PKC pathway leading to the phosphorylation and stabilization of CUGBP1. Both the sequestration of MBNL1 and stabilization of CUGBP1 lead to improper alternative splicing preventing proper isoform expression during development.

1.2.4.2 CUGBP1 activation and stabilization

In addition to MBNL1, CUBGP1 (CUG binding protein 1) is another RNA binding protein implicated in DM1 pathophysiology. Although its name implies that the protein binds to the hairpin structure formed by the pathogenic mRNA, and it was originally characterized as a protein capable of binding short single stranded CUG strands, it does not and in fact it shows no co-localization with DMPK mRNA foci (Fardaei et al., 2001; Mankodi et al., 2003; Timchenko et al., 1996). Nonetheless it appears to play a role in DM1 pathogenesis. Whereas MBN1's sequestration by DMPK mRNA prevents its inhibition of the inclusion of fetal exons during splicing events, CUGBP1 which in contrast to MBN1 is activated in DM1, does the opposite, promoting the inclusion of fetal exons in cTNT, IR and ClC - 1 (Philips et al., 1998; Savkur et al., 2001; Charlet-B et al., 2002). This apparent opposite and antagonistic function of the two proteins may serve as one means of mediating which isoforms of certain proteins are expressed during normal development. In keeping with this model, MBNL1 levels increase during development while CUGBP1 levels decrease (Lin et al., 2006; Kalsotra et al., 2008). An obvious question is how, in DM1, CUGBP1 is maintained at high levels which affect splicing well into adulthood when it normally decreases to levels with no or little impact on splicing events. The anomalous maintenance of CUGBP1 levels into adulthood observed in DM1 is mediated by an increase in PKC (Protein Kinase C) pathway activity, seemingly activated by the pathogenic mRNA through an unknown mechanism **(Fig.2)** (Lee and Cooper, 2009). Activation of the PKC pathway results in hyperphosphorylation of CUGBP1 which confers stability and allows it to persist well into adulthood (Kalsotra et al., 2008; Kuyumcu-Martinez et al., 2007). As was observed

with the MBNL1-knockout animals, CUGBP1 over expressing transgenic animals recapitulate aspects of DM1 at both the molecular and clinical level (Koshelev et al., 2010). This can be seen in cardiac tissue with dilated cardiomyopathy, conduction defects, and lethality observed in mice that overexpress CUGBP1 (Koshelev et al., 2010; Wang et al., 2007). This is particularly important as 80% of DM1 patients have some form of cardiac disease, which is the leading cause of death for the condition (Koshelev et al., 2010).

1.2.5 DM1 Treatment strategies

Although there are only a few DM1 clinical trials active at present, (U.S Institute of Health, 2011) the understanding of the role of CTG expansion in DM1 pathophysiology points to novel potential treatments for this largely untreatable illness.

1.2.5.1 Gene Therapy

One DM1 strategy includes the design of anti-sense oligonucleotides (AONS) which target the expanded mRNA either interfering in the interaction with RNA-binding protein or DNA sequences and/or accelerating DMPK mRNA degradation (Magana and Cisneros, 2011). In this regard, expression of an anti-sense RNA complementary to 13 CUG repeats resulted in a preferential decay of mutant DMPK over wild type DMPK and a reduction of the DM1 molecular pathology in DM1 myoblasts (Furling et al., 2003). Recently designed AONs have proven even more effective, reducing mutant DMPK levels by 90% in DM1 myoblasts and 80% in DM1 mouse models (Mulders et al., 2009).

A second AON that binds to expanded mRNA and blocks MBNL1 binding has been developed; this leads to the reversal of some of the dysregulated splicing events in DM1 mouse models (Wheeler et al., 2009). Similar to AONs, the pre-clinical application of siRNA, which can cleave RNA or inhibit translation, has been examined (Magana and Cisneros, 2011). Success has been marginal in this area with some concerns that siRNA is acting mainly in the cytoplasm with little nuclear translocation (Magana and Cisneros, 2011; Langlois et al., 2005). Although these approaches are promising, they are still in preliminary phases and it will be some time before it is known if they are applicable to patients. Clearly the appropriate validation including establishing ADME (absorption, distribution, metabolism, excretion), bioavailability and toxicology for each agent has to be undertaken.

1.2.5.2 MBNL1 up regulation

Alternative therapeutic strategies for DM1 have focused on correcting a number of putative downstream pathogenic mechanisms. Disrupting the interaction of the expanded mRNA with the alternative splicing factor MBNL1 is one area that has shown promise. Through a screen of compounds, the antimicrobial drug pentadamine was identified as capable of interfering with the interaction between MBNL1 and the pathogenic mRNA, leading to the reversal of aberrant splicing in DM1 cell lines (Warf et al., 2009). Unfortunately, the dose that prevented this interaction also caused lethality in mice (Warf et al., 2009). In addition to interfering with interactions between MBNL1 and pathogenic RNA, the effects of an overexpression of MBNL1 have been examined.

Overexpression of MBNL1 in a mouse model expressing expanded CTG repeats, reversed the misplicing and myotonia present in the mice (Kanadia et al., 2006).

1.2.5.3 CUGBP1 down regulation

There have been fewer attempts to modulate CUGBP1 levels in DM1 models due in part to a relative lack of knowledge of how the pathogenic mRNA activates the PKC pathway. There have, however, been some advances in decreasing CUGBP1 levels by modulating PKC activity. In a heart-specific mouse model overexpressing CUGBP1, inhibition of the PKC pathway using a known PKC inhibitor led to decreased CUGBP1 levels and correction of the RNA missplicing which are characteristic of this model (Wang et al., 2009).

1.2.5.4 Correction of alternative splicing

In addition to trying to correct the increase or decrease of RNA binding proteins in response to the pathogenic RNA, researchers have focused on the direct correction of the splicing defects caused by the abnormal levels of these proteins through AON technology similar to that previously discussed. AONs can be designed to bind to pre-mRNA and prevent splicing proteins from accessing specific splicing sites (Magana and Cisneros, 2011). One AON has been designed which blocks the inclusion of exon7a of the ClC-1 (a chloride channel affected in DM1) (Wheeler and Thornton, 2007). This exon, when included, causes malfunction of this channel in DM1 (Charlet-B et al., 2002;

Mankodi et al., 2002). This AON resulted in correction of ClC-1 function and reduction in myotonia in DM1 mice (Wheeler and Thornton, 2007).

1.2.5.5 Current treatments and future directions

Currently, the only option in improving outcomes for DM1 patients is to reduce pain and improve symptoms (e.g. sodium channel blockers to treat myotonia) (Logigian et al., 2010). Although a number of DM1 therapeutic approaches show promise and will likely ultimately be successful, none are currently ready for clinical use.

1.3 Duchenne Muscular Dystrophy (DMD)

1.3.1 DMD incidence and disease background

Another disorder that stands to benefit from pharmacological gene modulation is DMD. DMD is caused by mutations in the *dystrophin* gene (Blake et al., 2002). In the related Becker muscular dystrophy (BMD), dystrophin mutations lead to truncated forms of the protein and milder symptoms (Blake et al., 2002). DMD is an X-linked recessive disease, and one of the most common muscular disorders affecting 1 in 3500 males worldwide (Emery, 1993). Children with DMD are unaffected at birth but begin to present symptoms between the ages of 2-5 (Dubowitz, 1978; Jennekens et al., 1991). These children are often diagnosed when they fail to achieve normal motor milestones such as walking and climbing, and instead have a waddling gait (Jennekens et al., 1991).

In conjunction with these reductions in gross motor skills, the children develop pseudohypertrophy of the calf muscles and develop the Gowers' sign (use of hands when rising from kneeling or prone to standing position) due to proximal limb muscle weakness (Blake et al., 2002; Jennekens et al., 1991; Gowers, 1886). Muscle degeneration increases with age and most children are wheelchair-bound by the age of 12 (Emery, 1993). As the children progress through adolescence, the muscle weakness leads to progressive kyphoscoliosis and eventually a respiratory insufficiency with secondary pneumonia; survival beyond the third decade is rare (Blake et al., 2002). Cardiac dysfunction is common in the mid to later stages of DMD with cardiac myopathy and conduction defects being the most frequently reported symptoms (Emery, 1993).

1.3.2 Dystrophin protein structure, function and localization

Dystrophin appears to act as cellular scaffold, connecting the extracellular matrix to the intracellular actin network in the sarcolemma (Blake et al., 2002). The dystrophin protein is a cytoskeletal protein (427 kDa) which is a member of the β-spectrin/α-actinin protein family (Koenig et al., 1988). The protein is organized into four different regions with an actin binding domain at the N-terminal, a central rod domain (composed of 24 spectrin-like repeats), a cysteine rich domain, and a COOH-terminal domain **(Fig. 3)** (Blake et al., 2002). The rod domain accounts for the majority of the protein and is interrupted by four hinge regions (Koenig and Kunkel, 1990). While the N-terminal domain binds with actin, the portion of the protein near the COOH-terminal domain interacts with a group of proteins termed the dystrophin-associated protein complex

(DPC) **(Fig. 4)** (Blake et al., 2002). The α and β-dystroglycans are constituents of the complex that directly connect the extracellular network to dystrophin and the intracellular actin filaments (Blake et al., 2002). The extracellular matrix connects to the DPC through laminin or agrin which binds to α-dystroglycan on the extracellular side of the plasma membrane (Blake et al., 2002). α-Dystroglycan interacts with plasma membrane-spanning β-dystroglycan which in turn binds to the cysteine rich portion of dystrophin, forming the extracellular/intracellular connection (Blake et al., 2002). Another component of the DPC is the plasma membrane bound sarcoglycan complex composed of up to four sarcoglycan glycoproteins (α, β, γ, and δ) thought to play a role in intracellular signal transduction (Blake et al., 2002). The syntropin family of proteins (α, β-1, β-2, γ-1 and γ-2) are subunits of the DPC whose function is not fully elucidated, although they are thought to link membrane-associated proteins to the DPC (Blake et al., 2002). They have also been shown to bind to a number of molecules, for example nitric oxide synthase (nNOS) which catalyzes the production of nitric oxide from L-arginine and which has been found to be decreased at the sarcolemma in DMD patients (Chao et al., 1996). The last protein that makes up the DPC is the dystrobrevin family (α, β) of proteins. It appears that α-dystrobrevin isoforms bind and associate with the sarcoglycan complex (Yoshida et al., 2000). Similar to the other components of the DPC, the dystrobrevins role in the DPC at the sarcolemma are not fully elucidated, although a role in signal transduction has been proposed (Blake et al., 2002).

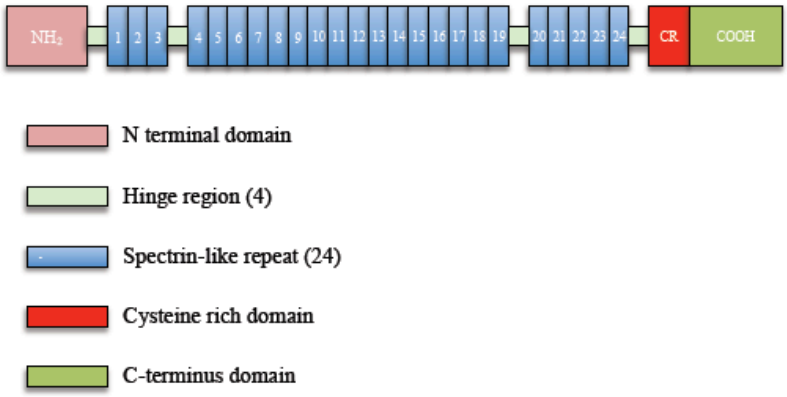

Figure 3 – Structural schematic of the full length dystrophin protein.

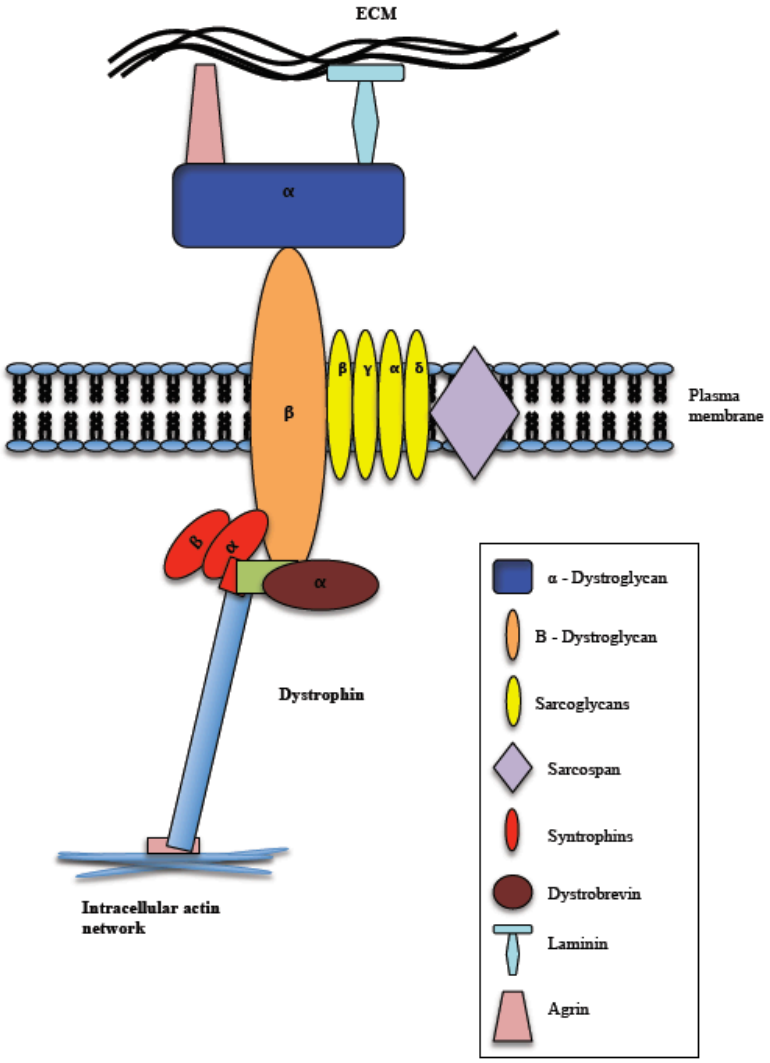

Figure 4 – Interaction of dystrophin with the dystrophin-glycoprotein complex at the sarcolemmal membrane.

Dystrophin and the DGC link the intracellular actin network to the extracellular matrix providing structural stability to the plasma membrane.

1.3.2 DMD diagnosis

DMD can be diagnosed through distinct histological features of the skeletal muscle even in ostensibly asymptomatic infants and young children. Skeletal muscle biopsies reveal widespread necrosis, degeneration (Blake et al., 2002) as well as hallmarks of inflammatory changes including macrophages and CD4+ lymphocytes present at perimysial and endomysial sites (Arahata and Engel, 1986; Arahata and Engel, 1984; McDouall et al., 1990). As patients grow and develop, their skeletal muscles continue a cycle of degeneration and regeneration (Schmalbruch, 1984). The regenerating muscle is a histochemical hallmark of the disease with its small fibres, a basophilic RNA-rich cytoplasm and the large centrally placed myonuclei in the fibres themselves (Blake et al., 2002; Schmalbruch, 1984; Bell and Conen, 1968; Bradley et al., 1972). The cycle of degeneration/regeneration continues until the body's ability to regenerate is exhausted, and the muscle is replaced by fibrous connective tissue and adipose tissue resulting in pseudohypertrophy (Blake et al., 2002). The loss of muscle tissue and increase in fibrosis is what eventually leads to the characteristic muscle weakness of the disease (Blake et al., 2002).

1.3.3 Dystrophin Gene

Dystrophin maps to Xp21 and is the largest human gene consisting of a 2.5Mb genomic sequence containing 79 exons encoding a 14-kb mRNA which is primarily expressed in muscle (skeletal and cardiac) and to a lesser degree in brain (Coffey et al.,

1992; Koenig et al., 1987; Monaco et al., 1986; Monaco et al., 1987; Monaco et al., 1992; Roberts et al., 1993; Boyd et al., 1986; Boyd and Buckle, 1986).

1.3.3.1 Dystrophin mutations

One common mutation does not underlie all DMD cases, although most mutations localize to two specific regions of the gene. The first area is between exons 45 and 53 and involves deletion of a portion of the rod domain, while the second mutational hotspot is between exons 2-20 encoding the actin binding sites and a portion of the rod domain (Koenig and Kunkel, 1990; Beggs et al., 1990; Koenig et al., 1989; Liechti-Gallati et al., 1989). Although these two areas most frequently contain DMD mutations, almost 1/3 of DMD cases are caused by small deletions or point mutations which often introduce premature stop codons leading to significantly reduced or even no protein (Roberts et al., 1994; Hoffman et al., 1987; Lenk et al., 1993).

1.3.4 DMD pathogenesis

The impact of mutated dystrophin on the sarcolemma is akin to the loss of an important cellular shock absorber, a component which normally provides structure and support to the sarcolemma when it undergoes stress. Thus when dystrophin is lost membrane instability ensues and ultimately a loss of membrane integrity occurs. This is evidenced by the abnormal positive staining for proteins such as albumin which are normally extracellular but found within diseased muscle (Blake et al., 2002; Clarke et al., 1993). The membrane permeability, which increases following mechanical stress (Blake

et al., 2002; Clarke et al., 1993) also leads to increased levels of calcium within muscle fibers (Tutdibi et al., 1999), an influx which leads to the activation and amplification of proteolysis. Protease activation can in turn exacerbate calcium dysregulation, leading to even more proteolysis; this cycle of degradation is a central mediator of the necrosis and fiber degradation characteristic of the disease (Blake et al., 2002).

1.3.5 DMD treatment options

There are currently no effective treatments for DMD. A number of non-genetic therapies has been investigated. Pharmacologic decrease of intracellular calcium concentration and protease inhibition have been two that have shown slight success (MacLennan et al., 1991; Turner et al., 1988).

1.3.5.1 Gene therapy

Perhaps the most promising therapeutic approaches for DMD involves either replacement of *dystrophin* or providing a functional replacement. Unfortunately, adenoviruses, like most gene therapy vectors have limitations in the size of gene payload, and with *dystrophin* being the largest human gene this method is not ideal (Odom et al., 2007). In some cases of BMD, however, a truncated form of dystrophin is expressed which on the basis of the milder symptoms obviously retains some residual function. Adenoviral vectors encoding variations of these truncated dystrophins have been constructed (Odom et al., 2007). An adenovirus containing a dystrophin cDNA with exons 17 to 48 deleted showed 50% uptake into muscle fiber; unfortunately severe

immune responses were also observed limiting prospects for this particular dystrophin variant (Ragot et al., 1993; Muruve et al., 1999; Muruve et al., 2004). With research ongoing into the use of other viral vectors such as lentivirus and adeno-associated viruses, it is possible that we will see a safer, more effective viral based delivery method for dystrophin or dystrophin variants in the future (Odom et al., 2007).

The use of AONs to promote exon skipping is another methodology which could be used as a treatment in DMD similar to applications discussed previously for DM1. This approach was tested in the mdx mouse (DMD mouse model) which contains an exon 23 nonsense mutation causing dystrophin synthesis to be stopped prematurely. Treatment with an exon 23 skipping AON resulted in as much as 20% dystrophin positive skeletal (though not cardiac) muscle (Lu et al., 2005). Another possibility is to simply inject naked plasmid DNA encoding dystrophin into muscle to restore its expression, an approach which has resulted in dystrophin expression in 10% of hind limb muscle tissue in mdx mice (Liang et al., 2004).

1.3.6 Utrophin a functional homologue of dystrophin

1.3.6.1 Utrophin background

There exists another avenue of therapy that is particularly appealing to our laboratory. Utrophin is a functional homologue of dystrophin, which can compensate for dystrophin loss/dysfunction by binding, securing and restoring the expression of the DPC at the sarcolemma (**Fig. 5**) (Blake et al., 2002; Perkins and Davies, 2002). It is highly

expressed during development, but is not found at the sarcolemma in adult tissue, remaining localized to the myotendinous and neuromuscular junction (NMJ) (Khurana et al., 1991; Ohlendieck et al., 1991; Clerk et al., 1993; Lin and Burgunder, 2000). Utrophin is a promising candidate for DMD therapy as relatively modest and attainable increases in utrophin protein (1.5-2x) are therapeutic in Mdx mice, and a general overexpression in other tissues is not detrimental (Miura et al., 2009; Miura and Jasmin, 2006; Fisher et al., 2001). Similar avenues of gene therapy, such as adenovirus mediated gene transfer, have been tested and show promising results, however the lingering problem of these genetic treatments in general (harmful immune response, tissue specificity, cell entry, inefficient dosing) reduce the likelihood of providing a positive impact for patients in a timely manner. In a manner analogous to dystrophin, utrophin gene therapy has been explored but suffers from the same hurdles outlined above for dystrophin (Rafael et al., 1998; Gilbert et al., 1999).

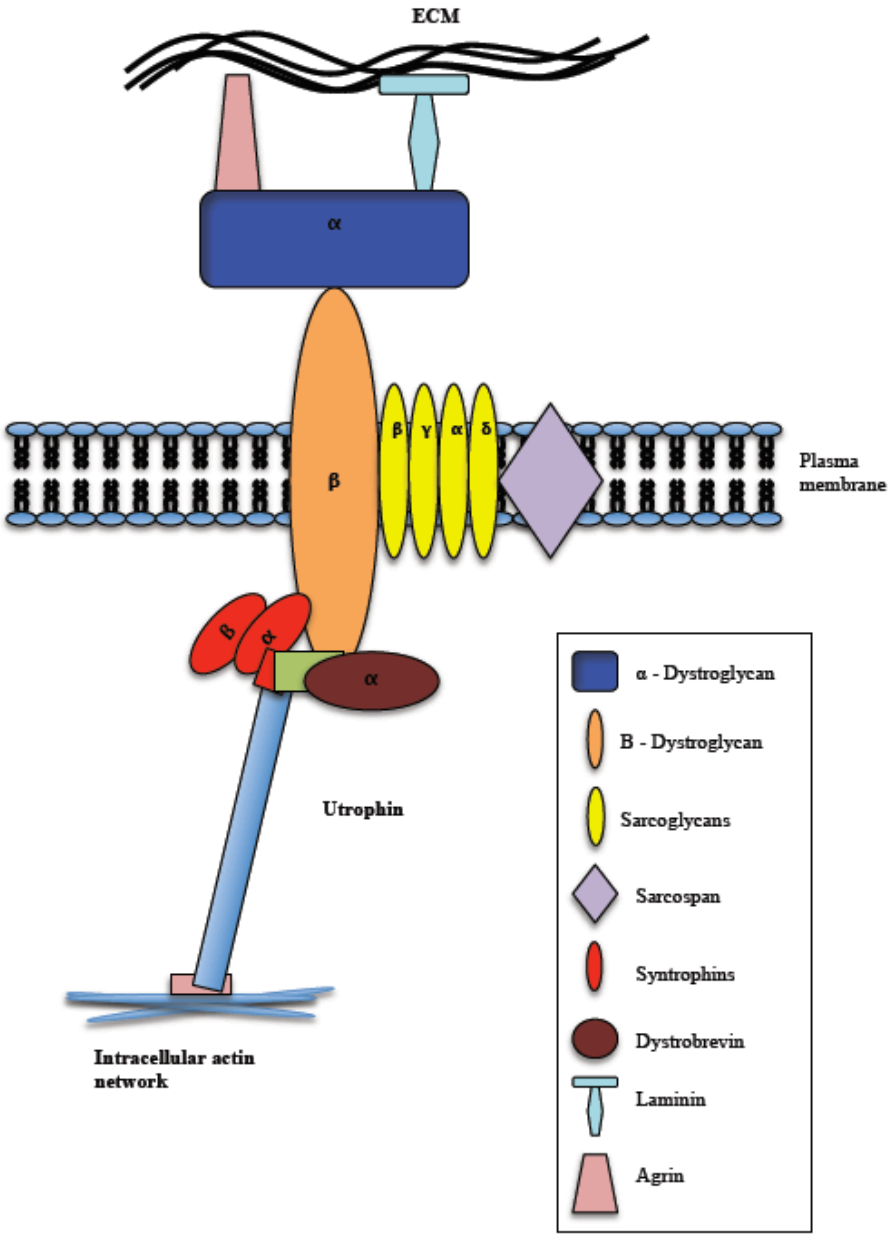

Figure 5 – Interaction of utrophin with the dystrophin-glycoprotein complex at the sarcolemmal membrane.

Utrophin and the DGC link the intracellular actin network to the extracellular matrix providing structural stability to the plasma membrane.

1.3.6.4 Utrophin transcriptional control

The beneficial effect of utrophin over expression on mdx mice (Miura et al., 2009; Miura and Jasmin, 2006; Fisher et al., 2001) (as well as the observation that DMD boys with higher level of utrophin have milder disease) (Kleopa et al., 2006) combined with the absence of deleterious effects of utrophin over-expression in non-dystrophic tissues, has prompted ongoing research into the up regulation of utrophin as a functional replacement of dystrophin. The *utrophin* gene, located on chromosome 6 is, after *dystrophin*, the second largest gene in the human genome with an approximate size of 1 Mb (Pearce et al., 1993). This large gene produces a large, 13kb, transcript that codes for a 395 kDa protein (Tinsley et al., 1992). Utrophin can be found in two different isoforms (A or B), with A being primarily expressed in skeletal muscle fibers, and B localizing to the vascular endothelium (Weir et al., 2002; Chakkalakal et al., 2003). Utrophin's expression at the neuromuscular junction appears to be driven through a N-box motif in utrophin-A's promoter region, targeted by GA-binding protein α and β (GABP), which are activated by an extracellular signal-related kinase (ERK) pathway through the release of nerve-derived trophic factor heregulin **(Fig. 6)** (Dennis et al., 1996; Schaeffer et al., 2004; Gramolini et al., 1997; Gramolini et al., 1998; Khurana et al., 1999; Gramolini et al., 1999). This allows utrophin expression to specifically occur at the neuromuscular junction. The utrophin-A promoter region also contains sites that bind the zinc finger-containing transcription factors Sp1 and 3, which activate transcription and are responsive to okadaic acid (Galvagni et al., 2001; Gyrd-Hansen et al., 2002; Rodova et al., 2004). A PPAR responsive element (PPRE) half site was found at the 5' end of the human utrophin A promoter; its stimulation by a peroxisome proliferator receptor

(PPAR)-β/δ activator also resulted in increased utrophin levels at the sarcolemma (Miura et al., 2009). Lastly, a nuclear factor of activated T cells (NFAT) binding site has been identified in the promoter region which is activated through calcineurin signaling and drives utrophin expression (Chakkalakal et al., 2003).

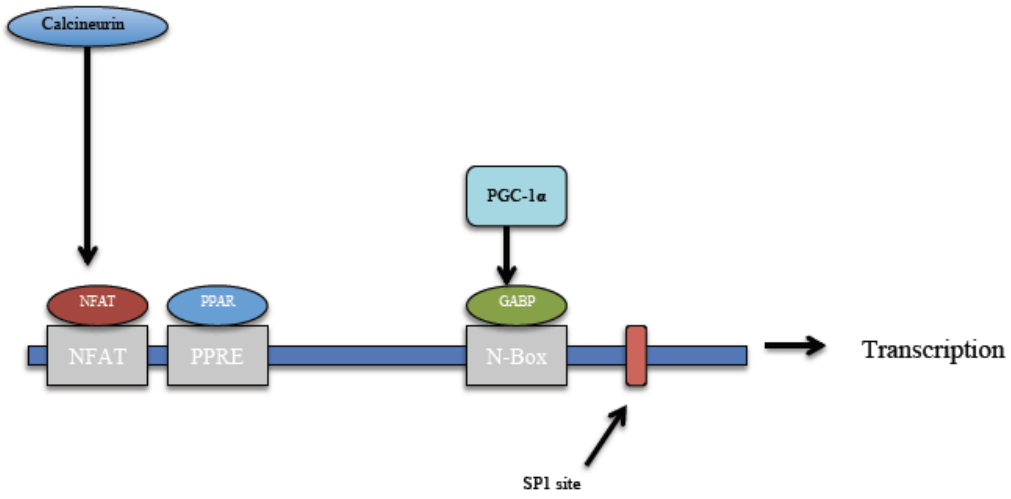

Figure 6 – Known transcriptional targets within the utrophin promoter region.

1.3.6.3 Utrophin protein

The utrophin protein shares 73% homology with dystrophin and its actin binding N-terminal domain shares 85% homology, while the DGC binding C-terminal domain shares 83% homology (Pearce et al., 1993; Tinsley et al., 1992; Love et al., 1989). Utrophin has two less spectrin-like repeats in its central rod domain (22 versus 24 in dystrophin), but has the same number of hinge regions giving it similar flexibility to dystrophin (**Fig. 7**) (Pearce et al., 1993; Rybakova et al., 2006; Amann et al., 1999).

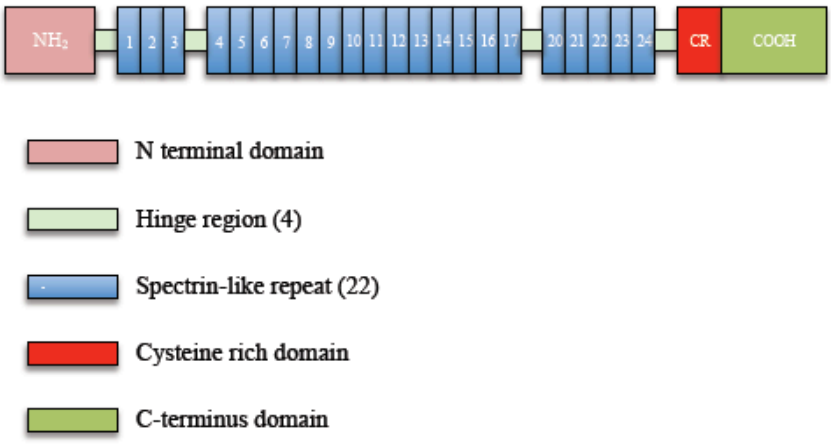

Figure 7 – Structural schematic of the full length utrophin protein.

1.4 Project Rational and Hypothesis

1.4.1 Need for treatment strategy

Although there have been promising advances in gene therapies for both Duchenne's and myotonic dystrophy, treatment options are not currently available and in all likelihood there remain large investments, both in terms of time and funding, required before they will be available for patients on a broad scale. This is highlighted by the limited number of trials testing new treatments for DMD and almost complete absence of any for myotonic dystrophy (U.S Institute of Health, 2011). Although gene therapy may ultimately present the best chance for a cure, treatments are needed in the interim both to improve the quality of life and increase the lifespan of patients until a cure is developed.

1.4.2 DM1 and DMD as candidate diseases

In both diseases, either decreasing (DMPK) or increasing (utrophin) transcript levels would hold excellent potential to provide a substantial effect to patients. As has been shown previously, there has been considerable interest in doing just this. Kay Davies and other DMD researchers have been advocating the up regulation of utrophin in the treatment of Duchenne muscular dystrophy for almost 20 years (Khurana and Davies, 2003). Indeed this approach is mirrored in other diseases as the induction of fetal hemoglobin as a treatment for sickle cell and other hemoglobinopathies has been a goal of hematologists for decades (Atweh and Loukopoulos, 2001). Nonetheless, if successful, the projects as outlined would serve as encouraging case studies for the wedding of recent

(and underutilized) system wide transcriptional databases and our rapidly expanding understanding of the genetic underpinnings of disease.

1.4.3 Use of *in silico* screen to identify disease modifying agents

We propose (and explore) here a novel approach to identify pharmacological transcript modulators that bypasses both the development and approval phases of drug development by screening pre-existing and approved drugs for this activity (**Fig. 8)**. Determining the genetic profiles of all potential compounds would be very expensive and labour-intensive. As a solution, it is possible to use pre-existing databases to identify candidate compounds at the outset.

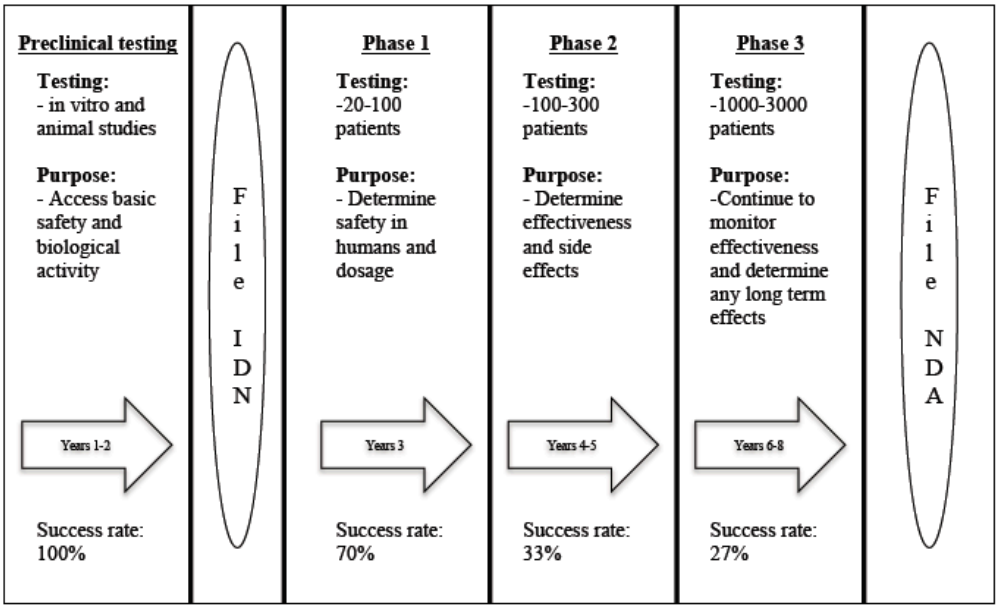

Figure 8 – Overview of FDA approval process.

Overview of FDA approval process with success rate through each phase. IDN – investigational new drug, NDA – new drug application (Med Scape, 2001).

1.4.4 The Broad Institute Connectivity Map

The Broad Institute is a joint venture between Harvard and the Massachusetts Institute of Technology (MIT) which has developed such a database, although for a slightly different purpose. The Broad Institute has developed what they have termed a Connectivity Map (Lamb, 2007; Lamb et al., 2006). This Connectivity Map has a straightforward methodology that incubates three human cancer cell lines (HELA, PC, MCF7 and HL60) with ~1300 compounds, the majority of which are FDA approved drugs (Lamb, 2007; Lamb et al., 2006). The transcriptional profiles generated by the Connectivity Map are then used as a novel means of classifying compounds as well as to possibly establish correlation between these profiles with the transcriptional profiles of a disease. For example if a certain type of cancer has a number of genes up regulated, the Connectivity Map could be used to find compound(s) which might correct this up regulation. Alternatively, the Connectivity Map could be used to identify drugs which have similar transcriptional profiles to others in the hopes of finding new compounds that could be used for other applications.

1.4.5 Issues with *in silico* mining for disease modulating transcript agents

1.4.5.1 Issues with Connectivity Map

The *in silico* analysis of system wide transcriptional databases for single transcript levels differs from the broader transcriptional profile analysis proposed by the Connectivity Map and raises a number of potential barriers The first is the indifferent

reproducibility of microarray experiments. When hundreds and even of thousands of genes comprise a Connectivity Map transcriptional profile this reproducibility becomes less of an issue; when focusing on a single transcript, however, there is the possibility that the readings are simply artifacts or errors,. A second issue with the Connectivity Map is that it screens solely on cancer cells. For the purposes of the Connectivity Map, these cells were ideal given the ease with which they can be cultured, as well as their suitability for a high throughput screening procedure (Lamb, 2007; Lamb et al., 2006). This means that our compounds of interest were not screened in a physiologically relevant cell line. Therefore, even if the microarray data is indeed correct, there is a risk that these compounds simply won't work in the relevant tissues.

1.4.5.2 RNA-protein disconnect

Finally for most disorders for which we shall be interested in modulating protein there is the issue of RNA-protein correlation. In addition to transcriptional control, there exists post-transcriptional modulation (e.g. protein stability, translation initiation) of protein expression, thus the mRNA level may not be a faithful reflection of final protein levels. Recent studies have examined the correlation between RNA and protein levels in response to drug treatment. This research determined that, of the 150 genes (35% of 425 screened) which showed significant changes at either the protein or mRNA levels, 76% exhibited changes for mRNA and their cognate proteins in the same direction (Tian et al., 2004). However, while 29 of the significant genes (20%) showed significant changes at both mRNA and protein levels, 67 genes (45%) showed significant changes at the mRNA

but not the protein levels, and 52 (35%) showed significant changes at the protein but not at the mRNA levels (Tian et al., 2004). There were also 2 (1.3%) which showed statistically significant opposite expression patterns between mRNA and protein. The correlation coefficient for the significant genes was determined to be 0.64 (Tian et al., 2004).

1.4.6 Further research opportunities

However even with these drawbacks, the prospect of identifying treatments for these presently untreatable diseases, in our opinion, outweigh the risks of dealing with false positives especially because the identification of FDA approved compounds would allow for significant time and financial savings in delivering these drugs to clinic (**Fig. 8**). It is currently estimated to cost approximately 800 million dollars to bring a new drug through all phases of testing and approval, while the chances of successfully attaining approval for a compound is ~6% (Dimasi, 2001; DiMasi et al., 2003; DiMasi et al., 2003). In addition to the translational promise of identifying such compounds, their identification may also elucidate the mechanisms through which they work, allowing other drugs to be developed to work through these pathways to modulate the transcripts more efficiently. The recent identification of the p38 kinase pathway in modulating the SMA related SMN2 gene following an analogous *in silico* screen is one example of this (Farooq et al., 2009). Elucidating the functional mechanism of such a compound (i.e. a new receptor involved in modulating the disease) may yield other avenues of research allowing other facets of the disease to be uncovered, revealing alternative avenues for further treatment development. This method of approaching drug discovery, followed by

mechanism discovery is highly appealing to us, and we believe that the possibilities for auxiliary research (discovery of new receptors, proteins, pathways involved in the disease) are very high.

Lastly, and perhaps most importantly, if we are able to identify compounds through the Broad Institute, we will not only be helping DM1 and DMD but other monogenic disorders in general. By showing the proof of concept that we were able to mine an *in silico* database and in a short time identify possible therapeutics for untreatable diseases, we would be opening the door for future experiments into many other monogenic disorders (estimates of the number of monogenic disorders are in the thousands) (McKusick-Nathans Institute of Genetic Medicine, Johns Hopkins University (Baltimore, MD) and National Center for Biotechnology Information, National Library of Medicine (Bethesda, MD), 2011). DM1 and DMD were chosen as diseases to be investigated in this way, as they represent distinct situations targeting up regulation or down regulation of a transcript of interest. Thus if we can show that the Broad Institute database is capable of predicting compounds capable of modulating transcripts in both ways, we will have shown that many monogenic disorders stand to benefit from this method of drug identification.

The Broad Institute has already suggested that other institutions take on similar projects, to increase the number of cell lines and compounds screened in an effort similar to the human genome project (Lamb, 2007; Lamb et al., 2006). We believe our own research will aid the call to generate a larger and better database, and if we can show

some success with a smaller, limited scope database, the possibilities for an even larger drug screen, across multiple cell lines would be significant.

Chapter 2

2. Methods

2.1 Connectivity Map Data Mining

Data mined form the Broad Institutes Connectivity Map project served as the starting point for this project. The Broad Institutes Connectivity Map is constituted of AffymetrixGeneChip U133-A microarray data generated with cRNA isolated from cell lines incubated with ~ 1300 drugs individually at a concentration of 10uM for 6 hours. The two different DMPK cDNA tags (37996_s_at, 217066_s_at), and utrophin cDNA tags (213023_at, 213022_s_at) on the GeneChip enabled the generation of two different lists (builds) of candidate compounds mitigating the variability inherent in microarray analyses. To compare across builds we took an average of the relative expression of both builds and ranked compounds according to their average effect. Connectivity Map drugs are tested from 1-100 times. In a further attempt to reduce false positive drug identification, we restricted most of our analyses to those compounds which had a minimum of 4 trials per build, leaving us with an aggregate minimum of 8 trials. This number was chosen as it reflects the highest number of trials that would allow a reasonable number of candidate drugs to be returned. This resulted in our candidate drug list shrinking to ~ 400 compounds that we included for further study. A small number of compounds were included that did not meet the 4 trial cut-off but whose suppression/induction capabilities were high. A very small number of compounds were removed after this stage due to the lack of availability. The majority of these were discontinued compounds, making them less than ideal candidate drugs.

2.2 Reagents

All compounds identified through the connectivity map and used for testing were purchased from Sigma-Aldrich.

2.3 Cell Culture

2.3.1 General culture

C2C12 myoblasts were cultured under standard conditions on 25 cm plates (Cell Star, Greiner Bio One) and kept at 37°C in a water-saturated environment which contained 5% $C0_2$. Dulbecco's modified Eagle's medium supplemented with 10% fetal calf serum (FCS) and 100 units/ml of penicillin-streptomycin was used as growth media. To prevent any differentiation of the myoblasts into myotubes, all growth plates were carefully monitored and were split when cells reached 70% confluence.

2.3.2 qPCR cell culture

For trials where RNA was to be extracted for qPCR, cells were split from 25 cm growth plates into 12- well (BD Biosciences, Falcon cell culture) plates. Depending on trial length (4, 16, 24 hour), cells were seeded at densities so as to never surpass 70-80% confluence. Cells were monitored before treatment and before lysis to ensure equal cell number between trials.

2.3.3 Protein cell culture

For trials where protein was to be extracted, cells were grown according to which protein was being analyzed. For DMPK protein analysis, an optimal amount of protein was attainable from the same 12-well plates used for qPCR analysis. For utrophin analysis, a larger amount of protein was needed. To account for this, cells used in trials assaying utrophin protein were grown on 10 cm (Corning Incorporated, NY) plates.

2.4 Drug treatment conditions

The mid-throughput screens conducted on *DMPK* suppressors candidate drugs were screened at 2 concentrations (1uM and 25uM), while utrophin inducer candidate drugs were screened at 4 concentrations (50nM, 1uM, 10uM, and 25uM). All drugs were diluted as per manufacturers recommendation in either sterile H20 or Dimethyl sulfide (DMSO). All compounds were diluted so that no vehicle surpassed 0.1% in cell media.

2.5 Animal Studies

Six-week-old CD1 mice were purchased from Charles River Laboratories (Boston, MA). They were cared for in approval with the University of Ottawa Animal Care and Use Committee which is compliant with the Guidelines of the Canadian Council on Animal Care and the Animals for Research Act. Animals were assessed daily by an animal care technician and were monitored before, during, and after treatment to ensure no negative effects of treatment. All treatments were given to mice through

intraperitoneal injection (I.P.), once daily. To reduce stress on animals small gauge needles (30 ½) were used. All tissues were extracted from mice within 8 hours of the last dose.

2.6 qPCR Analysis

2.6.1 *In vitro* RNA analysis

Total RNA was isolated according to the protocol provided by the manufacturer using the RNAeasy gDNA eliminator kit (Qiagen). This extraction included the gDNA elution step. For qPCR, cDNA was reverse transcribed from isolated RNA employing the provided primer mix (oligodT primers/random primers) provided with the Quantitect Reverse Transcription kit (Qiagen). cDNA synthesis was conducted following manufacturers instructions. The optional gDNA wipeout treatment was included during cDNA synthesis. The synthesized cDNA template was used for qPCR with PerfeCTa©Sybr green (Quanta Biosciences, MD) and analyzed on the Eppendorf Mastercycler realplex© using Eppendorf 96-well qPCR plates (white plastic bottom). β-2-microglobulin was chosen as the housekeeping gene and commercially available primers were obtained from Origene. Following qPCR, the delta delta Ct method of analysis was used to determine relative expression of our transcript of interest. Standard curves were generated for each primer pair to ensure our amplification and detection were occurring efficiently and within the linear range. The following primer sequences were used to detect DMPK, Utrophin and β-2-microglobulin:

DMPK (5'→3')

Forward: CTGCTCGACCTTCTCCTGG

Reverse: CACGCCCGATCACCTTCAA

Amplicon length: 166

Location: Spanning exon 1 (219)-exon 2 (384) of DMPK transcript

UtrophinA(5'→3')

Forward: GGCAGGAAGATTGCACAAGT

Reverse: CTGCTAGCCAAGTCCCAGAG

Primers were developed and described previously (Angus et al., 2005; McCarthy et al., 2007).

β-2-microglobulin(5'-3')

Forward: ACAGTTCCACCCGCCTCACATT

Reverse: TAGAAAGACCAGTCCTTGCTGAAG

Product length: 105

Location: Exon 2: 195-299

2.6.2 *In vivo* RNA analysis

Mice were individually euthanized by exposure to $C0_2$ and tissue (gastrocnemius and heart) were obtained, washed in sterile PBS, and frozen in liquid nitrogen. Dissection instruments were cleaned with RNAse Away (Molecular Bioproducts, CA) and RNA free H_20 water after each dissection to prevent contamination between samples. Samples were then stored at -80ºC. For RNA isolation, samples were lysed using the

Qiagen Tissue Lyser II©, in RNA free tubes utilizing steel balls. Total RNA was extracted using the RNeasy fibrous tissue midi kit (Qiagen), with the optional gDNA elimination step included, as per the manufactures instructions. cDNA synthesis and qPCR were performed on mouse samples in the same manner as described in **5.6.1**.

2.7 Western Blot Analysis

2.7.1 *In vitro* protein analysis

Cells were washed twice with Phospho-buffered saline (1 x PBS) and lysed with either 75ul (12 well plate), 300ul (5cm plate) of RIPA buffer containing 10mg/ml each of aprotinin, phenylmethylsulfonyl fluoride (PMSF) and leupeptin for 30 min at 4°C. Following lysis, the samples were centrifuged at 13,000g for 20 minutes at 4°C and supernatants were collected and frozen at -20°C. Protein concentrations were determined by Bradford protein assay using a Bio-Rad protein assay kit (Richmond, CA, USA).

2.7.1.1 DMPK protein assay

Before analysis, samples were boiled for 5 mins and equal amount of protein extracts were separated by 11% SDS-Page (80 volts 30min, 120V, 1 hour). Proteins were subsequently transferred (300 mA, 3 hours) to nitrocellulose membrane and the membrane was incubated in blocking solution (PBS, 5% milk, 0.2% Tween-20) for 1h at room temperature followed by overnight incubation with the primary antibody (anti-DMPK polyclonal provided by Dr. Chris Storbeck, Luke Sabourin (Ottawa) (Whiting et

al., 1995) at a dilution of 1:1000. A commercially available Tubulin (Abcam) was used at a concentration of 1:10,000. Membranes were washed with PBS-T (1x PBS, 0.2% Tween-20) three times followed by incubation with secondary antibody (anti-rabbit (DMPK), anti-mouse (Tubulin), Cell signaling) for 1 hour at room temperature. Antibody complexes were visualized by autoradiography using ECL western blotting system (GE Healthcare) and X-Ray film (Kodak). Quantification was performed by scanning the autoradiographs and signal intensities were determined by densitometry using the Image J software.

2.7.1.2 Utrophin protein assay

Before analysis, samples were boiled for 7 mins and equal amount of protein extracts were separated on a biphasic gel (25 min 80V, 100 V 4 hours). The large size of utrophin (395 kDA) renders immunoblots quantification problematic; by the time it has migrated through the stacking gel, reporter proteins have migrated off the gel usually making it necessary to run the markers on a different gel thereby weakening the quantification. To circumvent this problem, a student colleague (Jeremiah Hadwen) has developed a biphasic gel technique whereby a 6% gel is formed on top of a 15% gel containing glycerol. This allows utrophin to migrate into the less dense gel while retaining all proteins of the sample in the denser glycerol 15% gel. Using the biphasic gel approach, proteins were subsequently transferred overnight (300mA) at 4°C to nitrocellulose membrane and the membrane was incubated in 1:1 LiCor Odyssey blocking buffer (LiCor Biosciences) and 1x PBS for 30 min. Membranes were subsequently incubated with primary antibody Utrophin (Novacastra, UK) at a

concentration of 1:500, or Tubulin (Abcam) at a concentration of 1:10,000 diluted in the same 1:1 liCor:PBS solution + 0.05% Tween-20 overnight at 4°C. Membranes were then washed 4x with PBS-T. Secondary antibody, Alex 680 (Licor Biosciences) was diluted as per manufacturers instructions in 1:1 LiCor:PBS. Utrophin assays were incubated overnight at 4°C while tubulin assays were incubated for 1 hour at room temperature. Following secondary antibody incubation, samples were washed 4x with PBS-T and imaged and quantified using densitometry using the Odyssey hardware and software.

2.7.2 *In vivo* protein analysis

Mice were individually euthanized by exposure to $C0_2$ and tissue (gastrocnemius and heart) were obtained, washed in sterile PBS, and frozen in liquid nitrogen. Samples were then stored at -80C. Samples were prepared by lysing in either 500ul (Heart tissue), or 300ul (gastrocnemius tissue) of RIPA buffer containing 10mg/ml each of aprotinin, phenylmethylsulfonyl fluoride (PMSF) and leupeptin in the Qiagen Tissue Lyser II© until a smooth consistency was obtained. Following lysis, the samples were centrifuged at 13,000g for 30 min at 4°C and supernatants were collected and frozen at -80°C. Protein concentrations were determined by Bradford protein assay using a Bio-Rad protein assay kit (Richmond, CA, USA). Samples were analyzed in the same manner as was described in **5.7.1.1** except for heart tissue. Due to the high expression of DMPK protein in heart tissue, attempts were made to decrease the intensity of the bands reported. Even with limited exposure times, DMPK bands from heart tissue presented themselves as one large band. To address this heart protein levels were analyzed, and reported, as a total protein with no distinction made between protein isoforms.

2.8 Statistical Analysis

For statistical analysis of transcript/protein increases or decreases the students t-test (2 tailed, two-sample unequal variance test) was used for analysis. All graph error bars represent the standard error of the mean (SEM) or Standard deviation (SD) as is indicated in the figure caption.

Chapter 3

3. Results

3.1 Assessment of Connectivity Map to identify compound capable of decreasing a transcript of interest (DMPK)

3.1.1 Initial Screen for DMPK suppressing compounds

Our acquisition and analysis of the Broad Institute Connectivity Map data (see Chapter 5) resulted in a list of compounds that decrease DMPK mRNA in a number of cell lines (Lam et al., 2000). The list of candidate compounds shown in **Table 1** is comprised of agents which are both effective DMPK suppressors and readily attainable. Although this limitation meant some candidates were left out, these were largely experimental compounds with no FDA approval status making them less than ideal for this study.

3.1.2 Validation of Connectivity Map Screen

A central concern of ours was whether the DMPK mRNA suppression observed with the Connectivity Map cell lines (HL60, PC3, MCF7) would be recapitulated in more disease relevant tissues or cell lines. The C2C12 mouse myoblast cell line which are both easily cultured and represent a relevant muscle cell line were thus incubated for 4 and 24 hours in the presence of 1uM and 25uM of each putative DMPK suppressing agent. Data from three independent experiments are summarized in **Table 1** (**Supplemental Figures 1-20**). The cells were monitored for any signs of cell death (e.g. rounding, detachment

from plate); and any signs of cell death are noted asterisks in **Table 1**. The results of this study along with the initial Connectivity Map data revealed sodium channel blockers mexiletine, prilocaine, and procainamide as effective DMPK suppressors. A fourth sodium channel blocker, sparteine, also showed modest DMPK mRNA suppression in the Connectivity Map. Thus of ~1300 compounds, four from a relatively small drug class (9) appear in the top 11 DMPK mRNA suppressors. Furthermore other compounds which are known to modulate sodium channel activity, potentially through blockage, were also identified within the Connectivity Map (Trimetazadine) (Banach et al., 2008).

As encouraging as these results are it should be noted that there existed considerable variability between trials both in the Connectivity Map and our own initial assessment underlining the need for further validation (Sup. Figures 1-20).

Table 1 - Table summarizing mid-throughput qPCR screen for DMPK suppressors.

Each individual drugs class and optimal suppression at both time points are listed as identified through this initial screen. Connectivity map data indicates the original fold expression values provided by the Broad Institute used in initially ranking the compounds. Those compounds marked with an asterix denote compounds which elicited cell death at one of the concentrations tested.

Drug	Drug Class	DMPK mRNA level		
		Connectivity Map data (MCF7, HELA, PC3 cells)	Preliminary validation (C2C12) n=3	
		10uM, 6 hours (Fold Expression)	Optimal Down regulation (Fold Expression)	
			4 hours	24 hours
Tomelukast*	Leukotriene antagonist	0.56	0.98(25uM)	0.43(1uM)
Sulindac Sulfide*	Non-steroidal anti-inflammatory(NSAID)	0.64	0.03(25uM)	0.07(1uM)
8-Azaguanine	Purine analog	0.71	1.08(1uM)	0.04(25uM)
Santonin	Anthelminthic	0.72	1.08(25uM)	0.1(1uM)
Procainamide	Na Channel Blocker	0.75	0.18(25uM)	0.06(25uM)
Prilocaine	Na Channel Blocker	0.75	0.04(1uM)	0.01(25uM)
Splitomicin	Sirtuin inhibitor	0.76	0.94(25uM)	0.39(1uM)
Apigenin	Flavone(yellow), CYP2C9 inhibitor	0.80	0.06(1uM)	0.24(1uM)
Liothyronine	Thyroid hormone	0.80	0.52(1uM)	0.08(1uM)
Mexiletine	Na Channel Blocker	0.80	0.17(1uM)	0.11(1uM)
Sparteine	Na Channel Blocker	0.80	No FDA approval	
Kavain*		0.80	0.01(25uM)	0.05(25uM)
Thiabendazole	Anti-fungal agent	0.81	0.42(1uM)	0.93(25uM)
Ceterizine*	H1 receptor inverse agonist(Anti-histamine)	0.83	0.50(1uM)	0.02(1um)
Simvastatin	HMG-CoA reductase inhibitor	0.83	1.03(25uM)	0.63(1uM)
Nalidixic acid*	Quinolone antibiotic	0.83	0.01(25uM)	0.1(25uM)
Sulfamerazine	Sulfonamide antibacterial	0.83	0.39(1uM)	0.26(1uM)
Methylbenzethonium*	Microbicide	0.83	0.45(1uM)	0.0002(1uM)
Sulconazole	Anti fungal agent(Imidazole)	0.83	0.43(1uM)	0.43(25uM)
Trimetazadine	Anti-anginal(Metabolic agent)	0.83	0.63(1uM	1.03(25uM)
Metoprolol	β1 receptor blocker	0.84	0.32(1uM)	0.88(25uM)

3.1.3 Secondary Validation of Connectivity Map Screen for DMPK suppressors

3.1.3.1 Mexiletine verification and dose response generation

We elected to investigate the sodium channel blocker class of compounds (mexiletine, prilocaine, procainamide) in greater detail. In addition to these compounds, the β - blocker metoprolol was also included as it has been screened in a pilot trial ahead of the larger screen and had shown some promise in DMPK suppression. Four concentrations of drugs (50nM, 1uM, 10uM, 25uM) were assessed using C2C12 cells treated at 4 and 24 hours. A statistically significant decrease (77% decrease, $p<0.05$) in DMPK mRNA levels after 4 hours in response to mexiletine at 50nM was observed (**Fig. 9**). We also evaluated the impact of mexiletine on DMPK protein levels. Although we are aware it is the mRNA which is the pathogenic agent in DM1, we utilized protein levels as a biomarker which might help validate any observed DMPK mRNA decrease. No statistically significant decrease in DMPK protein was observed in response to any dose assayed, although a 30% decrease in DMPK protein isoforms D-F (67kDa) was observed in response to 50nM treatment with mexiletine (**Fig.10**). The optimal DMPK mRNA suppressing concentration (50nM) identified in this phase of the study is lower than serum levels of drug reported in studies examining mexiletine anti- arrhythmia properties in humans (2.8uM) although a wide range of therapeutic doses have been reported (Wang et al., 2004).

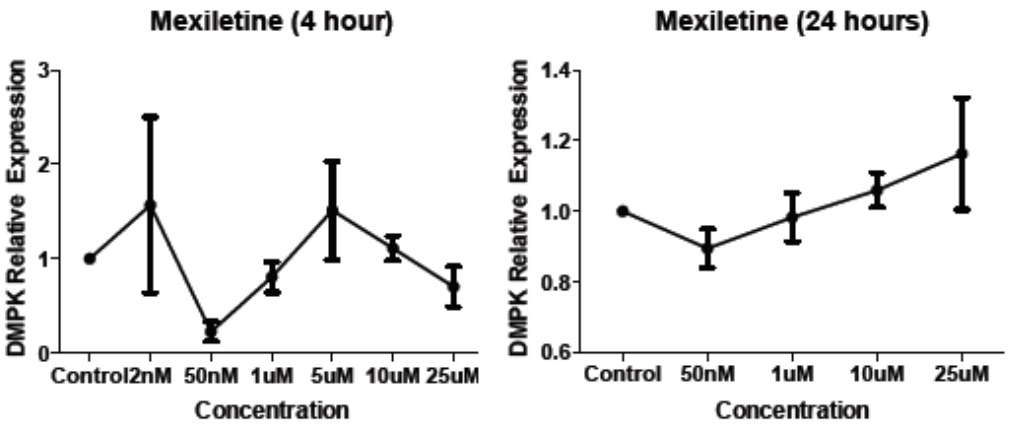

Figure 9 - Mexiletine decreases DMPK mRNA *in vitro*.

Mexiletine (50nM) treatment results in a 77% decrease ($p<0.05$) in DMPK mRNA levels following 4 hours of treatment and analysis of mRNA extracts by qPCR. Quantification of DMPK mRNA relative to β-2-Microglobulin in C2C12 cells (the ratio of control group set as 1). Mean ± SEM (bars) of 3 independent experiments for both 4 hours (treated n=12, control n=28) [4 hour 2nM n=6] and 24 hours (treated n=3, control n=6).

A

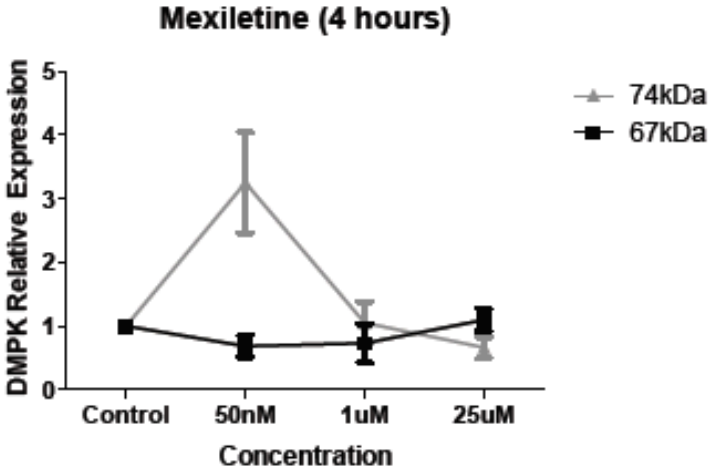

B

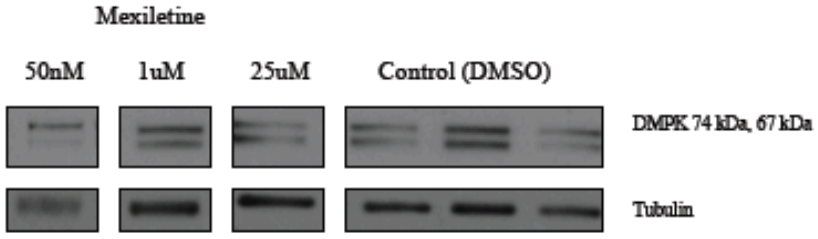

Figure 10 - Mexiletine results in no significant decrease of DMPK protein *in vitro*.

Mexiletine treatment resulted in no significant decrease in total DMPK protein, although a 30% decrease in DMPK isoforms D-F (67kD) was noted. A) Quantification of DMPK protein relative to tubulin from in C2C12 myoblasts (the ratio of control group set as 1) Mean ± SEM (bars) of 3 independent experiments (treated n=3, control n=3). B) Representative western blot.

3.1.3.2 Prilocaine verification and dose response generation

Prilocaine, which is a member of same sub-class of sodium channel blockers IB as mexiletine, also demonstrated a DMPK mRNA suppression in C2C12 cells similar to that seen with mexiletine. Following 4 hours of treatment, prilocaine resulted in statistically significant decreases in DMPK mRNA at the lower screened doses of 50nM and 1uM (**Fig. 11**, $p<0.05$). The 1uM dose proved to be the optimal dose with a 70% decrease in DMPK mRNA following 4 hours of treatment, a decrease that was lost after 24 hours (**Fig. 11**). DMPK protein levels did not decrease significantly following prilocaine treatment at 4 hours, although a 40% decrease in DMPK protein isoforms D-F was again noted (**Fig. 12**). The optimal DMPK mRNA suppressing concentrations for prilocaine fall within serum levels reported in patients receiving prilocaine infusions (~390nM) (Arthur et al., 1979) but are much lower than what has been reported to be required for complete block of neuronal sodium channels (~17uM) (Simon et al., 1997).

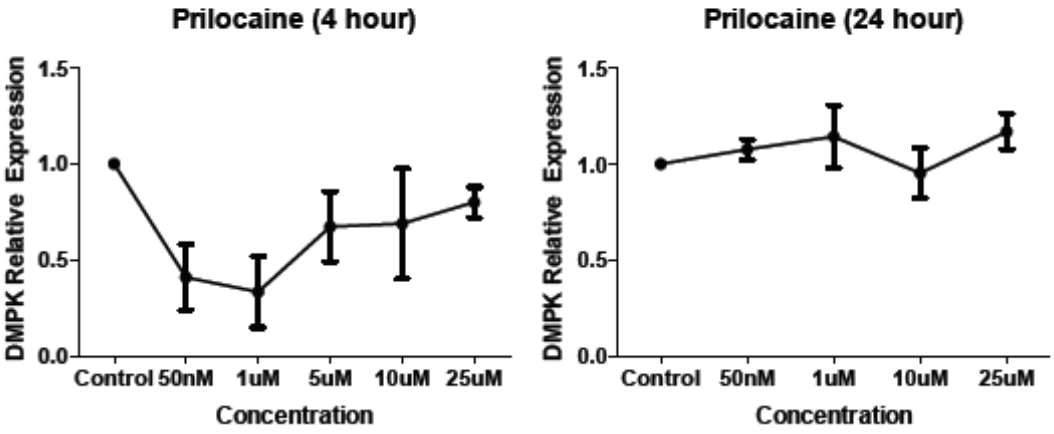

Figure 11 - Prilocaine decreases DMPK mRNA *in vitro*.

Prilocaine (1uM) treatment results in a 70% decrease ($p<0.05$) in DMPK mRNA levels following 4 hours of treatment and analysis of mRNA extracts by qPCR. Quantification of DMPK mRNA relative to β-2-Microglobulin in C2C12 cells (the ratio of control group set as 1). Mean ± SEM (bars) of 3 independent experiments for both 4 hours (treated n=9, control n=20) and 24 hours (treated n=3, control n=6).

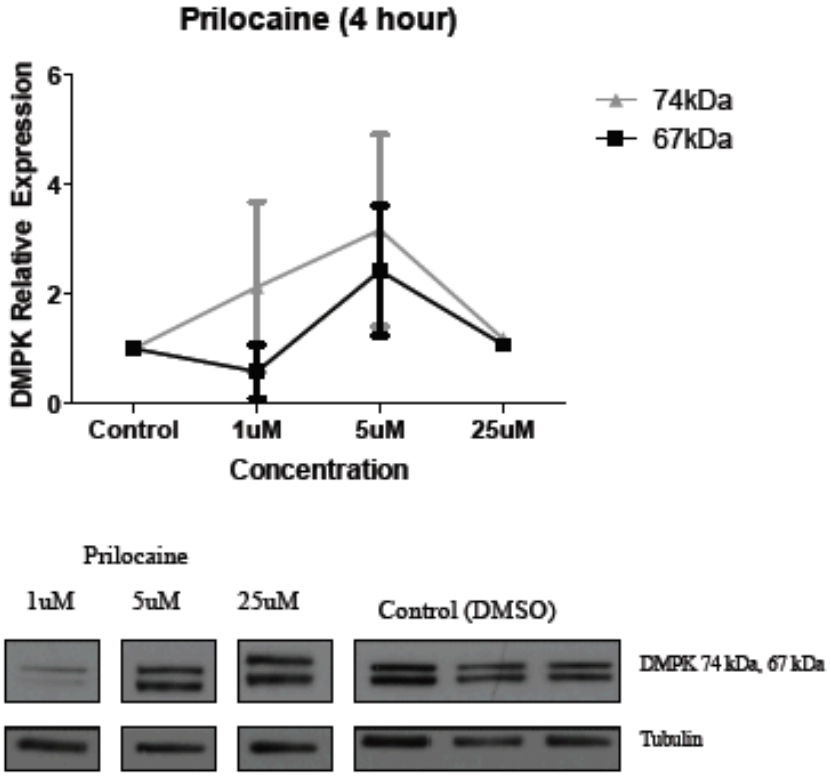

Figure 12 - Prilocaine results in no significant decrease of DMPK protein *in vitro*.

Prilocaine treatment resulted in no significant decrease in total DMPK protein, although a 40% decrease in DMPK isoforms D-F (67kD) was noted. A) Quantification of DMPK protein relative to tubulin from in C2C12 myoblasts (the ratio of control group set as 1) Mean ± SEM (bars) of 3 independent experiments (treated n=3, control n=3). B) Representative western blot.

3.1.3.3 Procainamide verification and dose response generation

Following both 4 and 24 hours of treatment with procainamide no statistically significant decrease in DMPK mRNA (**Fig. 13**) or protein (data not shown) was observed. This distinction may reflect the fact that it belongs to the IA class of sodium channel blockers while mexiletine and prilocaine are IB inhibitors. We believe the absence of effect is unlikely to be dose related as the maximal therapeutic dosage given to patients results in a serum level of ~18uM, well within the range of concentrations we have investigated (Myerburg et al., 1981).

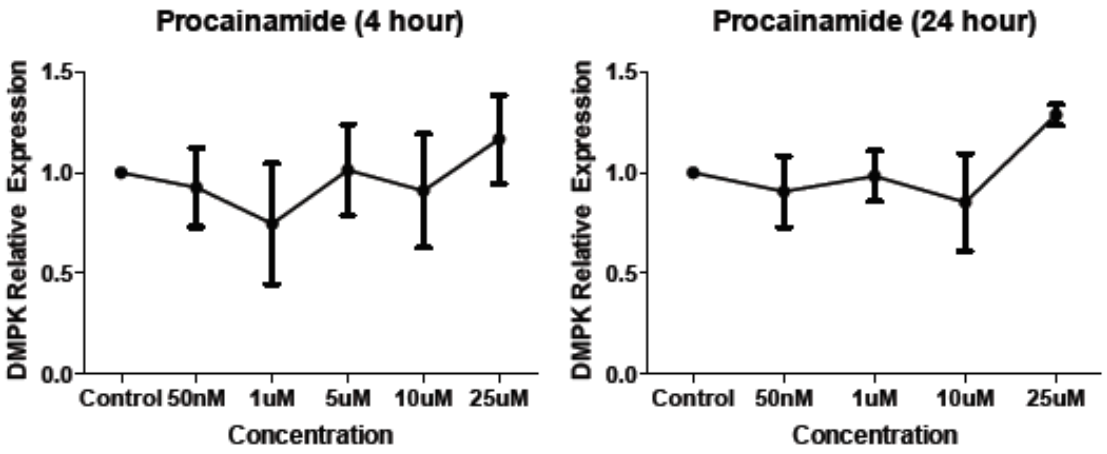

Figure 13 - Procainamide has no significant effect on DMPK mRNA *in vitro*.

Procainamide treatment results in no decrease in DMPK mRNA after treatment and analysis of mRNA extracts by qPCR. Quantification of DMPK mRNA relative to β-2-Microglobulin in C2C12 cells (the ratio of control group set as 1). Mean ± SEM (bars) of 3 independent experiments for both 4 hours (treated n=9, control n=20) and 24 hours (treated n=3, control n=6).

3.1.3.4 Metoprolol verification and dose response generation

Although the Connectivity Map data for metoprolol suggest an indifferent DMPK suppression **(Table 1)**, a small pilot study assaying a number of agents showed slight promise with metoprolol and so it was included in further stages of the study. Unfortunately upon further verification of metoprolol's effect on DMPK mRNA levels in vitro, we saw no significant decrease in DMPK levels at either 4 or 24 hours (**Fig. 14**). Again although DMPK mRNA was not decreased protein was assayed and no decrease was observed (data not shown).

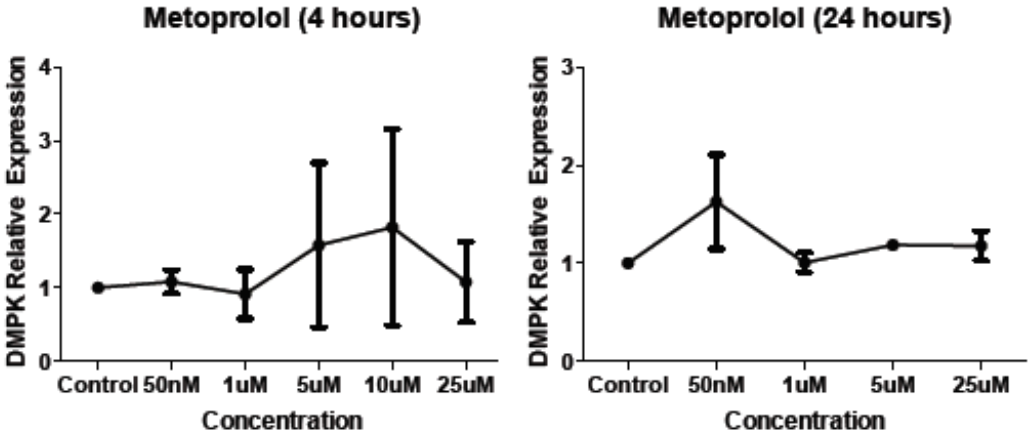

Figure 14 - Metoprolol has no significant effect on DMPK mRNA *in vitro*.

Metoprolol treatment results in no decrease in DMPK mRNA after treatment and analysis of mRNA extracts by qPCR. Quantification of DMPK mRNA relative to β-2-Microglobulin in C2C12 cells (the ratio of control group set as 1). Mean ± SEM (bars) of 3 independent experiments for both 4 hours (treated n=12, control n=27) and 24 hours (treated n=9, control n=15).

3.1.4 *In Vivo* Confirmation of DMPK suppression

The next phase in this research project was to determine if the DMPK suppression observed in cell culture was reproducible in live animals. For this purpose we treated wildtype CD-1 mice with our compounds for 5 days by daily IP injection over a number of doses. Dose selection was guided both by typical human clinical dosing, as well as attempting to approximate murine serum levels with the optimal DMPK suppressing concentrations observed in cell culture.

3.1.4.1 Mexiletine DMPK suppression *in vivo*

CD-1 mice were dosed with daily IP injections of either 50mg/kg, 25mg/kg, 12.5mg/kg, or 6.25mg/kg of mexiletine. Although following the 5 days of treatment no statistically significant DMPK mRNA decrease was observed in heart or gastrocnemius a 55% reduction in DMPK levels in response to 25mg/kg mexiletine was noted in gastrocnemius (**Fig. 15**). The lack of a statistically significant ($p=0.1$) result in this case may be the result of one animal which showed little DMPK mRNA suppression while the other two animals showed 70%, and 94% reduction at 25mg/kg. In this regard, in order to reduce the stress imposed on the animals the smallest volume that could be easily handled was injected, it may be that a missed injection (not penetrating peritoneal cavity) occurred, something that would not be easily detected. This coupled with the differences in metabolism of this drug that has been observed in patients might explain the failure to decrease DMPK mRNA in every animal (Logigian et al., 2010; Cambell, 1998a; Woosley et al., 1984; Campbell et al., 1978). The further observation of a decrease in

gastrocnemius DMPK mRNA (30%) in response to 50mg/kg treatment with mexiletine increases the likelihood of a bona fide *in vivo* decrease of DMPK mRNA in response to this dose (**Fig. 15**). No decrease in DMPK mRNA levels was observed in heart tissue at any of the doses tested (**Fig. 15**).

We next assayed DMPK protein in gastrocnemius in response to mexiletine treatment at the same doses (**Fig. 16**). Both the 25mg/kg and 50mg/kg doses resulted in decreases although only the 50mg/kg dose resulted in a statistically significant drop ($p<0.05$), while 25mg/kg resulted in a diminution very close to statistically significance ($p=0.06$). We believe our observation of DMPK protein reduction supports the probability of a true DMPK mRNA reduction conferred by mexiletine in skeletal muscle.

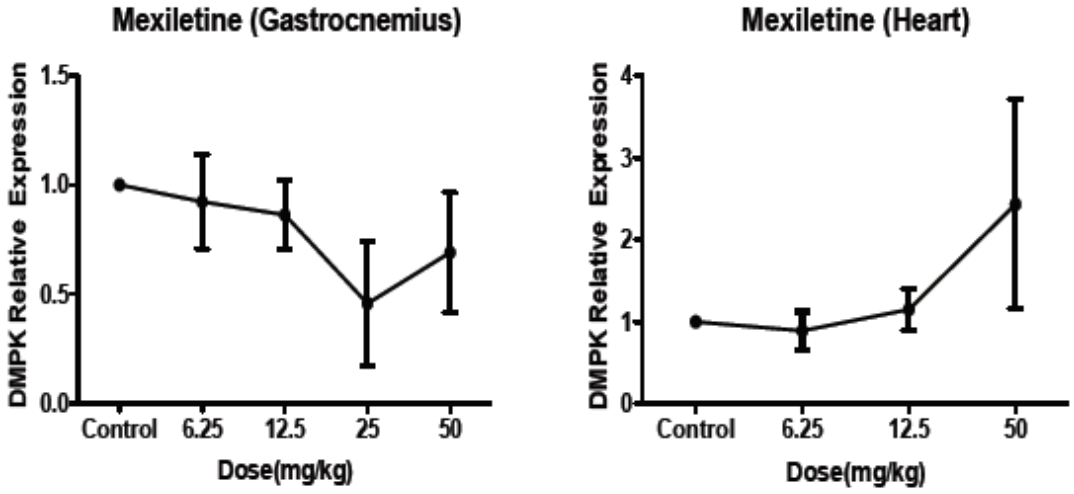

Figure 15 - Mexiletine decreases DMPK mRNA in gastrocnemius but not heart tissue.

Mexiletine (25mg/kg) treatment results in a non-significant (p=0.1) 55% decrease in DMPK mRNA levels in gastrocnemius tissue following treatment and analysis of mRNA extracts by qPCR. Relative DMPK mRNA levels in CD-1 gastrocnemius and heart tissue after 5 days (daily IP injection) of mexiletine. Quantification of DMPK mRNA relative to β-2-Microglobulin (the ratio of control group set as 1). Mean ± SEM (bars) of 1 experiment (Treated n= 3 animals) [heart 50mg/kg n=2]

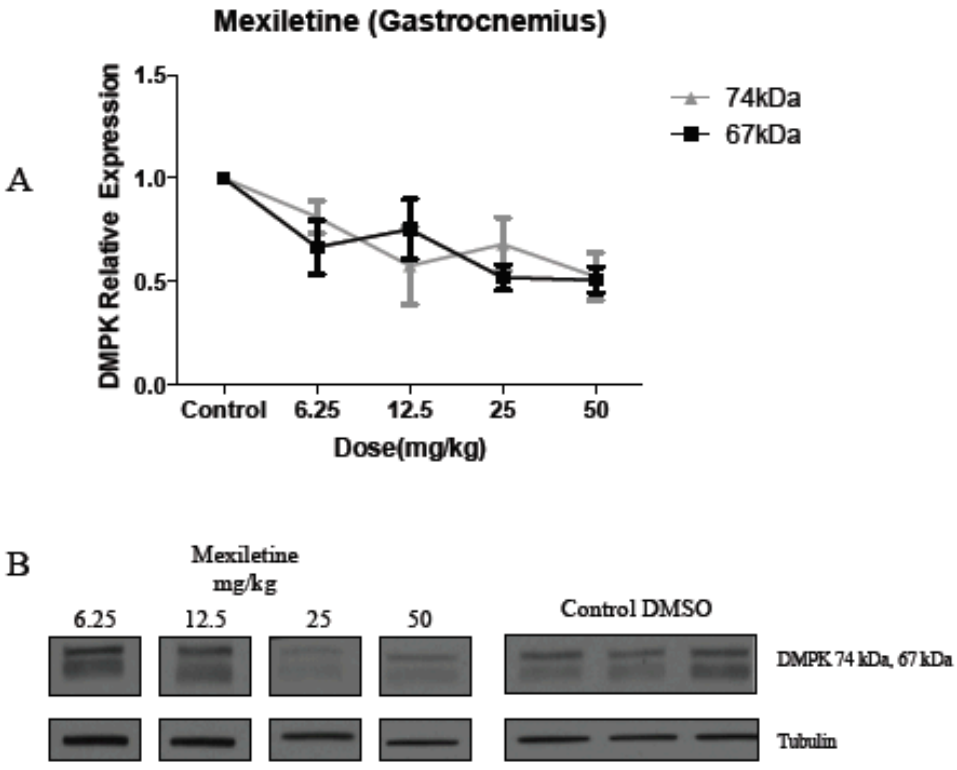

Figure 16 - Mexiletine decreases DMPK protein in gastrocnemius tissue.

Mexiletine treatment (50mg/kg) resulted in a decrease (48%, $p<0.05$) in total DMPK protein. CD-1 mice were treated with mexiletine for 5 days (daily IP injections). A) Quantification of DMPK protein relative to tubulin in CD-1 mice (the ratio of control group set as 1). Mean ± SEM (bars) of 1 experiment (n= 3 animals). B) Representative western blot.

3.1.4.2 Prilocaine DMPK suppression *in vivo*

Prilocaine was the most effective of our candidate compounds in decreasing DMPK mRNA in animal tissue. We tested three different dosages of prilocaine in CD-1 mice, 5mg/kg, 2.5mg/kg and 1.25mg/kg, with the highest dose representing a dosage in the upper allowable limits for human dosing. Following the 5 days of injections we saw a statistically significant decrease ($p<0.05$) in DMPK RNA levels in response to prilocaine in gastrocnemius tissue but not in heart (**Fig. 17**). Prilocaine was very efficient, and consistent, at knocking down DMPK RNA levels by 50% in all animals tested at the 1.25mg/kg dosage (**Fig. 17**). Prilocaine has slightly more toxicity than the other sodium channel blockers, its main use is as a local analgesic, and so the lower optimal DMPK mRNA suppression dose may be suitable for a longer term treatment. No sign of adverse effects or apparent toxicity was detected at any dose. A 1.25mg/kg dose of prilocaine conferred a significant ($p<0.05$) reduction of DMPK protein in gastrocnemius (**Fig. 18**).

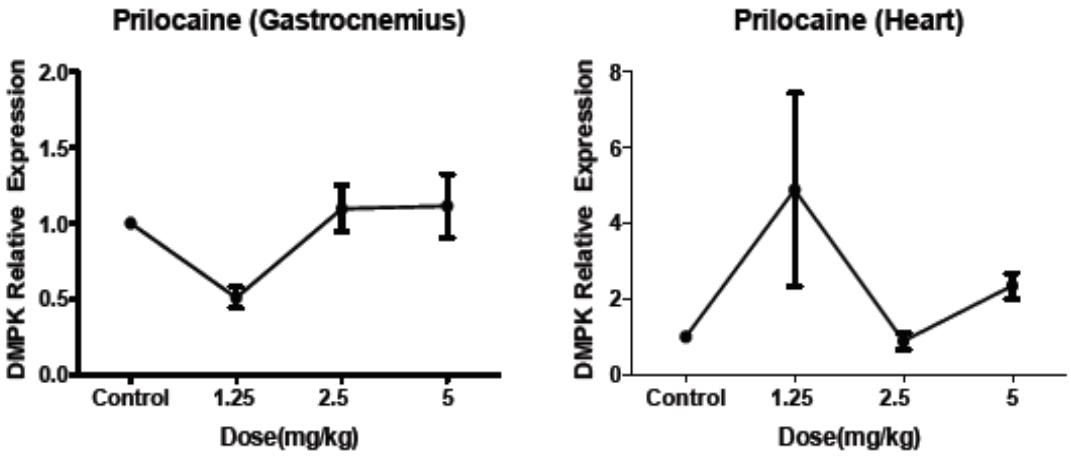

Figure 17 - Prilocaine decreases DMPK RNA in gastrocnemius but not heart tissue.

Prilocaine (1.25mg/kg) treatment results in a significant decrease (50%, $p<0.5$) in DMPK mRNA levels in gastrocnemius tissue following treatment and analysis of mRNA extracts by qPCR. Relative DMPK RNA levels in CD-1 gastrocnemius and heart tissue after 5 days (daily IP injection) of prilocaine. Quantification of DMPK mRNA relative to β-2-Microglobulin (the ratio of control group set as 1). Mean ± range (bars) of 1 experiment (Treated n= 3 animals) [gastroc 2.5mg/kg n=2]

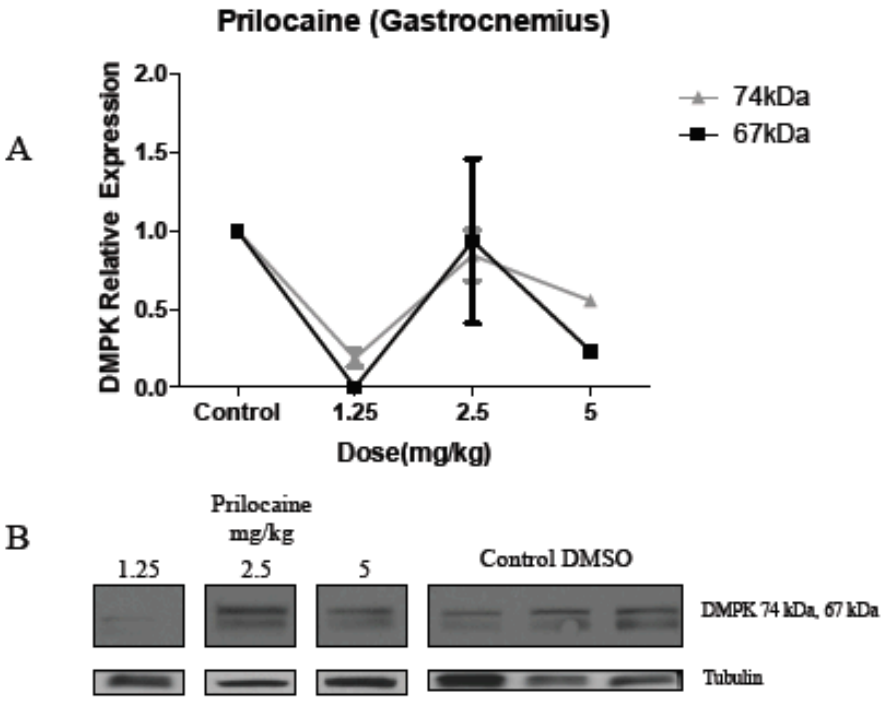

Figure 18 - Prilocaine decreases DMPK protein in gastrocnemius tissue.

Prilocaine treatment (1.25mg/kg) resulted in a decrease (90%, $p<0.05$) in total DMPK protein. CD-1 mice were treated with prilocaine for 5 days (daily IP injections). A) Quantification of DMPK protein relative to tubulin in CD-1 mice (the ratio of control group set as 1). Mean ± SEM (bars) of 1 experiment (n= 3 animals). B) Representative western blot.

3.1.4.3 Procainamide DMPK suppression *in vivo*

Although procainamide was not effective at decreasing DMPK in cell culture, it was effective in decreasing DMPK mRNA levels in both gastrocnemius and heart tissue in CD-1 mice (**Fig. 19**). CD-1 mice were treated with either 25mg/kg, 12.5mg/kg or 6.25mg/kg procainamide for 5 days. 25mg/kg of Procainamide decreased DMPK mRNA levels by 84% ($p<0.05$) in response to treatment, an effect that was very consistent across animals, reflected in the small error bars (**Fig. 19**). The mice were very tightly grouped together with DMPK knockdowns of 84%, 83% and 86%. A more modest DMPK reduction was observed in cardiac tissue (30% knockdown ,$p=0.09$) at 25mg/kg although the lower dose of 6.25mg/kg conferred a reduction of approximately 50% knockdown ($p<0.05$). We next assayed to see if DMPK protein is decreased in response to either the 25mg/kg dose of procainamide in gastrocnemius or at the doses that decreased DMPK mRNA in the heart (**Fig. 20-21**). We did not see a statistically significant decrease in DMPK isoforms overall, but a statistically significant ($p<0.05$) decrease in DMPK isoforms D-F (67kDa) was observed (**Fig. 20**), similar to the protein decrease in cell culture recorded in response to prilocaine and mexiletine (**Fig 10, 12**)

The high expression of cardiac DMPK renders clear delineation of protein isoform groups problematic; even at the smallest exposure times the isoforms merge into a single large band. We thus measure the entire blot reporting a total DMPK protein metric. We saw no decrease, significant or otherwise, in cardiac DMPK protein in response to procainamide (**Fig. 21**). Moreover it is possible that a transient modest decrease in DMPK protein in heart in response to the mRNA diminution might be missed

given both the high endogenous expression of DMPK protein and the fact that small differences can be difficult to detect by western blot.

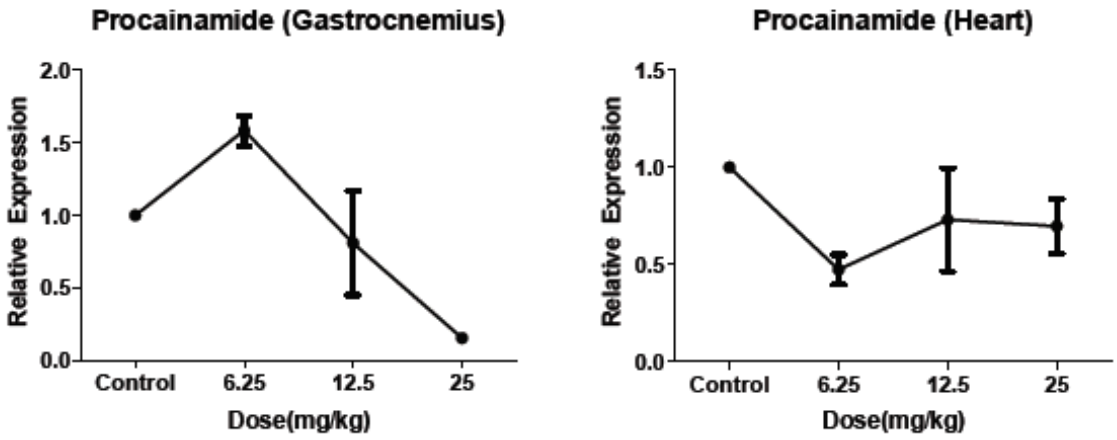

Figure 19 – Procainamide decreases DMPK mRNA in gastrocnemius and heart tissue.

Procainamide (25mg/kg, 6.25mg/kg) treatment results in a significant decrease (84%, $p<0.5$) in DMPK mRNA levels in gastrocnemius tissue, and in heart tissue (50%, $p<0.05$) following treatment and analysis of mRNA extracts by qPCR .Relative DMPK RNA levels in CD-1 gastrocnemius and heart tissue after 5 days (daily IP injection) of procainamide. Quantification of DMPK mRNA relative to β-2-Microglobulin (the ratio of control group set as 1). Mean ± SEM (bars) of 1 experiment (Treated n= 3 animals) [gastrocnemius 6.25mg/kg n=2]

A

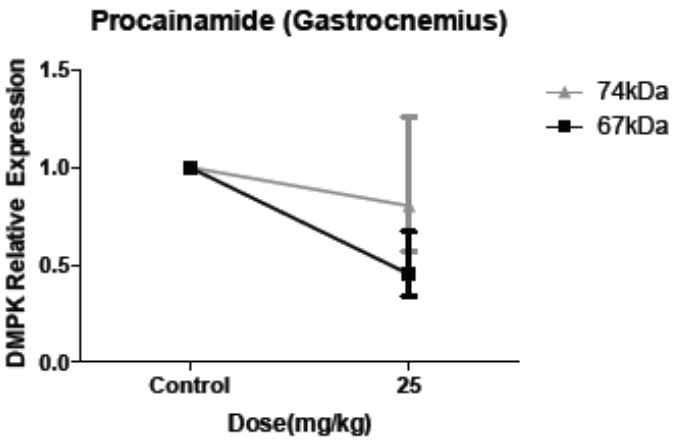

B

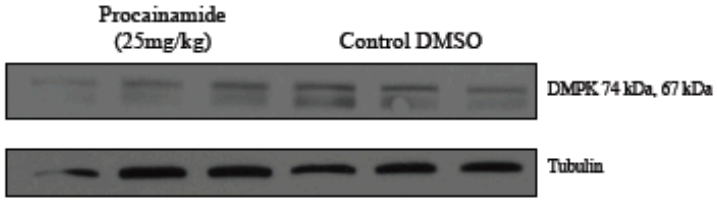

Figure 20 - Procainamide decreases DMPK protein gastroc tissue.

Procainamide treatment (25mg/kg) resulted in a decrease (54%, $p<0.05$) in DMPK isoforms D-F (67kDa). CD-1 mice were treated with procainamide for 5 days (daily IP injections). A) Quantification of DMPK protein relative to tubulin in CD-1 mice (the ratio of control group set as 1). Mean ± SEM (bars) of 1 experiment (n= 3 animals). B) Representative western blot.

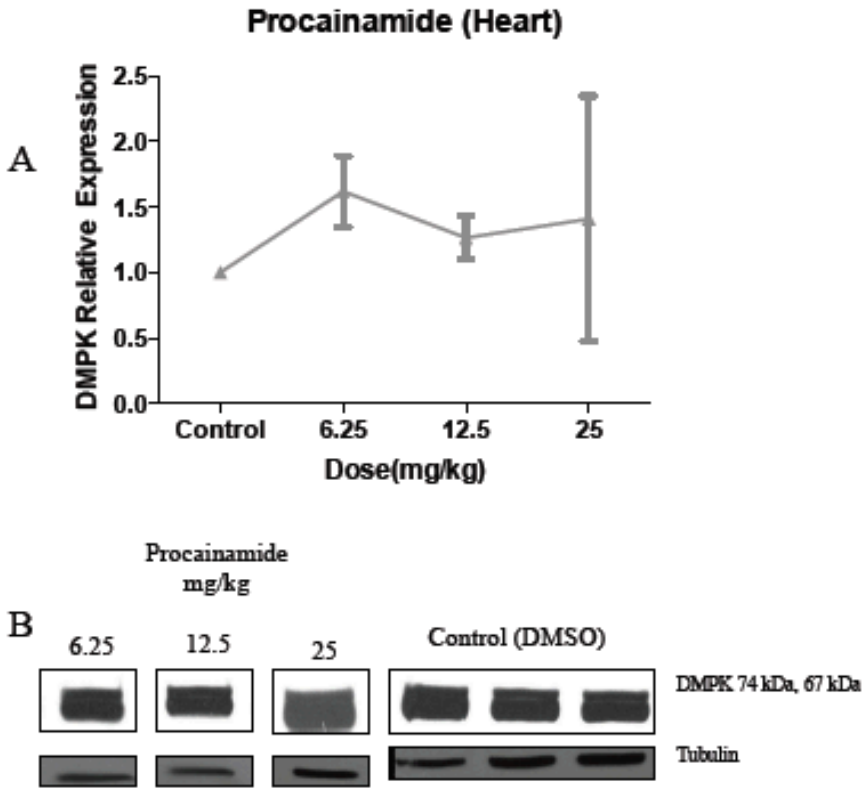

Figure 21 - Procainamide treatment does not affect DMPK protein levels in heart tissue.

Procainamide treatment resulted in no observable decrease in total DMPK protein levels. CD-1 mice were treated with procainamide for 5 days (daily IP injections). A) Quantification of DMPK protein relative to tubulin in CD-1 mice (the ratio of control group set as 1). Mean ± SEM (bars) of 1 experiment (n= 3 animals). B) Representative western blot.

3.1.4.4 Metoprolol DMPK suppression *in vivo*

Similar to what we observed following procainamide treatment, metoprolol resulted in greater DMPK suppression in CD-1 animals than was observed in cell culture. Metoprolol was included in this study due to an earlier pilot trial demonstrating a decrease in DMPK protein in CD-1 mice (gastrocnemius and heart) (data not shown). The impact of metoprolol treatment on DMPK mRNA was next assessed in CD-1 mice. Following 5 days of metoprolol treatment with either 1.2mg/kg, 0.6mg/kg, 0.3mg/kg, or 0.15mg/kg, we saw a statistically significant (60% knockdown, $p<0.05$) decrease in DMPK mRNA levels in gastrocnemius tissue at 0.15mg/kg (**Fig.22**) a dose similar to the 0.1mg/kg used in the pilot trial which decreased CD1 gastrocnemius DMPK protein (data not shown). Metoprolol (0.6 and 1.2mg/kg) also reduced DMPK mRNA in heart tissue (~ 60% knockdown, $p<0.05$) (**Fig. 22**). In contrast to the earlier pilot studies cited above, no corresponding metoprolol conferred reduction in DMPK protein levels was noted in gastrocnemius and heart (**Fig. 23-24**). We did not see a statistically significant decrease in DMPK protein overall in gastrocnemius, but we did see a statistically significant decrease ($p<0.05$) in DMPK isoforms D-F in response to the 0.15mg/kg dosage which caused DMPK mRNA to decrease (**Fig. 23**). A reduction of DMPK isoforms D-F was observed with all drugs tested; it is unclear if this is occurring through preferential degradation, splicing interference or transcriptional inhibition. Similar to the effects of procainamide, although we observed a decrease in DMPK mRNA levels in heart following metoprolol treatment, we saw no corresponding decrease in DMPK protein in heart tissue (**Fig. 24**).

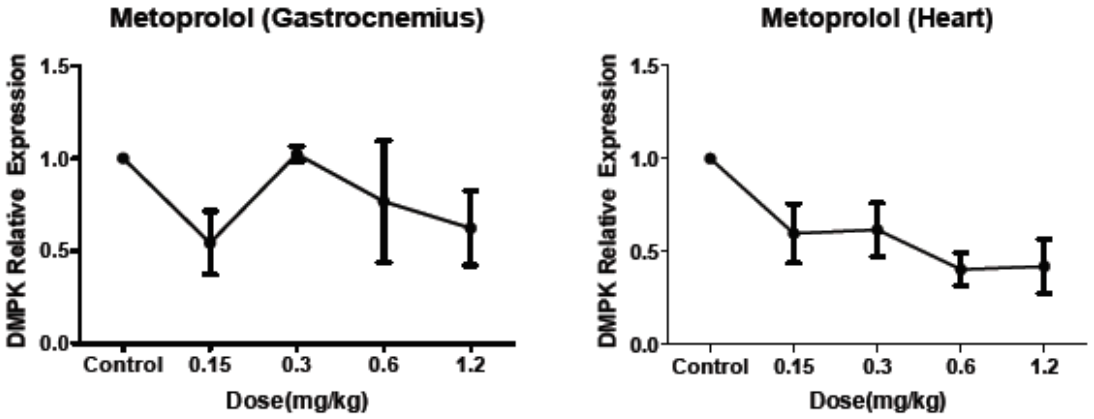

Figure 22 - Metoprolol decreases DMPK mRNA in heart and gastrocnemius tissue.

Metoprolol (0.15mg/kg, 0.6mg/kg) treatment results in a significant decrease (60%, $p<0.5$) in DMPK mRNA levels in gastrocnemius tissue, and in heart tissue (60%, $p<0.05$) following treatment and analysis of mRNA extracts by qPCR Relative DMPK RNA levels in CD-1 gastrocnemius and heart tissue after 5 days (daily IP injection) of metoprolol. Quantification of DMPK mRNA relative to β-2-Microglobulin (the ratio of control group set as 1). Mean ± SEM (bars) of 1 experiment (n= 3 animals).

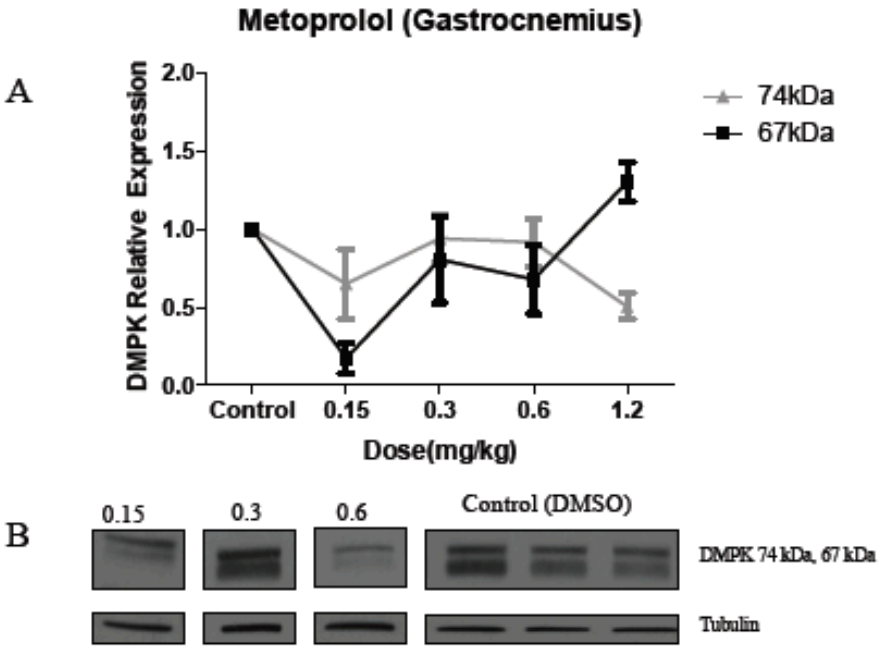

Figure 23 - Metoprolol decreases DMPK protein levels in gastrocnemius.

Metoprolol treatment (0.15mg/kg) resulted in a decrease (82%, $p<0.05$) in DMPK isoforms A-C (74kDa). CD-1 mice were treated with metoprolol for 5 days (daily IP injections). A) Quantification of DMPK protein relative to tubulin in CD-1 mice (the ratio of control group set as 1). Mean ± SEM (bars) of 1 experiment (n= 3 animals) [1.2mg/kg n=2]. B) Representative western blot.

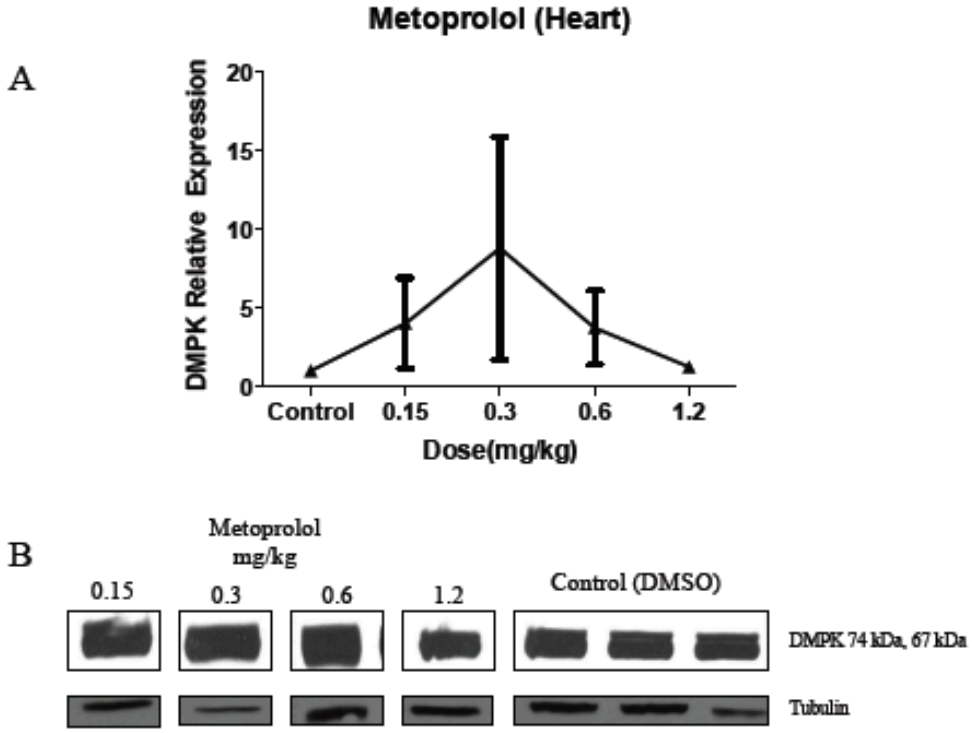

Figure 24 - Metoprolol treatment does not affect DMPK protein levels in heart tissue.

Metoprolol treatment resulted in no observable decrease in total DMPK protein levels. CD-1 mice were treated with metoprolol for 5 days (daily IP injections). A) Quantification of DMPK protein relative to tubulin in CD-1 mice (the ratio of control group set as 1). Mean ± SEM (bars) of 1 experiment (n= 3 animals). B) Representative western blot.

One finding we have observed from this phase of research is the need for the inclusion of a multitude of cell lines during screening as the apparent discord between our *in vitro* and *in vivo* results highlight. For future screening protocols of this nature it may be wise to increase the number of cell types the screen is conducted on to ensure that compounds are not missed, due to the inability of a given cell line to respond to them.

3.2 Assessment of Connectivity Map screen to identify compound capable of increasing a transcript of interest (Utrophin)

3.2.1 Initial Screen for Utrophin suppressing compounds

We next investigated whether Connectivity Map data would be useful in identifying agents which up regulate transcripts (in contrast to the DMPK mRNA down regulation), in this case a compound capable of up regulating the utrophin mRNA transcript as a potential therapy for Duchenne muscular dystrophy (DMD). The Connectivity Map had two builds for utrophin, as they did for DMPK, and we organized our data in a similar manner only this time ranking for compounds that up regulate our transcript of interest. Sixteen compounds which induced utrophin mRNA levels were identified in this manner (**Table 2**). Included in these compounds were three translational inhibitors which have also been implicated in activation of the p38 kinase; cycloheximide, anisomycin, and emetine (Sampieri et al., 2008; Islam et al., 2006). Additional compounds with p38 activation potential (Vitamin D, VPAC2, and celecoxib) were thus included for preliminary utrophin inducing assessment. In addition the STAT5 activator Prolactin, which our lab is currently working with looking for potential

treatments for Spinal Muscular Atrophy (SMA) was included in our assessment (Farooq et al., 2009).

Table 2 - Table summarizing mid-throughput qPCR screen for Utrophin inducers.

Each individual drugs class and optimal induction at both time points are listed as identified through this initial screen. Where available therapeutic serum levels obtained in human patients have been provided. Connectivity map data indicates the original fold expression values provided by the Broad Institute used in initially ranking the compounds. Those compounds marked with an asterix denote compounds which elicited cell death at one of the concentrations tested.

Drug	Drug Class	Utrophin mRNA level		
		Connectivity Map data (MCF7, HELA, PC3 cells)	Preliminary validation (C2C12) n=3	
		10uM, 6 hours(Fold Expression)	Optimal up regulation (Fold Expression)	
			4 hours	16 hours
Anisomycin	Protein synthesis inhibitor/p38 activator	1.5	1.15 (1nM)	52.95 (1nM)
Emetine	Protein synthesis inhibitor/p38 activator	1.47	1.24 (1nM)	0.77 (50nM)
Cycloheximide	Protein synthesis inhibitor/p38 activator	1.45	Extremely toxic	Extremely toxic
1,5 iosquinolinediol	Poly(ADP-ribose) synthetase inhibitor	1.45	0.93 (25uM)	0.79 (10uM)
Calmidazolium	Calmodulin antagonist	1.4	1.52 (50nM)	0.8 (1uM)
Chloroxazone	Skeletal muscle relaxant	1.4	0.59 (1uM)	0.15 (25uM)
Chelidonine	Poly(ADP-ribose) synthetase inhibitor	1.38	1.27 (1uM)	1.11 (50nM)
Linocomycin	Protein synthesis inhibitor(Antibiotic)	1.38	2.12 (1uM)	0.68 (1uM)
Loxapine	Antipsychotic	1.38	0.81 (1uM)	0.48 (25uM)
Tacrine	Cholinesteraase inhibitor	1.36	0.78 (25uM)	
Adiphenine	Smooth muscle relaxant	1.31	1.25 (50nM)	1.06 (1uM)
Benzebromarone	Uricosic agent	1.3	29.75 (25uM)	1.02 (10uM)
Biotin	Vitamin B7	1.3	1.11 (10uM)	0.71 (1uM)
Dapsone	Sulfone antibiotic	1.3	1.14 (25uM)	0.56 (50nM)
Nimelsulide	Cyclooxygenase-2 inhibitor	1.29	0.47 (25uM)	0.96 (50nM)
Canavanine	iNOS inhibitor	1.29	0.83 (10uM)	1.38 (50nM)
Biperiden*	Anticholinergenic	1.27	0.83 (1uM)	1.57(10uM)
Vitamin D	Vitamin	NA	0.68 (6.25nM)	0.56 (0.625nM)
VPAC 2	Adenylate cyclase activator(p38 activator)	NA	0.45 (26nM)	0.88(1uM)
Prolactin	Hormone, STAT5 activator	NA	0.54 (0.05mg/l)	0.59 (0.01mg/L)
Celecoxib	NSAID, cox-2 inhibitor	NA	2.1 (10uM)	0.70 (10uM)

3.2.2 Validation of Connectivity Map Screen

Our experience from the DMPK screen prompted us to increase the number of concentrations investigated to four (50nM, 1uM, 10uM, 25uM) at 4 and 16 hours for each compound. In this manner we identified a number of compounds (anisomycin, lincomycin, benzbromarone, calmidazolium, and celecoxib) which appeared to up regulate utrophin consistently (**Table 2, Supplemental figures 21-40**). Two of the p38 inducing compounds (celecoxib and anisomycin) passed this initial phase of verification, suggesting a possible role in the p38 pathway in utrophin induction.

3.2.3 Secondary Validation of Connectivity Map Screen for Utrophin Inducers

3.2.3.1 Celecoxib verification and dose response generation

A further dose finding analysis (50nM, 1, 10, 25uM; 4, 16 h) was next undertaken. The greatest celecoxib mediated increase in C2C12 utrophin mRNA (1.97 fold, $p<0.05$) was observed at 4 hours at 10 uM (**Fig. 25**). This effect was largely lost after 16 hours, although we did see occasional induction between trials (**Fig. 25**).

Celecoxib also conferred C2C12 utrophin protein induction at 24 hours (1.8x increase, p=0.11 **Fig. 26**) although this increase was mediated by the lower concentrations of celecoxib (0.1uM, 1uM) than that which induced the mRNA at 4 hours (10uM).

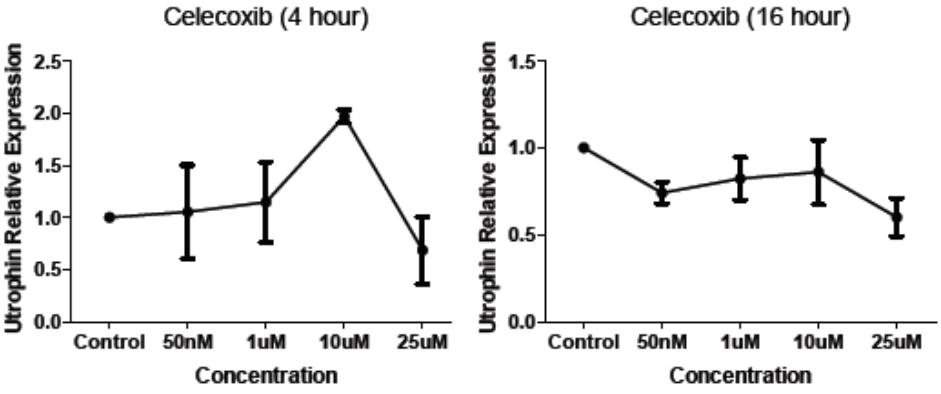

Figure 25 - Celecoxib up regulates Utrophin mRNA *in vitro*.

Celecoxib (10uM) treatment results in a 1.97 fold induction ($p<0.05$) in utrophin mRNA levels following 4 hours of treatment and analysis of mRNA extracts by qPCR. Quantification of utrophin mRNA relative to β-2-Microglobulin in C2C12 cells (the ratio of control group set as 1). Mean ± SEM (bars) of 3 independent experiments for both 4 hour (treated n=9, control n=14) and 16 hours (treated n=9, control n =21).

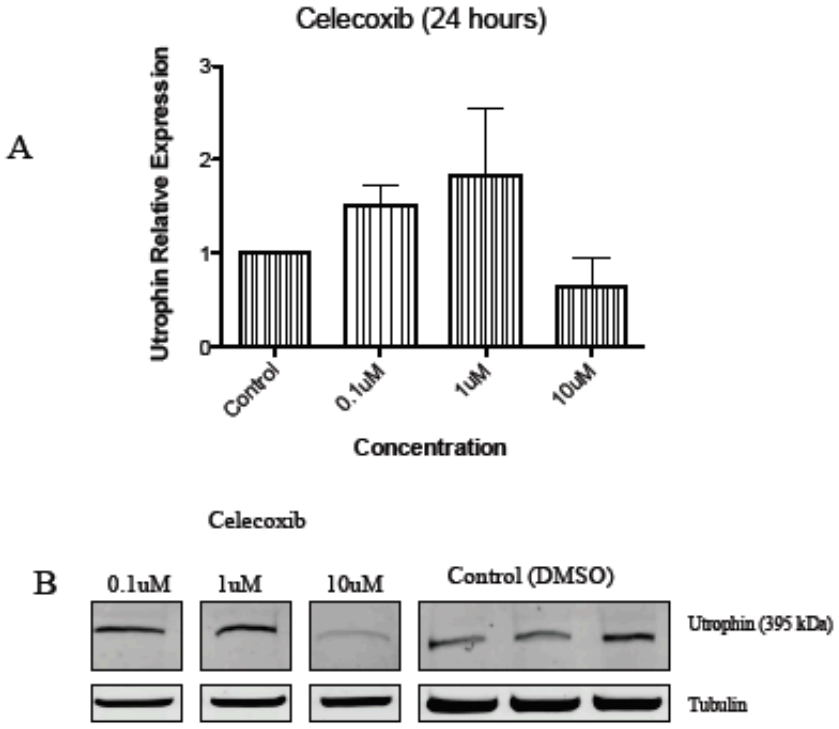

Figure 26 - Celecoxib induces utrophin protein *in vitro*.

Celecoxib treatment resulted in non - significant increase in utrophin protein (1.8 fold, p=0.11). A) Quantification of DMPK protein relative to tubulin from in C2C12 myoblasts (the ratio of control group set as 1) Mean ± SD (bars) of 3 independent experiments (treated n=3, control n=3). B) Representative western blot.

3.2.3.2 Benzbromarone verification and dose response generation

Increases in utrophin mRNA were observed following 4 hours of both 25uM (1.5x increase, $p<0.05$), and 10uM benzbromarone (1.99x increase, $p=0.07$) (**Fig. 27**). This effect was lost after 16 hours (**Fig. 27**). Utrophin protein levels in response to benzbromarone paralleled utrophin mRNA to a certain extent with 1.5x increase ($p=0.07$) observed at 10uM (**Fig. 28**).

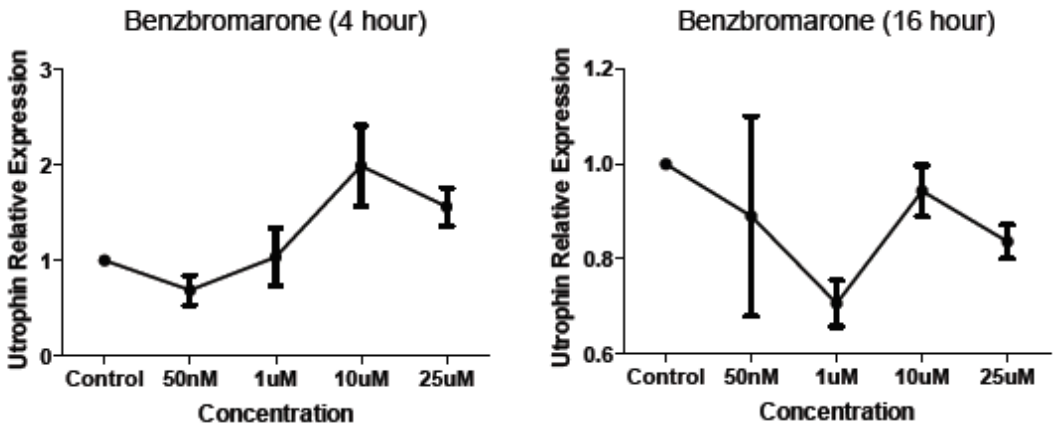

Figure 27 - Benzbromarone up regulates utrophin mRNA *in vitro*.

Benzbromarone (25uM) treatment results in a 1.5 fold induction ($p<0.05$) in utrophin mRNA levels following 4 hours of treatment and analysis of mRNA extracts by qPCR. Quantification of utrophin mRNA relative to β-2-Microglobulin in C2C12 cells (the ratio of control group set as 1). Mean ± SEM (bars) of 3 independent experiments for both 4 hour (treated n=9, control n=11) and 16 hours (treated n=9, control n =18).

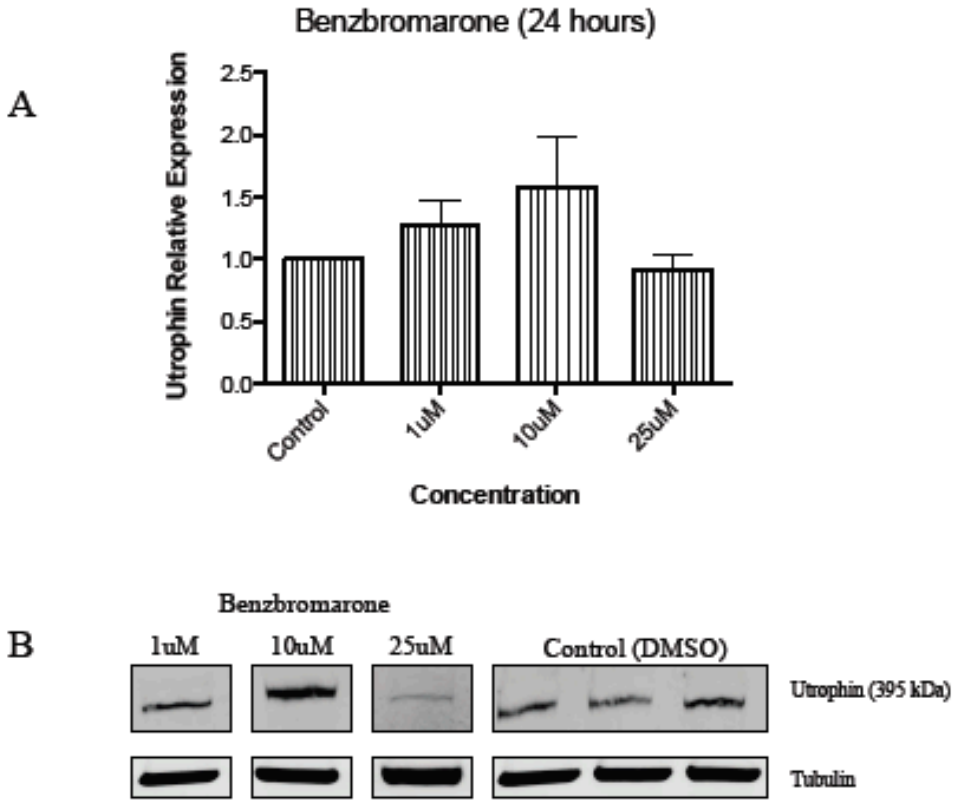

Figure 28 - Benzbromarone induces utrophin protein *in vitro*.

Benzbromarone treatment resulted in non - significant increase in utrophin protein (1.5 fold, p=0.07). A) Quantification of utrophin protein relative to tubulin from in C2C12 myoblasts (the ratio of control group set as 1) Mean ± SD (bars) of 3 independent experiments (treated n=3, control n=3). B) Representative western blot. Representative western blot.

3.2.3.3 Anisomycin, Lincomycin, Calmidazolium verification and dose response generation

Celecoxib and benzbromarone were the most effective utrophin inducing compounds identified by our screen with a more modest impact recorded for the other compounds: anisomycin (**Fig. 29, 30**), lincomycin (**Fig. 31, 32**), calmidazolium (**Fig. 33, 34**) all showed variable results. Anisomycin was only screened at two low concentrations due to cytotoxicity observed at higher concentrations. Following quantification, slight increases in utrophin protein in response to lincomycin, anisomycin, and calmidazolium were noted, although review of the blots show that the increases are not easily observable and may not be wholly accurate. Indeed wide variation between trials prevented any significant increases from being observed. Coupling this with the lack of an mRNA increase observed at those doses makes us hesitant to believe they are truly causing utrophin increase.

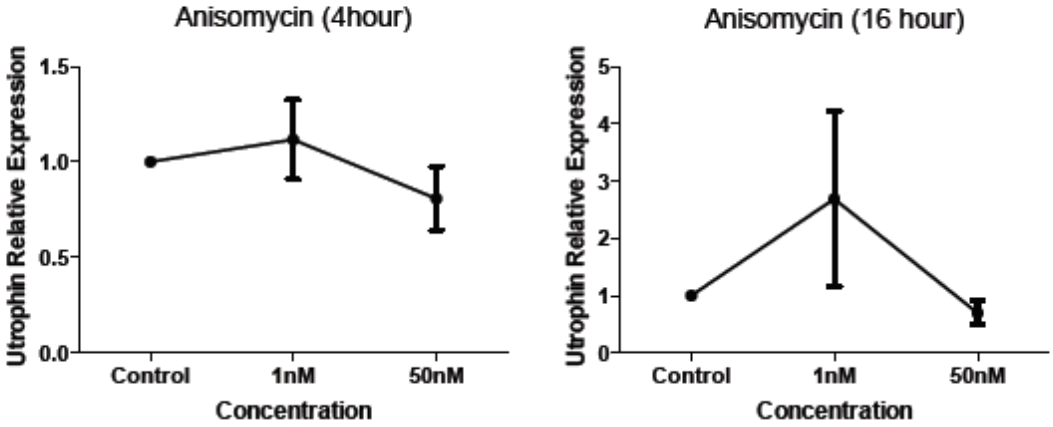

Figure 29 - Anisomycin does not affect utrophin mRNA *in vitro*.

No statistically significant increase in utrophin mRNA occurred following treatment with anisomycin analysis of mRNA extracts by qPCR. Quantification of Utrophin mRNA relative to β-2-Microglobulin in C2C12 cells (the ratio of control group set as 1). Mean ± SEM (bars) of 3 independent experiments for both 4 hour (treated n=9, control n=18) and 16 hours (treated n=9, control n =20).

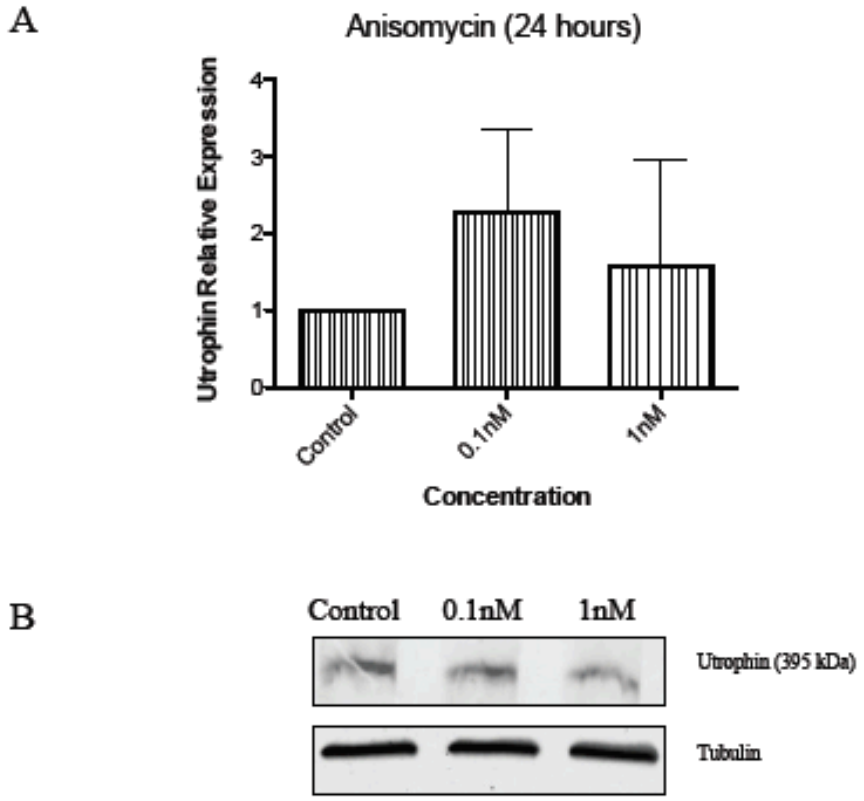

Figure 30 - Anisomycin treatment results in a non-significant increase in utrophin protein *in vitro*.

Anisomycin treatment resulted in no significant increase in utrophin protein in C2C12 myoblasts following 24 hour treatment. A) Quantification of DMPK protein relative to tubulin from in C2C12 myoblasts (the ratio of control group set as 1) (treated n=4, control n=4). B) Representative western blot.

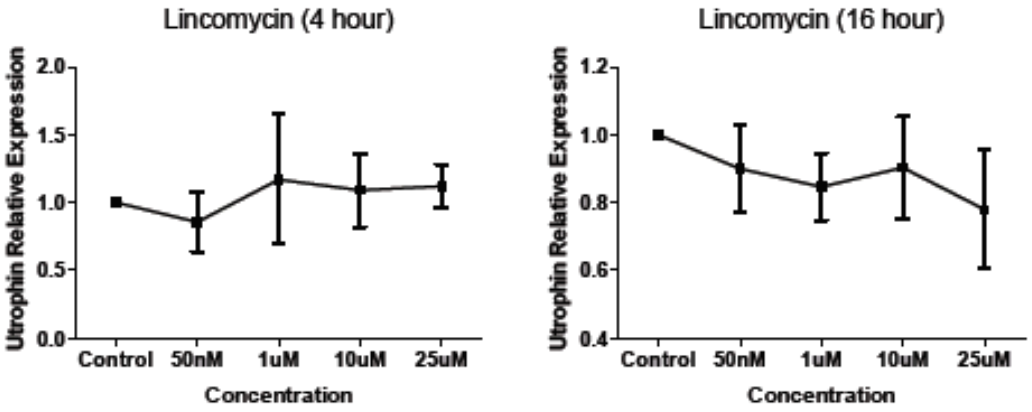

Figure 31 - Lincomycin does not affect utrophin mRNA *in vitro*.

No observable increase in utrophin RNA occurred following treatment with lincomycin and analysis of mRNA extracts by qPCR. Quantification of utrophin mRNA relative to β-2-Microglobulin in C2C12 cells (the ratio of control group set as 1). Mean ± SEM (bars) of 3 independent experiments for both 4 hour (treated n=9, control n=18) and 16 hours (treated n=9, control n =17).

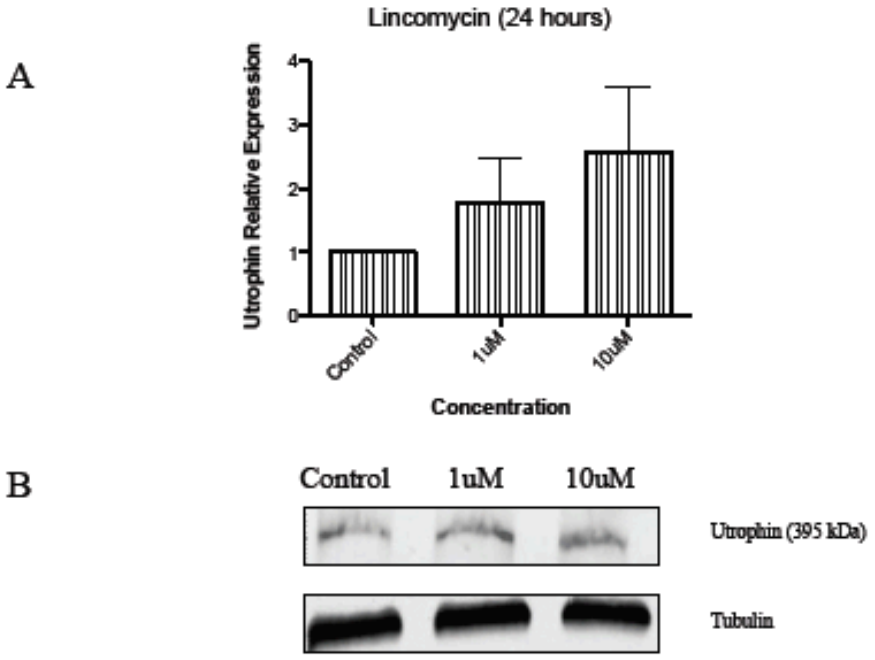

Figure 32 - Lincomycin treatment results in a non-significant increase in utrophin protein *in vitro*.

Lincomycin treatment results in no statistically significant induction of utrophin protein in C2C12 myoblasts following 24 hour treatment. A) Quantification of DMPK protein relative to tubulin from in C2C12 myoblasts (the ratio of control group set as 1) (treated n=4, control n=4). B) Representative western blot.

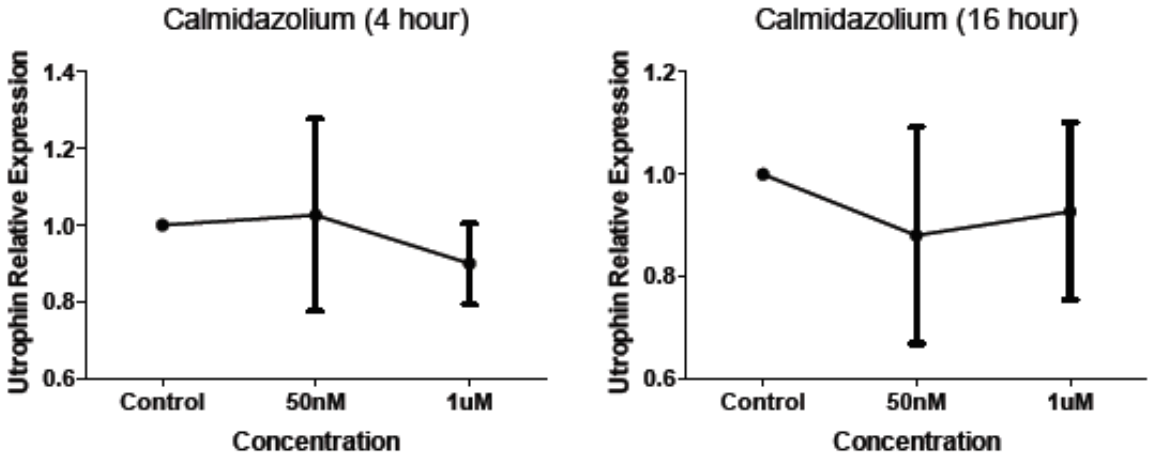

Figure 33 - Calmidazolium does not affect utrophin mRNA *in vitro*.

No observable increase in utrophin RNA occurred following treatment with calmidazolium. Quantification of Utrophin mRNA relative to β-2-Microglobulin in C2C12 cells (the ratio of control group set as 1). Mean ± SEM (bars) of 3 independent experiments for both 4 hour (treated n=9, control n=18) and 16 hours (treated n=9, control n =20).

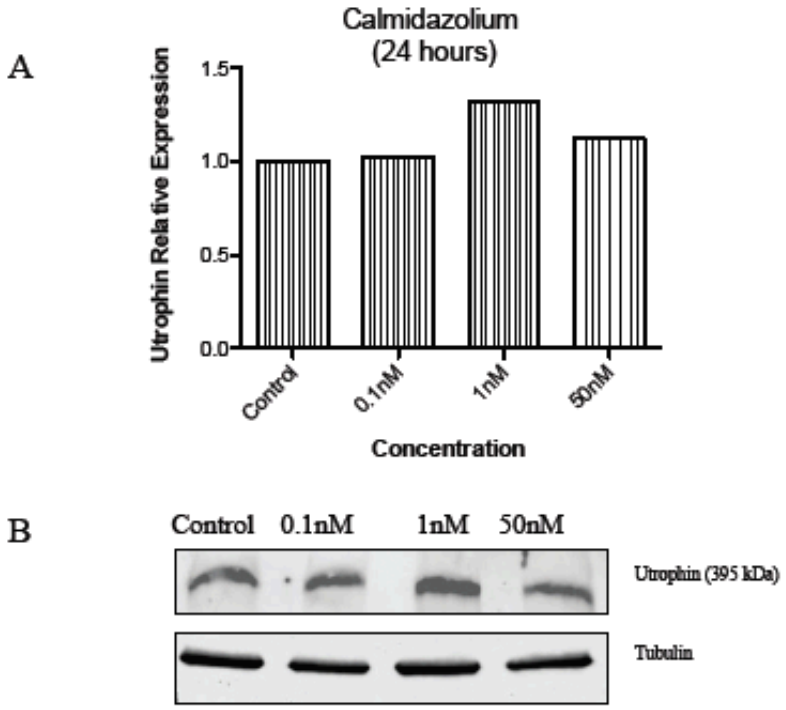

Figure 34 - Calmidazolium does not increase utrophin protein *in vitro*.

Calmidazolium treatment results in no statistically relevant increase in utrophin protein in C2C12 myoblasts following 24 hour treatment. A) Quantification of DMPK protein relative to tubulin from in C2C12 myoblasts (the ratio of control group set as 1) (treated n=1, control n=3). B) Representative western blot.

Chapter 4

4. Discussion

4.1 General Discussion

In addition to this study, our laboratory has had some prior success in mining *in silico* databases for the purposes of new rare disease treatment identification. Using a database compiled by Johnson & Johnson©**,** our lab has identified the role of the p38 kinase pathway in activating the spinal muscular atrophy (SMA) modulating SMN2 gene (Farooq et al., 2009). The purpose of the current study was to determine if using other databases (The Connectivity Map) could yield similarly successful results. Myotonic dystrophy and Duchenne muscular dystrophy represent two ideal candidate diseases upon which to perform such an analysis particularly as they represent opposite scenarios, i.e. requiring an up or down regulation of a transcript respectively.

Although we focus here on results from the Connectivity Map database, we believe that this approach will be broadly generalizable utilizing similar databases either from academic centers or pharmaceutical companies. By analyzing the Connectivity Map data for candidate compounds we hoped to not only validate data from the Connectivity Map itself as a useful screening tool, but increase our level of understanding about the effectiveness and usefulness of these types of databases in drug discovery. The benefits of this type of discovery have already been discussed earlier.

4.2 *In silico* mining

Over the course of the project, we have made two observations which hold true for both diseases studied. The first is that the agents identified usually have more effect on the transcripts in the short term (4 hours) compared with the long term (16-24 hours). The brevity of this effect may be true of the impact most small molecules have on most transcript levels or it may be that given the Connectivity Map read-out is at 6 hours, the assay is biased towards drugs which act rapidly and for a limited time only. Given that the Connectivity Map data may preferentially identify those compounds which act quickly on a transcript, it may also be that the chief mechanism shall involve modulation of transcript stability and not of transcription rates themselves; i.e. this approach will identify transcript stabilizers/destabilizers more readily than drugs which modulate transcription rates. This naturally is contingent upon the length of time it takes to transcribe a gene and here estimates of gene transcription times range widely from as little as under two hours for utrophin ((Singh and Padgett, 2009)) and as high as 16 hours for Dystrophin ((Tennyson et al., 1995)). If the shorter transcription time is accurate, it is possible that a 6 hour trial will encompass both transcriptional repressors/activators as well as stabilizers/degraders.

Regardless, given the single time point/single dose nature of the Connectivity Map data, it may be that there are either slower acting drugs or ones which act at concentrations greater or less than 10uM that are not being detected in our current approach. For example, although the half life of a given drug in a whole organism is often comparatively brief as a result of hepatic uptake and general metabolism, there is the possibility that some compounds exert their effect on a long term basis, necessitating

constant administration to get the desired effect. Despite such a possibility, we believe that less than 100% ascertainment is a fact of most if not all screens of this nature and the value of identifying some drugs with a true effect outweighs the risk of missing others.

The second general observation that we made was that while our analysis is an effective method of identifying agents which modulate mRNA, as anticipated, protein modulation does not always faithfully mirror the mRNA changes. As was discussed previously this imperfect relationship has been observed elsewhere (Tian et al., 2004). Indeed it appears more likely (45% of proteins studied in one report (Tian et al., 2004)) that one will observe significant mRNA changes with no corresponding protein increases. As well, we believe that RNA screens may be more biased towards compounds capable of decreasing proteins than those which increase protein, given that the reduction of a transcript will likely have a higher probability of reducing protein expression than an increase in transcript will result in protein elevation.

4.3 Myotonic Dystrophy

The discovery of sodium channel blockers as effective DMPK modulators both *in vivo* and *in vitro* highlights the potential value of our screen for DMPK suppressors. Although the individual drugs identified in this manner appear to be efficient suppressors, we are particularly interested in the identification of the class of compounds as a whole. The use of the Connectivity Map data to elucidate this novel and unanticipated class effect of DMPK mRNA repression by sodium channel blocking is in our view a validation of this approach.

4.3.1 Sodium channel blockers; an established DM1 myotonia therapy

Interestingly a number of the sodium channel blockers we identified in this screen have already been used as DM1 treatments. Procainamide was identified as an effective anti-myotonia treatment in 1955 (Geshwind and Simpson, 1955). While the sodium channel blocking properties of the compound may account for the amelioration of myotonia, procainamide appears to treat other symptoms of DM1 as well, dyspnea (shortness of breath) being one example (Fitting and Leuenberger, 1989). It is conceivable that procainamide is decreasing the expanded DMPK mRNA resulting in this improvement. Mexiletine has also recently been recognized as an effective treatment for myotonia in DM1 patients (Logigian et al., 2010). In keeping with the broader effects seen with procainamide, a group in Rochester, NY report an impact on a number of DM1 signs and symptoms beyond myotonia, triggering their effort to have mexiletine re-labeled as a broader therapeutic for myotonic dystrophy (beyond its normal use as an anti-myotonia sodium channel blocker), (pers commun Dr. Chad Heatwole, Rochester: (Heatwole, 2011)). We have thus identified DMPK mRNA suppressing agents which may be being corroborated by experience in humans; confirmation is clearly needed starting with the assessment of both of DMPK mRNA levels as well as intranuclear RNA foci in the tissue of patients being treated with either sodium channel blocker.

Prilocaine was the most consistent DMPK suppressor, and could be the most effective DMPK suppressor in humans as well. Although the effect of procainamide and mexiletine on DM1 has been the subject of published reports, no analogous studies have been conducted utilizing prilocaine, possibly a result of the comparative toxicity of this

drug (Santa Cruz Biotechnology, 2011). Clinical trials will be needed to both establish prilocaine safety and whether the compound shows greater clinical efficacy than mexiletine and procainamide.

4.3.2 Role of sodium channel in DMPK suppression

The mechanism by which sodium channel blockers decrease DMPK is not known. C2C12 cells do appear to express skeletal muscle sodium channels (Na_v 1.4) and can be induced to express the cardiac muscle sodium channel (Na_v1.5) by culturing them in the presence of cardiomyocytes (Zebedin et al., 2007; Deschenes et al., 2002). Although this expression pattern is consistent with the involvement of these specific sodium channels in DMPK mRNA suppression more in depth studies must be conducted on C2C12 sodium channel expression to fully elucidate which channels are expressed in this cell line.

It is possible that the suppression of DMPK mRNA is occurring by a mechanism other than that of the sodium channel blockade. Procainamide, in particular, has been shown to modulate gene expression through its actions as an inhibitor of methyltransferases in certain cancers leading to the restoration of normal gene expression in cancer models of mice (Lin et al., 2001). However the diversity of mexiletine, procainamide and prilocaine, in addition to the fact that the sole trait they have in common (to our knowledge) is sodium channel blockade, makes it likely that it is this property that is responsible for DMPK mRNA reduction.

Interestingly DMPK itself appears to modulate sodium channel expression; DMPK knockout mice have a reduced concentration of sodium channels present in skeletal muscle (Mounsey et al., 2000). The reduced channels also appear more active as they are observed to be open more frequently and with longer bursts of activity (Mounsey et al., 2000). Furthermore, a direct interaction between the DMPK protein and sodium channels has been shown to occur whereby the kinase phosphorylates sodium channels, thereby decreasing their activity (Mounsey et al., 1995; Chahine and George, 1997).

One might therefore envision the following feedback mechanism: with the reduction in sodium channel activity, an attempt is made by the cell to offset this by blocking the inhibitory DMPK phosphorylation of sodium channel by rapidly reducing DMPK mRNA with the attendant drop in DMPK protein that we have shown. This is a credible negative feedback loop in which a reduction in channel inhibition results from a reduction in channel activity. Clearly the precise mechanism by which this may occur remains to be elucidated, although it is noteworthy that a link between sodium channel blockade and modulation of sodium channel alpha subunit mRNA has been previously observed (Duff et al., 1992).

The tissue specific response we observed in our treatment with prilocaine, mexiletine, and procainamide may represent another clue to the relationship between DMPK levels and sodium channel activity. Prilocaine and mexiletine both worked well as DMPK suppressors in skeletal muscle tissue (gastrocnemius) but failed to have any effect on DMPK levels in heart tissue. It has been observed that although DMPK appears

to modulate skeletal muscle expression of sodium channels (Nav 1.4), it has no effect on the sodium channel isoform (Nav 1.5) present in heart tissue (Chahine and George, 1997). There may exist an element of reciprocity then; only in tissues in which DMPK modulates sodium channel activity will blocking the sodium channel have an effect on DMPK mRNA and protein levels. Interestingly absent DMPK levels in mice result in mild cardiac defects (rhythm disturbances and conduction defects) later in life (Lee et al., 2003); if sodium channel blockers decreased cardiac DMPK, they might not be the effective treatments they are today as this would exacerbate the conditions they are being used to treat. In fact, mexiletine has been implicated in the up regulation of the cardiac sodium channel in rats given the drug on a long term basis (Kang et al., 1997).

It remains unclear why procainamide would work in heart tissue, however. One difference that does occur between these compounds is the type of sodium channel blocking signal they cause. Procainamide has been shown to block channels slowly and muscle is slower to recover from such a type of block (Ehring et al., 1988). Mexiletine and prilocaine, on the other hand, act to block channels quickly and muscle tissues also recovers from this block quickly as well (Ehring et al., 1988). Perhaps a long persistent presence of drug is what is needed to decrease DMPK in the heart. This absence of a long persistent signal might be heightened in healthy mice as mexiletine has been shown to affect sodium channel activity more in patients with arrhythmias than in healthy patients (Campbell et al., 1978; Cambell, 1998b). Mexiletine even appears to be metabolized more slowly in sick patients as heightened plasma levels have been observed in patients

versus healthy individuals administered the same amount of mexiletine (Woosley et al., 1984).

Sodium channel blocker specificity aside, it may simply be that the dose required to actually cause sodium channel blockage of cardiac muscle tissue is too high to be obtained effectively by these drugs. Indeed a study using the potent sodium channel blocker tetrodotoxin (TTX) found that the IC_{50} for cardiac tissue cells required a 400x greater dose of TTX than what was required to achieve the IC_{50} for skeletal muscle tissue (Clare et al., 2000). This was conceivably due to a single residue (Cys374) which is different between skeletal and cardiac sodium channels and confers resistance to blockage by TTX (Clare et al., 2000; Sivilotti et al., 1997).

4.3.3 Metoprolol mediated DMPK suppression

The mechanism by which metoprolol appears to be suppressing DMPK mRNA *in vivo* is not clear. Metoprolol is a β-blocker and similar compounds (Propanol) have been shown to interact and block sodium channels, specifically cardiac and neuronal voltage gated channels (Wang et al., 2010). Unfortunately the same study reported no blocking effect on these channels by metoprolol (Wang et al., 2010).

4.3.3 Myotonic dystrophy concluding thoughts and future directions

We have shown here a consistent decrease in DMPK mRNA levels in response to our candidate compounds at both *in vitro* and *in vivo* levels. The next phase of research

shall be to characterize these compounds effects on the pathogenic DMPK RNA. A potential limitation of our approach is the possibility for differences between the response of the disease and the wildtype transcript to the agents identified in the Connectivity Map. The lack of genetically and physiologically relevant faithful disease cell lines, and methods adaptable to a mid-throughput screening method, prevented us from being able to conduct a screen with cells containing the expanded transcript in a timely and cost efficient manner. With the observation that DM1 patients appear improved in response to these compounds, we have a reasonable expectation that DMPK mRNA suppression by the compounds ability will be identified (Logigian et al., 2010; Geshwind and Simpson, 1955; Fitting and Leuenberger, 1989). We believe that the observation by clinicians that these compounds improve patient symptoms supports our approach showing that we were able to identify a possible treatment option in a comparatively brief period of 18 months.

4.4 Duchenne Muscular Dystrophy (DMD)

In order to further make the case for the use of *in silico* screens for novel treatments in rare diseases we next analyzed DMD, a disease in which we would be trying to increase a transcript. Our observation of maximal DMPK suppression at concentrations higher and lower than the connectivity map's 10uM resulted in the inclusion of a larger number of screened concentrations (50nM, 1uM, 10uM, 25uM) during the DMD Connectivity Map verification phase. With the observation that the Connectivity Map data may be biased to detect fast acting drugs, we also lowered our second screening time point from 24 to 16 hours. This generated a significantly larger

workload, but the increase in sensitivity that we obtained for our assay by increasing the dosages was significant.

4.4.1 Possible role of p38 activation in utrophin mRNA stabilization

As was the case with our observation of sodium channel blockers down regulating DMPK, a class effect was also noted for DMD inducers; the translational inhibitors anisomycin, emetine, and cyclohexamide all up regulate utrophin **(Table 2**). In addition all three have been shown at lower doses to be activators of the p38 pathway (Sampieri et al., 2008; Islam et al., 2006) suggesting that this signaling cascade may play a role in utrophin induction.

Our lab has already had experience in activating the p38 pathway to induce a transcript of interest (SMN2) as a potential treatment for SMA (Farooq et al., 2009). SMA is caused by deletion of the SMN1 gene causing a loss of a protein vital for proper neuromuscular function. The disease is similar to DMD insofar as the induction of a homologous SMN2 gene can offset loss of SMN1 preventing or attenuating SMA severity. It has been shown that p38 activation can lead to the stabilization of mRNA which possess AU-rich elements (ARE) in their 3' un-translated region; this transcript stabilization may be accompanied by an increase in the expression of the protein encoded by the mRNA (Dean et al., 2004). Interestingly the utrophin transcript possess just such a AU-rich element **(Fig. 6)** (Chakkalakal et al., 2008). With the possibility that p38 activating compounds increase utrophin we decided to include a number of p38 activating

compounds identified within our own lab (celecoxib, vitamin D, and a VPAC-2 inhibitor; unpublished data: (Farooq and MacKenzie, 2010)) to our screen.

Following our initial screen it appeared as though the p38 activators (anisomycin and celecoxib) induced utrophin mRNA levels (**Table 2)**. Further verification of these compounds, however, showed no significant increase in utrophin mRNA or protein in response to anisomycin. There was, however, an increase in both mRNA and protein in response to celecoxib. The absence of significant utrophin protein induction in response to anisomycin suggests there may also be an inhibition of protein synthesis so that increases in transcript level are outweighed by translational inhibition. Although these compounds might not ultimately lead to a viable treatment option they do help validate the ability of the Connectivity Map to identify actual compounds capable of modulating transcripts.

4.4.2 Possible role of PPAR mediation activation in utrophin mRNA transcriptional activation

Benzbromarone is commonly used as a treatment for gout, and is both effective and well tolerated (Heel et al., 1977). It has also been shown to be a potent activator of peroxisome proliferator-activated receptors (PPAR) αand γ (Kunishima et al., 2007). It is noteworthy that there is PPRE responsive element present in the utrophin transcript (**Fig. 6)** and its modulation by PPAR-β/δ activators leads to increases of both utrophin mRNA and protein (Miura et al., 2009). There does appear to be a disconnect, however, between which PPAR activators modulate utrophin (β/δ) and which PPAR motifs benzbromarone

activates (α/γ) (Miura et al., 2009; Kunishima et al., 2007). Even with this potential disconnect we believe it is possible that benzbromarone is increasing utrophin levels through PPAR-γ activation because of two observations. First, benzbromarone has been shown to have optimal PPAR-γ activation at 10uM, while PPAR-α activation requires a much large dose (100uM) (Kunishima et al., 2007). This maximal PPAR-γ activation mirrors the optimal induction we have observed in utrophin in response to this concentration (**Fig. 27)**. Second, in addition to activating the p38 pathway, celecoxib has been shown to activate PPAR-γ specifically (Lopez-Parra et al., 2005). This observation that the concentration that results in optimal utrophin induction is the same concentration required for maximal PPAR-γ induction and that a second (unrelated) compound is capable of activating the same receptor suggests a role of PPAR-γ activation in utrophin induction.

4.4.3 DMD concluding thoughts and future directions

Similar to our experience in the DM1 screen, our screen for utrophin inducers has identified compounds that appear to regulate pathways and transcriptional activation sites that have been previously implicated in utrophin induction. Unlike DM1 wherein the causative mRNA is qualitatively different from the wild type mRNA used in our screen (and thus may respond differently to the putative DMPK mRNA suppressors), there is no difference between the utrophin transcript in our screen or the disease and so there may be a higher probability that compounds we have identified in wild type cells will lead to effective utrophin induction in animal models. Assessment of the effect of

benzbromarone and celecoxib on utrophin in the Mdx mice (DMD mouse model) is currently being undertaken.

4.5 Conclusions

Our unbiased drug screen has identified some agents which modulate pathways known to be have some potential therapeutic impact (e.g. sodium channel blockers and DM1; PPAR activators and utrophin induction) and others which offer novel approaches (p38 activation and utrophin levels).

Some obvious issues remain; for DM1 the main question is if our candidate compounds decrease pathogenically expanded DMPK mRNA, and for DMD it needs to be shown that the significant utrophin mRNA increases will lead to substantial protein expression *in vivo*. These concerns highlight the complexity and unpredictability of both how our genome works, and how changes in gene expression are modulated and what implications these changes have. In reality, screens based entirely on mRNA levels will likely be hit or miss when attempting to predict disease modifiers, especially when transcripts differ in the disease or protein, or when other downstream effects are desired. Nonetheless, until research methods allow us to assay protein, abnormal transcript variants or other disease specific assays in a high throughput manner microarrays measuring mRNA are likely our best tool for generating these types of databases. Screens based on mRNA levels also have their benefits. Although they may not always

represent the best screen to use on a specific disease they do represent the best method for generating a general database applicable to many diseases. Screens based on protein levels would completely neglect RNA/genetic based disorders. Screens based on mRNA levels, however, are applicable to disorders that occur through both protein and mRNA abnormalities and mutations. For this reason even if assays are developed similar to a microarray but for protein or other variables it is likely that mRNA screens will remain a very useful resource for *in silico* databases used for drug discovery.

With one of the goals of this study being to bypass a number of the lengthy, and expensive, phases of clinical research required for drug approval, actual approval for the use of these identified compounds is paramount to the success of this project. In addition, there are other avenues of research that this type of screening has spawned that would allow for new discoveries into the regulation of these diseases. For example, the discovery of sodium channel blockers, and possibly sodium channels themselves, as regulators of DMPK expression may lead to a better understanding of DM1 and the mechanisms through which DMPK expression in controlled. Even if the sodium channel blockers fail to be approved as effective treatments for DM1, our hope would be that advances in the understanding of the mechanisms of DMPK expression elucidated while these compounds were discovered could lead to new drug development, albeit ones that would need the standard lengthy approval process

In conclusion, the considerable number of compounds identified in this study, both for DM1 and DMD, currently in or entering into preclinical assessment in disease

models give us reason to expect a fairly prompt judgment and hopefully the identification of agents worthy of continued clinical exploration.

Success in these animal models may also enable better predictions of how drug identification from the Broad Institute, or similar *in silico* screens will ultimately lead to therapies for disease.

Chapter 5

5. References

Amack, J.D., S.R. Reagan, and M.S. Mahadevan. 2002. Mutant DMPK 3'-UTR transcripts disrupt C2C12 myogenic differentiation by compromising MyoD *J.Cell Biol.* 159:419-429.

Amann, K.J., A.W. Guo, and J.M. Ervasti. 1999. Utrophin lacks the rod domain actin binding activity of dystrophin *J.Biol.Chem.* 274:35375-35380.

Angus, L.M., J.V. Chakkalakal, A. Mejat, J.K. Eibl, G. Belanger, L.A. Megeney, E.R. Chin, L. Schaeffer, R.N. Michel, and B.J. Jasmin. 2005. Calcineurin-NFAT signaling, together with GABP and peroxisome PGC-1{alpha}, drives utrophin gene expression at the neuromuscular junction *Am.J.Physiol.Cell.Physiol.* 289:C908-17.

Arahata, K., and A.G. Engel. 1986. Monoclonal antibody analysis of mononuclear cells in myopathies. III: Immunoelectron microscopy aspects of cell-mediated muscle fiber injury *Ann.Neurol.* 19:112-125.

Arahata, K., and A.G. Engel. 1984. Monoclonal antibody analysis of mononuclear cells in myopathies. I: Quantitation of subsets according to diagnosis and sites of accumulation and demonstration and counts of muscle fibers invaded by T cells *Ann.Neurol.* 16:193-208.

Arthur, G.R., D.H. Scott, R.N. Boyes, and D.B. Scott. 1979. Pharmacokinetic and clinical pharmacological studies with mepivacaine and prilocaine *Br.J.Anaesth.* 51:481-485.

Atweh, G.F., and D. Loukopoulos. 2001. Pharmacological induction of fetal hemoglobin in sickle cell disease and beta-thalassemia *Semin.Hematol.* 38:367-373.

Banach, M., J. Rysz, A. Goch, D.P. Mikhailidis, and G.M. Rosano. 2008. The role of trimetazidine after acute myocardial infarction *Curr.Vasc.Pharmacol.* 6:282-291.

Beggs, A.H., M. Koenig, F.M. Boyce, and L.M. Kunkel. 1990. Detection of 98% of DMD/BMD gene deletions by polymerase chain reaction *Hum.Genet.* 86:45-48.

Bell, C.D., and P.E. Conen. 1968. Histopathological changes in Duchenne muscular dystrophy *J.Neurol.Sci.* 7:529-544.

Benders, A.A., P.J. Groenen, F.T. Oerlemans, J.H. Veerkamp, and B. Wieringa. 1997. Myotonic dystrophy protein kinase is involved in the modulation of the Ca2+ homeostasis in skeletal muscle cells *J.Clin.Invest.* 100:1440-1447.

Berul, C.I., C.T. Maguire, M.J. Aronovitz, J. Greenwood, C. Miller, J. Gehrmann, D. Housman, M.E. Mendelsohn, and S. Reddy. 1999. DMPK dosage alterations result in atrioventricular conduction abnormalities in a mouse myotonic dystrophy model *J.Clin.Invest.* 103:R1-7.

Blake, D.J., A. Weir, S.E. Newey, and K.E. Davies. 2002. Function and genetics of dystrophin and dystrophin-related proteins in muscle *Physiol.Rev.* 82:291-329.

Boyd, Y., V. Buckle, S. Holt, E. Munro, D. Hunter, and I. Craig. 1986. Muscular dystrophy in girls with X;autosome translocations *J.Med.Genet.* 23:484-490.

Boyd, Y., and V.J. Buckle. 1986. Cytogenetic heterogeneity of translocations associated with Duchenne muscular dystrophy *Clin.Genet.* 29:108-115.

Bradley, W.G., P. Hudgson, P.F. Larson, T.A. Papapetropoulos, and M. Jenkison. 1972. Structural changes in the early stages of Duchenne muscular dystrophy *J.Neurol.Neurosurg.Psychiatry.* 35:451-455.

Brook, J.D., M.E. McCurrach, H.G. Harley, A.J. Buckler, D. Church, H. Aburatani, K. Hunter, V.P. Stanton, J.P. Thirion, and T. Hudson. 1992. Molecular basis of myotonic dystrophy: expansion of a trinucleotide (CTG) repeat at the 3' end of a transcript encoding a protein kinase family member *Cell.* 68:799-808.

Brouwer, J.R., R. Willemsen, and B.A. Oostra. 2009. Microsatellite repeat instability and neurological disease. *BioEssays : News and Reviews in Molecular, Cellular and Developmental Biology.* 31:71-83.

Cambell, R. 1998a. *Cardiac Electrophysiology Review.* 2:194-196.

Cambell, R. 1998b. Mexiletine. *Cardiac Electrophysiology Review.* 2:194-196.

Campbell, N.P., J.G. Kelly, A.A. Adgey, and R.G. Shanks. 1978. The clinical pharmacology of mexiletine *Br.J.Clin.Pharmacol.* 6:103-108.

Canicio, J., P. Ruiz-Lozano, M. Carrasco, M. Palacin, K. Chien, A. Zorzano, and P. Kaliman. 2001. Nuclear factor kappa B-inducing kinase and Ikappa B kinase-alpha signal skeletal muscle cell differentiation *J.Biol.Chem.* 276:20228-20233.

Carrasco, M., J. Canicio, M. Palacin, A. Zorzano, and P. Kaliman. 2002. Identification of intracellular signaling pathways that induce myotonic dystrophy protein kinase expression during myogenesis *Endocrinology.* 143:3017-3025.

Chahine, M., and A.L. George Jr. 1997. Myotonic dystrophy kinase modulates skeletal muscle but not cardiac voltage-gated sodium channels *FEBS Lett.* 412:621-624.

Chakkalakal, J.V., P. Miura, G. Belanger, R.N. Michel, and B.J. Jasmin. 2008. Modulation of utrophin A mRNA stability in fast versus slow muscles via an AU-rich element and calcineurin signaling *Nucleic Acids Res.* 36:826-838.

Chakkalakal, J.V., M.A. Stocksley, M.A. Harrison, L.M. Angus, J. Deschenes-Furry, S. St-Pierre, L.A. Megeney, E.R. Chin, R.N. Michel, and B.J. Jasmin. 2003. Expression of utrophin A mRNA correlates with the oxidative capacity of skeletal muscle fiber types and is regulated by calcineurin/NFAT signaling *Proc.Natl.Acad.Sci.U.S.A.* 100:7791-7796.

Chao, D.S., J.R. Gorospe, J.E. Brenman, J.A. Rafael, M.F. Peters, S.C. Froehner, E.P. Hoffman, J.S. Chamberlain, and D.S. Bredt. 1996. Selective loss of sarcolemmal nitric oxide synthase in Becker muscular dystrophy *J.Exp.Med.* 184:609-618.

Charlet-B, N., R.S. Savkur, G. Singh, A.V. Philips, E.A. Grice, and T.A. Cooper. 2002. Loss of the muscle-specific chloride channel in type 1 myotonic dystrophy due to misregulated alternative splicing *Mol.Cell.* 10:45-53.

Clare, J.J., S.N. Tate, M. Nobbs, and M.A. Romanos. 2000. Voltage-gated sodium channels as therapeutic targets *Drug Discov.Today.* 5:506-520.

Clarke, M.S., R. Khakee, and P.L. McNeil. 1993. Loss of cytoplasmic basic fibroblast growth factor from physiologically wounded myofibers of normal and dystrophic muscle *J.Cell.Sci.* 106 (Pt 1):121-133.

Clerk, A., G.E. Morris, V. Dubowitz, K.E. Davies, and C.A. Sewry. 1993. Dystrophin-related protein, utrophin, in normal and dystrophic human fetal skeletal muscle *Histochem.J.* 25:554-561.

Coffey, A.J., R.G. Roberts, E.D. Green, C.G. Cole, R. Butler, R. Anand, F. Giannelli, and D.R. Bentley. 1992. Construction of a 2.6-Mb contig in yeast artificial chromosomes spanning the human dystrophin gene using an STS-based approach *Genomics.* 12:474-484.

Davis, B.M., M.E. McCurrach, K.L. Taneja, R.H. Singer, and D.E. Housman. 1997. Expansion of a CUG trinucleotide repeat in the 3' untranslated region of myotonic dystrophy protein kinase transcripts results in nuclear retention of transcripts *Proc.Natl.Acad.Sci.U.S.A.* 94:7388-7393.

Dean, J.L., G. Sully, A.R. Clark, and J. Saklatvala. 2004. The involvement of AU-rich element-binding proteins in p38 mitogen-activated protein kinase pathway-mediated mRNA stabilisation *Cell.Signal.* 16:1113-1121.

Dennis, C.L., J.M. Tinsley, A.E. Deconinck, and K.E. Davies. 1996. Molecular and functional analysis of the utrophin promoter *Nucleic Acids Res.* 24:1646-1652.

Deschenes, I., N. Neyroud, D. DiSilvestre, E. Marban, D.T. Yue, and G.F. Tomaselli. 2002. Isoform-specific modulation of voltage-gated Na(+) channels by calmodulin *Circ.Res.* 90:E49-57.

DiMasi, J.A., R.W. Hansen, and H.G. Grabowski. 2003. The price of innovation: new estimates of drug development. *J. Health. Econ.* 22:151-185.

Dimasi, J.A. 2001. Risks in new drug development: approval success rates for investigational drugs *Clin.Pharmacol.Ther.* 69:297-307.

DiMasi, J.A., R.W. Hansen, and H.G. Grabowski. 2003. The price of innovation: new estimates of drug development costs *J.Health Econ.* 22:151-185.

Dubowitz, V. 1978. Muscle disorders in childhood *Major Probl.Clin.Pediatr.* 16:iii-xiii, 1-282.

Duff, H.J., J. Offord, J. West, and W.A. Catterall. 1992. Class I and IV antiarrhythmic drugs and cytosolic calcium regulate mRNA encoding the sodium channel alpha subunit in rat cardiac muscle *Mol.Pharmacol.* 42:570-574.

Ebralidze, A., Y. Wang, V. Petkova, K. Ebralidse, and R.P. Junghans. 2004. RNA leaching of transcription factors disrupts transcription in myotonic dystrophy *Science.* 303:383-387.

Ehring, G.R., J.W. Moyer, and L.M. Hondeghem. 1988. Quantitative structure activity studies of antiarrhythmic properties in a series of lidocaine and procainamide derivatives *J.Pharmacol.Exp.Ther.* 244:479-492.

Emery, A.E. 1993. Duchenne Muscular Dystrophy. *In* Duchenne Muscular Dystrophy. Oxford Monographs on Medical Genetics, Oxford, UK. 392.

Fardaei, M., K. Larkin, J.D. Brook, and M.G. Hamshere. 2001. In vivo co-localisation of MBNL protein with DMPK expanded-repeat transcripts *Nucleic Acids Res.* 29:2766-2771.

Farooq, F., S. Balabanian, X. Liu, M. Holcik, and A. MacKenzie. 2009. p38 Mitogen-activated protein kinase stabilizes SMN mRNA through RNA binding protein HuR *Hum.Mol.Genet.* 18:4035-4045.

Farooq, F., and A. MacKenzie. 2010. Celebrex, VPAC-2, and Vitamin D increase SMN2 protein through p38 pathway induction.

Fisher, R., J.M. Tinsley, S.R. Phelps, S.E. Squire, E.R. Townsend, J.E. Martin, and K.E. Davies. 2001. Non-toxic ubiquitous over-expression of utrophin in the mdx mouse *Neuromuscul.Disord.* 11:713-721.

Fitting, J.W., and P. Leuenberger. 1989. Procainamide for dyspnea in myotonic dystrophy *Am.Rev.Respir.Dis.* 140:1442-1445.

Fu, Y.H., D.L. Friedman, S. Richards, J.A. Pearlman, R.A. Gibbs, A. Pizzuti, T. Ashizawa, M.B. Perryman, G. Scarlato, and R.G. Fenwick Jr. 1993. Decreased expression of myotonin-protein kinase messenger RNA and protein in adult form of myotonic dystrophy *Science.* 260:235-238.

Furling, D., G. Doucet, M.A. Langlois, L. Timchenko, E. Belanger, L. Cossette, and J. Puymirat. 2003. Viral vector producing antisense RNA restores myotonic dystrophy myoblast functions *Gene Ther.* 10:795-802.

Galvagni, F., S. Capo, and S. Oliviero. 2001. Sp1 and Sp3 physically interact and co-operate with GABP for the activation of the utrophin promoter *J.Mol.Biol.* 306:985-996.

Geshwind, N., and J.A. Simpson. 1955. Procaine amide in the treatment of myotonia *Brain.* 78:81-91.

Gilbert, R., J. Nalbantoglu, B.J. Petrof, S. Ebihara, G.H. Guibinga, J.M. Tinsley, A. Kamen, B. Massie, K.E. Davies, and G. Karpati. 1999. Adenovirus-mediated utrophin gene transfer mitigates the dystrophic phenotype of mdx mouse muscles *Hum.Gene Ther.* 10:1299-1310.

Gowers, W.R. 1886. A Manual of Diseases of the Nervous System. J. & A. Churchill, London.

Gramolini, A.O., L.M. Angus, L. Schaeffer, E.A. Burton, J.M. Tinsley, K.E. Davies, J.P. Changeux, and B.J. Jasmin. 1999. Induction of utrophin gene expression by heregulin in skeletal muscle cells: role of the N-box motif and GA binding protein *Proc.Natl.Acad.Sci.U.S.A.* 96:3223-3227.

Gramolini, A.O., E.A. Burton, J.M. Tinsley, M.J. Ferns, A. Cartaud, J. Cartaud, K.E. Davies, J.A. Lunde, and B.J. Jasmin. 1998. Muscle and neural isoforms of agrin increase utrophin expression in cultured myotubes via a transcriptional regulatory mechanism *J.Biol.Chem.* 273:736-743.

Gramolini, A.O., C.L. Dennis, J.M. Tinsley, G.S. Robertson, J. Cartaud, K.E. Davies, and B.J. Jasmin. 1997. Local transcriptional control of utrophin expression at the neuromuscular synapse *J.Biol.Chem.* 272:8117-8120.

Groenen, P.J., D.G. Wansink, M. Coerwinkel, W. van den Broek, G. Jansen, and B. Wieringa. 2000. Constitutive and regulated modes of splicing produce six major myotonic dystrophy protein kinase (DMPK) isoforms with distinct properties *Hum.Mol.Genet.* 9:605-616.

Gyrd-Hansen, M., T.O. Krag, A.G. Rosmarin, and T.S. Khurana. 2002. Sp1 and the ets-related transcription factor complex GABP alpha/beta functionally cooperate to activate the utrophin promoter *J.Neurol.Sci.* 197:27-35.

Harley, H.G., S.A. Rundle, W. Reardon, J. Myring, S. Crow, J.D. Brook, P.S. Harper, and D.J. Shaw. 1992. Unstable DNA sequence in myotonic dystrophy *Lancet.* 339:1125-1128.

Harmon, E.B., M.L. Harmon, T.D. Larsen, A.F. Paulson, and M.B. Perryman. 2008. Myotonic dystrophy protein kinase is expressed in embryonic myocytes and is required for myotube formation *Dev.Dyn.* 237:2353-2366.

Harper, P. 2001. Myotonic Dystrophy. W.B Saunders, London.

Heatwole, C.R. 2011. Personal Communication.

Heel, R.C., R.N. Brogden, T.M. Speight, and G.S. Avery. 1977. Benzbromarone: a review of its pharmacological properties and therapeutic use in gout and hyperuricaemia *Drugs.* 14:349-366.

Ho, T.H., N. Charlet-B, M.G. Poulos, G. Singh, M.S. Swanson, and T.A. Cooper. 2004. Muscleblind proteins regulate alternative splicing *EMBO J.* 23:3103-3112.

Hoffman, E.P., R.H. Brown Jr, and L.M. Kunkel. 1987. Dystrophin: the protein product of the Duchenne muscular dystrophy locus *Cell.* 51:919-928.

Hunter, A., C. Tsilfidis, G. Mettler, P. Jacob, M. Mahadevan, L. Surh, and R. Korneluk. 1992. The correlation of age of onset with CTG trinucleotide repeat amplification in myotonic dystrophy *J.Med.Genet.* 29:774-779.

Islam, Z., J.S. Gray, and J.J. Pestka. 2006. p38 Mitogen-activated protein kinase mediates IL-8 induction by the ribotoxin deoxynivalenol in human monocytes *Toxicol.Appl.Pharmacol.* 213:235-244.

Jansen, G., P. Willems, M. Coerwinkel, W. Nillesen, H. Smeets, L. Vits, C. Howeler, H. Brunner, and B. Wieringa. 1994. Gonosomal mosaicism in myotonic dystrophy patients: involvement of mitotic events in (CTG)n repeat variation and selection against extreme expansion in sperm *Am.J.Hum.Genet.* 54:575-585.

Jennekens, F.G., L.P. ten Kate, M. de Visser, and A.R. Wintzen. 1991. Diagnostic criteria for Duchenne and Becker muscular dystrophy and myotonic dystrophy *Neuromuscul.Disord.* 1:389-391.

Jiang, H., A. Mankodi, M.S. Swanson, R.T. Moxley, and C.A. Thornton. 2004. Myotonic dystrophy type 1 is associated with nuclear foci of mutant RNA, sequestration of muscleblind proteins and deregulated alternative splicing in neurons *Hum.Mol.Genet.* 13:3079-3088.

Jin, S., M. Shimizu, A. Balasubramanyam, and H.F. Epstein. 2000. Myotonic dystrophy protein kinase (DMPK) induces actin cytoskeletal reorganization and apoptotic-like blebbing in lens cells *Cell Motil.Cytoskeleton.* 45:133-148.

Kaliman, P., and E. Llagostera. 2008. Myotonic dystrophy protein kinase (DMPK) and its role in the pathogenesis of myotonic dystrophy 1 *Cell.Signal.* 20:1935-1941.

Kalsotra, A., X. Xiao, A.J. Ward, J.C. Castle, J.M. Johnson, C.B. Burge, and T.A. Cooper. 2008. A postnatal switch of CELF and MBNL proteins reprograms alternative splicing in the developing heart *Proc.Natl.Acad.Sci.U.S.A.* 105:20333-20338.

Kanadia, R.N., K.A. Johnstone, A. Mankodi, C. Lungu, C.A. Thornton, D. Esson, A.M. Timmers, W.W. Hauswirth, and M.S. Swanson. 2003. A muscleblind knockout model for myotonic dystrophy *Science.* 302:1978-1980.

Kanadia, R.N., J. Shin, Y. Yuan, S.G. Beattie, T.M. Wheeler, C.A. Thornton, and M.S. Swanson. 2006. Reversal of RNA missplicing and myotonia after muscleblind overexpression in a mouse poly(CUG) model for myotonic dystrophy *Proc.Natl.Acad.Sci.U.S.A.* 103:11748-11753.

Kang, J.X., Y. Li, and A. Leaf. 1997. Regulation of sodium channel gene expression by class I antiarrhythmic drugs and n - 3 polyunsaturated fatty acids in cultured neonatal rat cardiac myocytes *Proc.Natl.Acad.Sci.U.S.A.* 94:2724-2728.

Khurana, T.S., and K.E. Davies. 2003. Pharmacological strategies for muscular dystrophy *Nat.Rev.Drug Discov.* 2:379-390.

Khurana, T.S., A.G. Rosmarin, J. Shang, T.O. Krag, S. Das, and S. Gammeltoft. 1999. Activation of utrophin promoter by heregulin via the ets-related transcription factor complex GA-binding protein alpha/beta *Mol.Biol.Cell.* 10:2075-2086.

Khurana, T.S., S.C. Watkins, P. Chafey, J. Chelly, F.M. Tome, M. Fardeau, J.C. Kaplan, and L.M. Kunkel. 1991. Immunolocalization and developmental expression of dystrophin related protein in skeletal muscle *Neuromuscul.Disord.* 1:185-194.

Kleopa, K.A., A. Drousiotou, E. Mavrikiou, A. Ormiston, and T. Kyriakides. 2006. Naturally occurring utrophin correlates with disease severity in Duchenne muscular dystrophy *Hum.Mol.Genet.* 15:1623-1628.

Klesert, T.R., D.H. Cho, J.I. Clark, J. Maylie, J. Adelman, L. Snider, E.C. Yuen, P. Soriano, and S.J. Tapscott. 2000. Mice deficient in Six5 develop cataracts: implications for myotonic dystrophy *Nat.Genet.* 25:105-109.

Koenig, M., A.H. Beggs, M. Moyer, S. Scherpf, K. Heindrich, T. Bettecken, G. Meng, C.R. Muller, M. Lindlof, and H. Kaariainen. 1989. The molecular basis for Duchenne versus Becker muscular dystrophy: correlation of severity with type of deletion *Am.J.Hum.Genet.* 45:498-506.

Koenig, M., E.P. Hoffman, C.J. Bertelson, A.P. Monaco, C. Feener, and L.M. Kunkel. 1987. Complete cloning of the Duchenne muscular dystrophy (DMD) cDNA and preliminary genomic organization of the DMD gene in normal and affected individuals *Cell.* 50:509-517.

Koenig, M., and L.M. Kunkel. 1990. Detailed analysis of the repeat domain of dystrophin reveals four potential hinge segments that may confer flexibility *J.Biol.Chem.* 265:4560-4566.

Koenig, M., A.P. Monaco, and L.M. Kunkel. 1988. The complete sequence of dystrophin predicts a rod-shaped cytoskeletal protein *Cell.* 53:219-228.

Koshelev, M., S. Sarma, R.E. Price, X.H. Wehrens, and T.A. Cooper. 2010. Heart-specific overexpression of CUGBP1 reproduces functional and molecular abnormalities of myotonic dystrophy type 1 *Hum.Mol.Genet.* 19:1066-1075.

Kunishima, C., I. Inoue, T. Oikawa, H. Nakajima, T. Komoda, and S. Katayama. 2007. Activating effect of benzbromarone, a uricosuric drug, on peroxisome proliferator-activated receptors *PPAR Res.* 2007:36092.

Kuyumcu-Martinez, N.M., G.S. Wang, and T.A. Cooper. 2007. Increased steady-state levels of CUGBP1 in myotonic dystrophy 1 are due to PKC-mediated hyperphosphorylation *Mol.Cell.* 28:68-78.

Lam, L.T., Y.C. Pham, T.M. Nguyen, and G.E. Morris. 2000. Characterization of a monoclonal antibody panel shows that the myotonic dystrophy protein kinase, DMPK, is expressed almost exclusively in muscle and heart *Hum.Mol.Genet.* 9:2167-2173.

Lamb, J. 2007. The Connectivity Map: a new tool for biomedical research *Nat.Rev.Cancer.* 7:54-60.

Lamb, J., E.D. Crawford, D. Peck, J.W. Modell, I.C. Blat, M.J. Wrobel, J. Lerner, J.P. Brunet, A. Subramanian, K.N. Ross, M. Reich, H. Hieronymus, G. Wei, S.A. Armstrong, S.J. Haggarty, P.A. Clemons, R. Wei, S.A. Carr, E.S. Lander, and T.R. Golub. 2006. The Connectivity Map: using gene-expression signatures to connect small molecules, genes, and disease *Science.* 313:1929-1935.

Langlois, M.A., C. Boniface, G. Wang, J. Alluin, P.M. Salvaterra, J. Puymirat, J.J. Rossi, and N.S. Lee. 2005. Cytoplasmic and nuclear retained DMPK mRNAs are targets for RNA interference in myotonic dystrophy cells *J.Biol.Chem.* 280:16949-16954.

Le Mee, G., N. Ezzeddine, M. Capri, and O. Ait-Ahmed. 2008. Repeat length and RNA expression level are not primary determinants in CUG expansion toxicity in Drosophila models *PLoS One.* 3:e1466.

Lee, H.C., M.K. Patel, D.J. Mistry, Q. Wang, S. Reddy, J.R. Moorman, and J.P. Mounsey. 2003. Abnormal Na channel gating in murine cardiac myocytes deficient in myotonic dystrophy protein kinase *Physiol.Genomics.* 12:147-157.

Lee, J.E., and T.A. Cooper. 2009. Pathogenic mechanisms of myotonic dystrophy *Biochem.Soc.Trans.* 37:1281-1286.

Lenk, U., R. Hanke, H. Thiele, and A. Speer. 1993. Point mutations at the carboxy terminus of the human dystrophin gene: implications for an association with mental retardation in DMD patients *Hum.Mol.Genet.* 2:1877-1881.

Liang, K.W., M. Nishikawa, F. Liu, B. Sun, Q. Ye, and L. Huang. 2004. Restoration of dystrophin expression in mdx mice by intravascular injection of naked DNA containing full-length dystrophin cDNA *Gene Ther.* 11:901-908.

Liechti-Gallati, S., M. Koenig, L.M. Kunkel, D. Frey, E. Boltshauser, V. Schneider, S. Braga, and H. Moser. 1989. Molecular deletion patterns in Duchenne and Becker type muscular dystrophy *Hum.Genet.* 81:343-348.

Lin, S., and J.M. Burgunder. 2000. Utrophin may be a precursor of dystrophin during skeletal muscle development *Brain Res.Dev.Brain Res.* 119:289-295.

Lin, X., K. Asgari, M.J. Putzi, W.R. Gage, X. Yu, B.S. Cornblatt, A. Kumar, S. Piantadosi, T.L. DeWeese, A.M. De Marzo, and W.G. Nelson. 2001. Reversal of GSTP1 CpG island hypermethylation and reactivation of pi-class glutathione S-transferase (GSTP1) expression in human prostate cancer cells by treatment with procainamide *Cancer Res.* 61:8611-8616.

Lin, X., J.W. Miller, A. Mankodi, R.N. Kanadia, Y. Yuan, R.T. Moxley, M.S. Swanson, and C.A. Thornton. 2006. Failure of MBNL1-dependent post-natal splicing transitions in myotonic dystrophy *Hum.Mol.Genet.* 15:2087-2097.

Liquori, C.L., K. Ricker, M.L. Moseley, J.F. Jacobsen, W. Kress, S.L. Naylor, J.W. Day, and L.P. Ranum. 2001. Myotonic dystrophy type 2 caused by a CCTG expansion in intron 1 of ZNF9 *Science.* 293:864-867.

Logigian, E.L., W.B. Martens, R.T. Moxley 4th, M.P. McDermott, N. Dilek, A.W. Wiegner, A.T. Pearson, C.A. Barbieri, C.L. Annis, C.A. Thornton, and R.T. Moxley 3rd. 2010. Mexiletine is an effective antimyotonia treatment in myotonic dystrophy type 1 *Neurology.* 74:1441-1448.

Lopez-Parra, M., J. Claria, E. Titos, A. Planaguma, M. Parrizas, J.L. Masferrer, W. Jimenez, V. Arroyo, F. Rivera, and J. Rodes. 2005. The selective cyclooxygenase-2 inhibitor celecoxib modulates the formation of vasoconstrictor eicosanoids and activates PPARgamma. Influence of albumin *J.Hepatol.* 42:75-81.

Love, D.R., D.F. Hill, G. Dickson, N.K. Spurr, B.C. Byth, R.F. Marsden, F.S. Walsh, Y.H. Edwards, and K.E. Davies. 1989. An autosomal transcript in skeletal muscle with homology to dystrophin *Nature.* 339:55-58.

Lu, Q.L., A. Rabinowitz, Y.C. Chen, T. Yokota, H. Yin, J. Alter, A. Jadoon, G. Bou-Gharios, and T. Partridge. 2005. Systemic delivery of antisense oligoribonucleotide restores dystrophin expression in body-wide skeletal muscles *Proc.Natl.Acad.Sci.U.S.A.* 102:198-203.

MacLennan, P.A., A. McArdle, and R.H. Edwards. 1991. Effects of calcium on protein turnover of incubated muscles from mdx mice *Am.J.Physiol.* 260:E594-8.

Magana, J.J., and B. Cisneros. 2011. Perspectives on gene therapy in myotonic dystrophy type 1 *J.Neurosci.Res.* 89:275-285.

Mankodi, A., E. Logigian, L. Callahan, C. McClain, R. White, D. Henderson, M. Krym, and C.A. Thornton. 2000. Myotonic dystrophy in transgenic mice expressing an expanded CUG repeat *Science.* 289:1769-1773.

Mankodi, A., M.P. Takahashi, H. Jiang, C.L. Beck, W.J. Bowers, R.T. Moxley, S.C. Cannon, and C.A. Thornton. 2002. Expanded CUG repeats trigger aberrant splicing of ClC-1 chloride channel pre-mRNA and hyperexcitability of skeletal muscle in myotonic dystrophy *Mol.Cell.* 10:35-44.

Mankodi, A., P. Teng-Umnuay, M. Krym, D. Henderson, M. Swanson, and C.A. Thornton. 2003. Ribonuclear inclusions in skeletal muscle in myotonic dystrophy types 1 and 2 *Ann.Neurol.* 54:760-768.

McCarthy, J.J., K.A. Esser, and F.H. Andrade. 2007. MicroRNA-206 is overexpressed in the diaphragm but not the hindlimb muscle of mdx mouse *Am.J.Physiol.Cell.Physiol.* 293:C451-7.

McDouall, R.M., M.J. Dunn, and V. Dubowitz. 1990. Nature of the mononuclear infiltrate and the mechanism of muscle damage in juvenile dermatomyositis and Duchenne muscular dystrophy *J.Neurol.Sci.* 99:199-217.

McKusick-Nathans Institute of Genetic Medicine, Johns Hopkins University (Baltimore, MD) and National Center for Biotechnology Information, National Library of Medicine (Bethesda, MD). Online Mendelian Inheritance in Man, OMIM (TM). http://www.ncbi.nlm.nih.gov/omim/. 2011.

Med Scape. 2001. The Drug Approval Process: Drug Development. {http://www.medscape.com/viewarticle/405869_4}. 2011:1.

Miller, J.W., C.R. Urbinati, P. Teng-Umnuay, M.G. Stenberg, B.J. Byrne, C.A. Thornton, and M.S. Swanson. 2000. Recruitment of human muscleblind proteins to (CUG)(n) expansions associated with myotonic dystrophy *EMBO J.* 19:4439-4448.

Miura, P., J.V. Chakkalakal, L. Boudreault, G. Belanger, R.L. Hebert, J.M. Renaud, and B.J. Jasmin. 2009. Pharmacological activation of PPARbeta/delta stimulates utrophin A expression in skeletal muscle fibers and restores sarcolemmal integrity in mature mdx mice *Hum.Mol.Genet.* 18:4640-4649.

Miura, P., and B.J. Jasmin. 2006. Utrophin upregulation for treating Duchenne or Becker muscular dystrophy: how close are we? *Trends Mol.Med.* 12:122-129.

Monaco, A.P., C.J. Bertelson, C. Colletti-Feener, and L.M. Kunkel. 1987. Localization and cloning of Xp21 deletion breakpoints involved in muscular dystrophy *Hum.Genet.* 75:221-227.

Monaco, A.P., R.L. Neve, C. Colletti-Feener, C.J. Bertelson, D.M. Kurnit, and L.M. Kunkel. 1986. Isolation of candidate cDNAs for portions of the Duchenne muscular dystrophy gene *Nature.* 323:646-650.

Monaco, A.P., A.P. Walker, I. Millwood, Z. Larin, and H. Lehrach. 1992. A yeast artificial chromosome contig containing the complete Duchenne muscular dystrophy gene *Genomics.* 12:465-473.

Mounsey, J.P., D.J. Mistry, C.W. Ai, S. Reddy, and J.R. Moorman. 2000. Skeletal muscle sodium channel gating in mice deficient in myotonic dystrophy protein kinase *Hum.Mol.Genet.* 9:2313-2320.

Mounsey, J.P., P. Xu, J.E. John 3rd, L.T. Horne, J. Gilbert, A.D. Roses, and J.R. Moorman. 1995. Modulation of skeletal muscle sodium channels by human myotonin protein kinase *J.Clin.Invest.* 95:2379-2384.

Mulders, S.A., W.J. van den Broek, T.M. Wheeler, H.J. Croes, P. van Kuik-Romeijn, S.J. de Kimpe, D. Furling, G.J. Platenburg, G. Gourdon, C.A. Thornton, B. Wieringa, and D.G. Wansink. 2009. Triplet-repeat oligonucleotide-mediated reversal of RNA toxicity in myotonic dystrophy *Proc.Natl.Acad.Sci.U.S.A.* 106:13915-13920.

Muruve, D.A., M.J. Barnes, I.E. Stillman, and T.A. Libermann. 1999. Adenoviral gene therapy leads to rapid induction of multiple chemokines and acute neutrophil-dependent hepatic injury in vivo *Hum.Gene Ther.* 10:965-976.

Muruve, D.A., M.J. Cotter, A.K. Zaiss, L.R. White, Q. Liu, T. Chan, S.A. Clark, P.J. Ross, R.A. Meulenbroek, G.M. Maelandsmo, and R.J. Parks. 2004. Helper-dependent adenovirus vectors elicit intact innate but attenuated adaptive host immune responses in vivo *J.Virol.* 78:5966-5972.

Myerburg, R.J., K.M. Kessler, I. Kiem, K.C. Pefkaros, C.A. Conde, D. Cooper, and A. Castellanos. 1981. Relationship between plasma levels of procainamide, suppression of premature ventricular complexes and prevention of recurrent ventricular tachycardia *Circulation.* 64:280-290.

Napierala, M., and W.J. Krzyzosiak. 1997. CUG repeats present in myotonin kinase RNA form metastable "slippery" hairpins *J.Biol.Chem.* 272:31079-31085.

Odom, G.L., P. Gregorevic, and J.S. Chamberlain. 2007. Viral-mediated gene therapy for the muscular dystrophies: successes, limitations and recent advances *Biochim.Biophys.Acta.* 1772:243-262.

Ohlendieck, K., J.M. Ervasti, K. Matsumura, S.D. Kahl, C.J. Leveille, and K.P. Campbell. 1991. Dystrophin-related protein is localized to neuromuscular junctions of adult skeletal muscle *Neuron.* 7:499-508.

Okoli, G., N. Carey, K.J. Johnson, and D.J. Watt. 1998. Over expression of the murine myotonic dystrophy protein kinase in the mouse myogenic C2C12 cell line leads to inhibition of terminal differentiation *Biochem.Biophys.Res.Commun.* 246:905-911.

Otten, A.D., and S.J. Tapscott. 1995. Triplet repeat expansion in myotonic dystrophy alters the adjacent chromatin structure *Proc.Natl.Acad.Sci.U.S.A.* 92:5465-5469.

Oude Ophuis, R.J., S.A. Mulders, R.E. van Herpen, R. van de Vorstenbosch, B. Wieringa, and D.G. Wansink. 2009. DMPK protein isoforms are differentially expressed in myogenic and neural cell lineages *Muscle Nerve.* 40:545-555.

Pearce, M., D.J. Blake, J.M. Tinsley, B.C. Byth, L. Campbell, A.P. Monaco, and K.E. Davies. 1993. The utrophin and dystrophin genes share similarities in genomic structure *Hum.Mol.Genet.* 2:1765-1772.

Perkins, K.J., and K.E. Davies. 2002. The role of utrophin in the potential therapy of Duchenne muscular dystrophy *Neuromuscul.Disord.* 12 Suppl 1:S78-89.

Philips, A.V., L.T. Timchenko, and T.A. Cooper. 1998. Disruption of splicing regulated by a CUG-binding protein in myotonic dystrophy *Science.* 280:737-741.

Rafael, J.A., J.M. Tinsley, A.C. Potter, A.E. Deconinck, and K.E. Davies. 1998. Skeletal muscle-specific expression of a utrophin transgene rescues utrophin-dystrophin deficient mice *Nat.Genet.* 19:79-82.

Ragot, T., N. Vincent, P. Chafey, E. Vigne, H. Gilgenkrantz, D. Couton, J. Cartaud, P. Briand, J.C. Kaplan, and M. Perricaudet. 1993. Efficient adenovirus-mediated transfer of a human minidystrophin gene to skeletal muscle of mdx mice *Nature.* 361:647-650.

Ranum, L.P., and T.A. Cooper. 2006. RNA-mediated neuromuscular disorders *Annu.Rev.Neurosci.* 29:259-277.

Ranum, L.P., P.F. Rasmussen, K.A. Benzow, M.D. Koob, and J.W. Day. 1998. Genetic mapping of a second myotonic dystrophy locus *Nat.Genet.* 19:196-198.

Roberts, R.G., A.J. Coffey, M. Bobrow, and D.R. Bentley. 1993. Exon structure of the human dystrophin gene *Genomics.* 16:536-538.

Roberts, R.G., R.J. Gardner, and M. Bobrow. 1994. Searching for the 1 in 2,400,000: a review of dystrophin gene point mutations *Hum.Mutat.* 4:1-11.

Rodova, M., K. Brownback, and M.J. Werle. 2004. Okadaic acid augments utrophin in myogenic cells *Neurosci.Lett.* 363:163-167.

Rybakova, I.N., J.L. Humston, K.J. Sonnemann, and J.M. Ervasti. 2006. Dystrophin and utrophin bind actin through distinct modes of contact *J.Biol.Chem.* 281:9996-10001.

Sampieri, C.L., R.K. Nuttall, D.A. Young, D. Goldspink, I.M. Clark, and D.R. Edwards. 2008. Activation of p38 and JNK MAPK pathways abrogates requirement for new protein synthesis for phorbol ester mediated induction of select MMP and TIMP genes *Matrix Biol.* 27:128-138.

Santa Cruz Biotechnology, I. 2011. Prilocaine hydrochloride: sc-253317 (Material Safety Data Sheet). :1-4.

Savkur, R.S., A.V. Philips, and T.A. Cooper. 2001. Aberrant regulation of insulin receptor alternative splicing is associated with insulin resistance in myotonic dystrophy *Nat.Genet.* 29:40-47.

Schaeffer, P.J., A.R. Wende, C.J. Magee, J.R. Neilson, T.C. Leone, F. Chen, and D.P. Kelly. 2004. Calcineurin and calcium/calmodulin-dependent protein kinase activate distinct metabolic gene regulatory programs in cardiac muscle *J.Biol.Chem.* 279:39593-39603.

Schmalbruch, H. 1984. Regenerated muscle fibers in Duchenne muscular dystrophy: a serial section study *Neurology.* 34:60-65.

Simon, M.A., M.J. Gielen, N. Alberink, T.B. Vree, and J. van Egmond. 1997. Intravenous regional anesthesia with 0.5% articaine, 0.5% lidocaine, or 0.5% prilocaine. A double-blind randomized clinical study *Reg.Anesth.* 22:29-34.

Singh, J., and R.A. Padgett. 2009. Rates of in situ transcription and splicing in large human genes *Nat.Struct.Mol.Biol.* 16:1128-1133.

Sivilotti, L., K. Okuse, A.N. Akopian, S. Moss, and J.N. Wood. 1997. A single serine residue confers tetrodotoxin insensitivity on the rat sensory-neuron-specific sodium channel SNS *FEBS Lett.* 409:49-52.

Smith, K.P., M. Byron, C. Johnson, Y. Xing, and J.B. Lawrence. 2007. Defining early steps in mRNA transport: mutant mRNA in myotonic dystrophy type I is blocked at entry into SC-35 domains *J.Cell Biol.* 178:951-964.

Suominen, T., L.L. Bachinski, S. Auvinen, P. Hackman, K.A. Baggerly, C. Angelini, L. Peltonen, R. Krahe, and B. Udd. 2011. Population frequency of myotonic dystrophy: higher than expected frequency of myotonic dystrophy type 2 (DM2) mutation in Finland *Eur.J.Hum.Genet.*

Tennyson, C.N., H.J. Klamut, and R.G. Worton. 1995. The human dystrophin gene requires 16 hours to be transcribed and is cotranscriptionally spliced *Nat.Genet.* 9:184-190.

Thornton, C.A., J.P. Wymer, Z. Simmons, C. McClain, and R.T. Moxley 3rd. 1997. Expansion of the myotonic dystrophy CTG repeat reduces expression of the flanking DMAHP gene *Nat.Genet.* 16:407-409.

Tian, Q., S.B. Stepaniants, M. Mao, L. Weng, M.C. Feetham, M.J. Doyle, E.C. Yi, H. Dai, V. Thorsson, J. Eng, D. Goodlett, J.P. Berger, B. Gunter, P.S. Linseley, R.B. Stoughton, R. Aebersold, S.J. Collins, W.A. Hanlon, and L.E. Hood. 2004. Integrated genomic and proteomic analyses of gene expression in Mammalian cells *Mol.Cell.Proteomics.* 3:960-969.

Timchenko, L.T., N.A. Timchenko, C.T. Caskey, and R. Roberts. 1996. Novel proteins with binding specificity for DNA CTG repeats and RNA CUG repeats: implications for myotonic dystrophy *Hum.Mol.Genet.* 5:115-121.

Tinsley, J.M., D.J. Blake, A. Roche, U. Fairbrother, J. Riss, B.C. Byth, A.E. Knight, J. Kendrick-Jones, G.K. Suthers, and D.R. Love. 1992. Primary structure of dystrophin-related protein *Nature.* 360:591-593.

Turner, P.R., T. Westwood, C.M. Regen, and R.A. Steinhardt. 1988. Increased protein degradation results from elevated free calcium levels found in muscle from mdx mice *Nature.* 335:735-738.

Tutdibi, O., H. Brinkmeier, R. Rudel, and K.J. Fohr. 1999. Increased calcium entry into dystrophin-deficient muscle fibres of MDX and ADR-MDX mice is reduced by ion channel blockers *J.Physiol.* 515 (Pt 3):859-868.

U.S Institute of Health. Clinical Trials Database {http://clinicaltrials.gov/}. 2011.

van Herpen, R.E., R.J. Oude Ophuis, M. Wijers, M.B. Bennink, F.A. van de Loo, J. Fransen, B. Wieringa, and D.G. Wansink. 2005. Divergent mitochondrial and endoplasmic reticulum association of DMPK splice isoforms depends on unique sequence arrangements in tail anchors *Mol.Cell.Biol.* 25:1402-1414.

Vignaud, A., A. Ferry, A. Huguet, M. Baraibar, C. Trollet, J. Hyzewicz, G. Butler-Browne, J. Puymirat, G. Gourdon, and D. Furling. 2010. Progressive skeletal muscle weakness in transgenic mice expressing CTG expansions is associated with the activation of the ubiquitin-proteasome pathway *Neuromuscul.Disord.* 20:319-325.

Wang, D., M. Mistry, K. Kahlig, J. Kearney, J. Xiang, and A. George Jr. 2010. Propranolol blocks cardiac and neuronal voltage-gated sodium channels. *Frontiers in Pharmacology.* 1:1-12.

Wang, G.K., C. Russell, and S.Y. Wang. 2004. Mexiletine block of wild-type and inactivation-deficient human skeletal muscle hNav1.4 Na+ channels *J.Physiol.* 554:621-633.

Wang, G.S., D.L. Kearney, M. De Biasi, G. Taffet, and T.A. Cooper. 2007. Elevation of RNA-binding protein CUGBP1 is an early event in an inducible heart-specific mouse model of myotonic dystrophy *J.Clin.Invest.* 117:2802-2811.

Wang, G.S., M.N. Kuyumcu-Martinez, S. Sarma, N. Mathur, X.H. Wehrens, and T.A. Cooper. 2009. PKC inhibition ameliorates the cardiac phenotype in a mouse model of myotonic dystrophy type 1 *J.Clin.Invest.* 119:3797-3806.

Wansink, D.G., R.E. van Herpen, M.M. Coerwinkel-Driessen, P.J. Groenen, B.A. Hemmings, and B. Wieringa. 2003. Alternative splicing controls myotonic dystrophy protein kinase structure, enzymatic activity, and subcellular localization *Mol.Cell.Biol.* 23:5489-5501.

Warf, M.B., M. Nakamori, C.M. Matthys, C.A. Thornton, and J.A. Berglund. 2009. Pentamidine reverses the splicing defects associated with myotonic dystrophy *Proc.Natl.Acad.Sci.U.S.A.* 106:18551-18556.

Weir, A.P., E.A. Burton, G. Harrod, and K.E. Davies. 2002. A- and B-utrophin have different expression patterns and are differentially up-regulated in mdx muscle *J.Biol.Chem.* 277:45285-45290.

Wheeler, T.M., K. Sobczak, J.D. Lueck, R.J. Osborne, X. Lin, R.T. Dirksen, and C.A. Thornton. 2009. Reversal of RNA dominance by displacement of protein sequestered on triplet repeat RNA *Science.* 325:336-339.

Wheeler, T.M., and C.A. Thornton. 2007. Myotonic dystrophy: RNA-mediated muscle disease *Curr.Opin.Neurol.* 20:572-576.

Whiting, E.J., J.D. Waring, K. Tamai, M.J. Somerville, M. Hincke, W.A. Staines, J.E. Ikeda, and R.G. Korneluk. 1995. Characterization of myotonic dystrophy kinase (DMK) protein in human and rodent muscle and central nervous tissue *Hum.Mol.Genet.* 4:1063-1072.

Woosley, R.L., T. Wang, W. Stone, L. Siddoway, K. Thompson, H.J. Duff, I. Cerskus, and D. Roden. 1984. Pharmacology, electrophysiology, and pharmacokinetics of mexiletine *Am.Heart J.* 107:1058-1065.

Yoshida, M., H. Hama, M. Ishikawa-Sakurai, M. Imamura, Y. Mizuno, K. Araishi, E. Wakabayashi-Takai, S. Noguchi, T. Sasaoka, and E. Ozawa. 2000. Biochemical evidence for association of dystrobrevin with the sarcoglycan-sarcospan complex as a basis for understanding sarcoglycanopathy *Hum.Mol.Genet.* 9:1033-1040.

Zebedin, E., M. Mille, M. Speiser, T. Zarrabi, W. Sandtner, B. Latzenhofer, H. Todt, and K. Hilber. 2007. C2C12 skeletal muscle cells adopt cardiac-like sodium current properties in a cardiac cell environment *Am.J.Physiol.Heart Circ.Physiol.* 292:H439-50.

Chapter 6

Supplemental Figures:

The following figures represent the data contained in tables 1 and 2, which was generated based on C2C12 RNA levels analyzed by qPCR treated at the indicated time intervals and concentrations.

6. Supplemental Figures

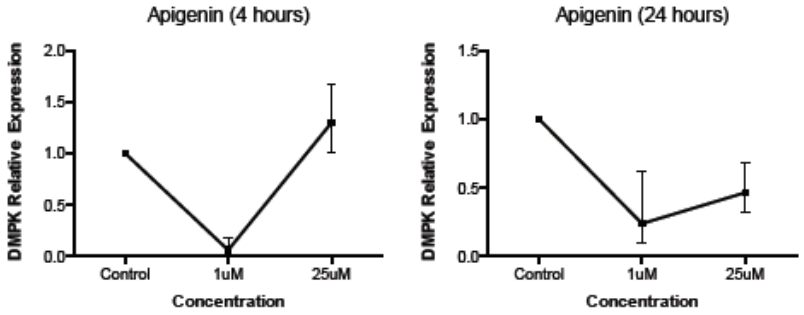

Supplemental Figure 1 - Apigenin Initial Screen Data.

Relative DMPK RNA levels of C2C12 myoblasts after 4 and 24 hour treatments. Quantification of DMPK mRNA relative to β-2-Microglobulin in C2C12 cells (the ratio of control group set as 1). Mean ± SD (bars) of 3 separate experiments (Treated n= 3).

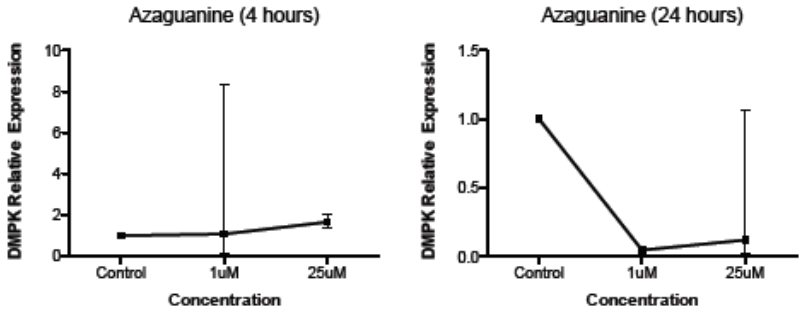

Supplemental Figure 2 - Azaguanine Initial Screen Data.

Relative DMPK RNA levels of C2C12 myoblasts after 4 and 24 hour treatments. Quantification of DMPK mRNA relative to β-2-Microglobulin in C2C12 cells (the ratio of control group set as 1). Mean ± SD (bars) of 3 separate experiments (Treated n= 3).

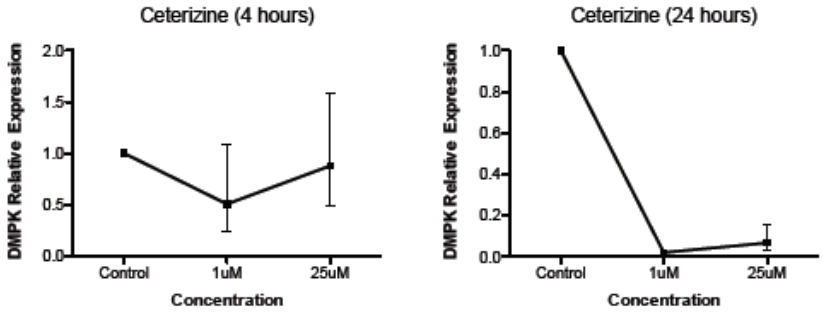

Supplemental Figure 3 - Ceterizine Initial Screen Data.

Relative DMPK RNA levels of C2C12 myoblasts after 4 and 24 hour treatments. Quantification of DMPK mRNA relative to β-2-Microglobulin in C2C12 cells (the ratio of control group set as 1). Mean ± SD (bars) of 3 separate experiments (Treated n= 3).

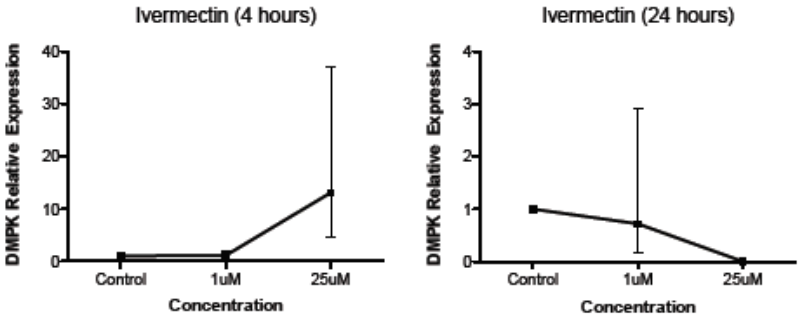

Supplemental Figure 4 - Ivermectin Initial Screen Data.

Relative DMPK RNA levels of C2C12 myoblasts after 4 and 24 hour treatments. Quantification of DMPK mRNA relative to β-2-Microglobulin in C2C12 cells (the ratio of control group set as 1). Mean ± SD (bars) of 3 separate experiments (Treated n= 3).

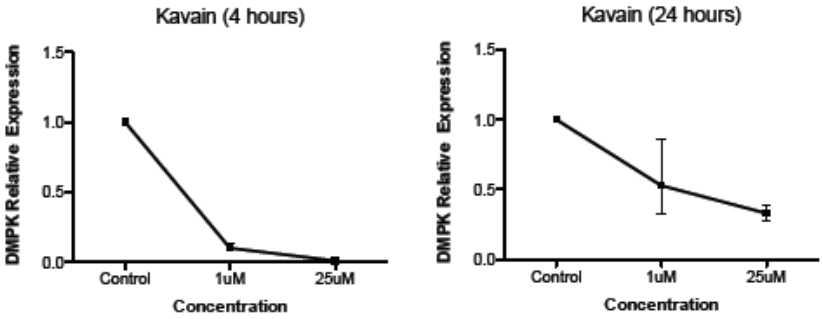

Supplemental Figure 5 - Kavain Initial Screen Data.

Relative DMPK RNA levels of C2C12 myoblasts after 4 and 24 hour treatments. Quantification of DMPK mRNA relative to β-2-Microglobulin in C2C12 cells (the ratio of control group set as 1). Mean ± SD (bars) of 3 separate experiments (Treated n= 3).

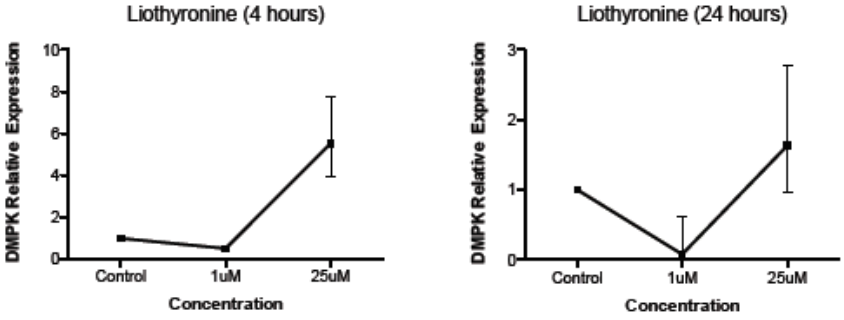

Supplemental Figure 6 - Liothyronine Initial Screen Data.

DMPK RNA levels of C2C12 myoblasts after 4 and 24 hour treatments. Quantification of DMPK mRNA relative to β-2-Microglobulin in C2C12 cells (the ratio of control group set as 1). Mean ± SD (bars) of 3 separate experiments (Treated n= 3).

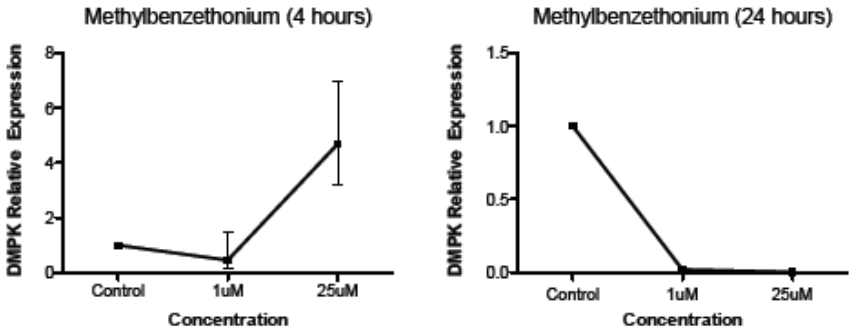

Supplemental Figure 7 - Methylbenzethonium Initial Screen Data.

Relative DMPK RNA levels of C2C12 myoblasts after 4 and 24 hour treatments. Quantification of DMPK mRNA relative to β-2-Microglobulin in C2C12 cells (the ratio of control group set as 1). Mean ± SD (bars) of 3 separate experiments (Treated n= 3).

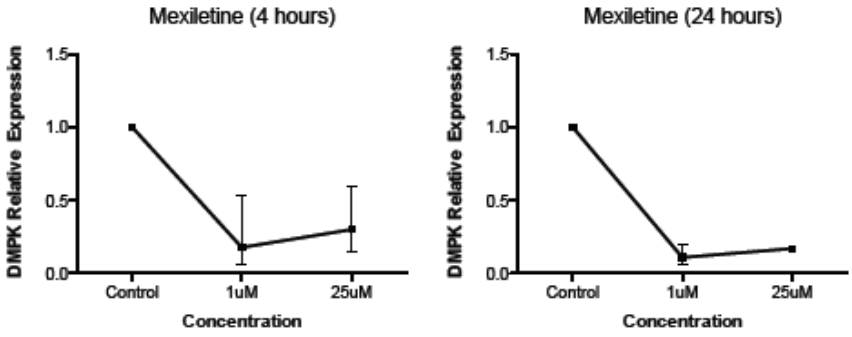

Supplemental Figure 8 - Mexiletine Initial Screen Data.

Relative DMPK RNA levels of C2C12 myoblasts after 4 and 24 hour treatments. Quantification of DMPK mRNA relative to β-2-Microglobulin in C2C12 cells (the ratio of control group set as 1). Mean ± SD (bars) of 3 separate experiments (Treated n= 3).

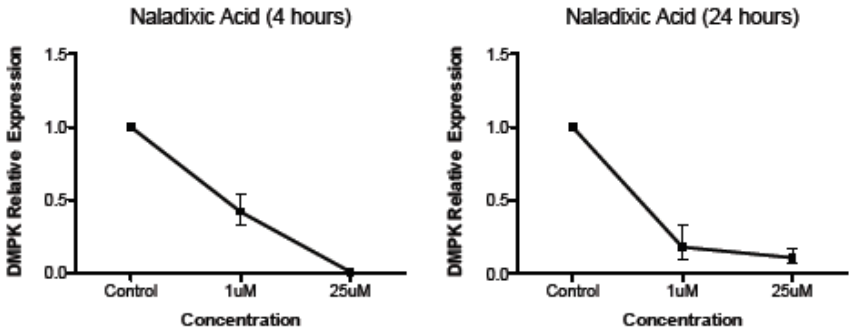

Supplemental Figure 9 - Naladixic Acid Initial Screen Data.

Relative DMPK RNA levels of C2C12 myoblasts after 4 and 24 hour treatments. Quantification of DMPK mRNA relative to β-2-Microglobulin in C2C12 cells (the ratio of control group set as 1). Mean ± SD (bars) of 3 separate experiments (Treated n= 3).

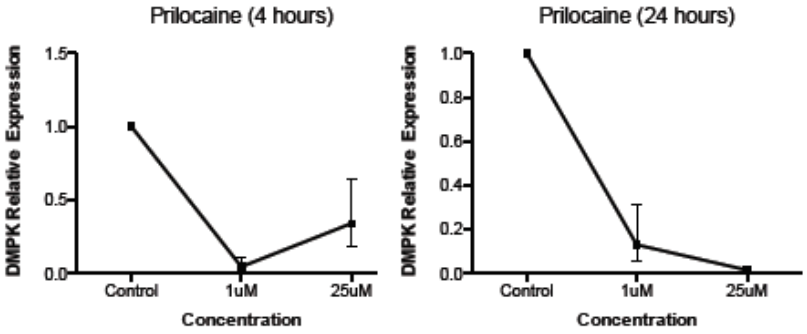

Supplemental Figure 10 - Prilocaine Initial Screen Data.

Relative DMPK RNA levels of C2C12 myoblasts after 4 and 24 hour treatments. Quantification of DMPK mRNA relative to β-2-Microglobulin in C2C12 cells (the ratio of control group set as 1). Mean ± SD (bars) of 3 separate experiments (Treated n= 3).

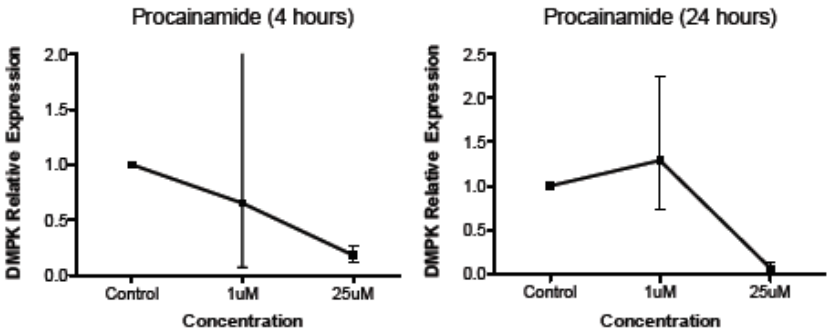

Supplemental Figure 11. Procainamide Initial Screen Data.

Relative DMPK RNA levels of C2C12 myoblasts after 4 and 24 hour treatments. Quantification of DMPK mRNA relative to β-2-Microglobulin in C2C12 cells (the ratio of control group set as 1). Mean ± SD (bars) of 3 separate experiments (Treated n= 3).

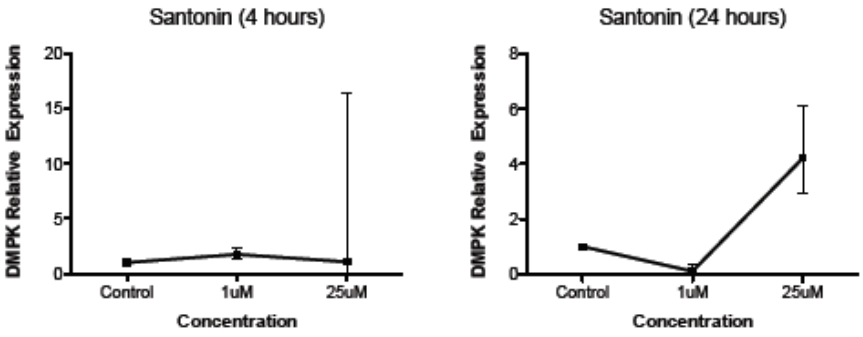

Supplemental Figure 12 - Santonin Initial Screen Data.

Relative DMPK RNA levels of C2C12 myoblasts after 4 and 24 hour treatments. Quantification of DMPK mRNA relative to β-2-Microglobulin in C2C12 cells (the ratio of control group set as 1). Mean ± SD (bars) of 3 separate experiments (Treated n= 3).

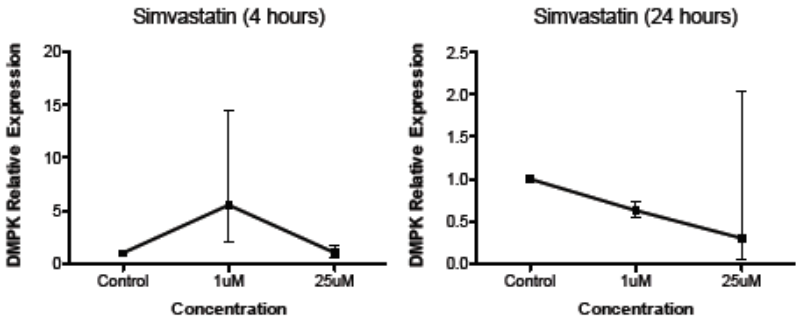

Supplemental Figure 13 - Simvastatin Initial Screen Data.

Relative DMPK RNA levels of C2C12 myoblasts after 4 and 24 hour treatments. Quantification of DMPK mRNA relative to β-2-Microglobulin in C2C12 cells (the ratio of control group set as 1). Mean ± SD (bars) of 3 separate experiments (Treated n= 3).

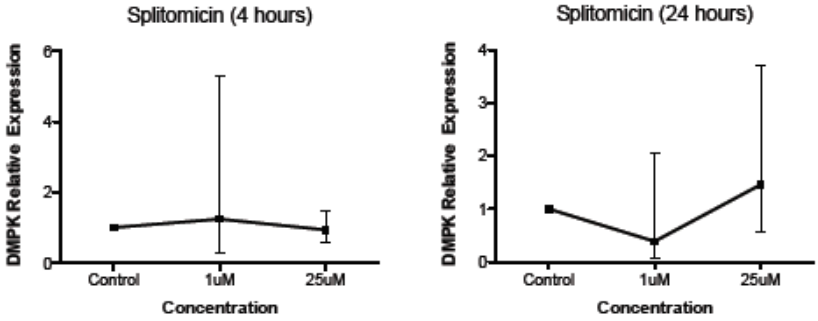

Supplemental Figure 14 - Splitomicin Initial Screen Data.

Relative DMPK RNA levels of C2C12 myoblasts after 4 and 24 hour treatments. Quantification of DMPK mRNA relative to β-2-Microglobulin in C2C12 cells (the ratio of control group set as 1). Mean ± SD (bars) of 3 separate experiments (Treated n= 3).

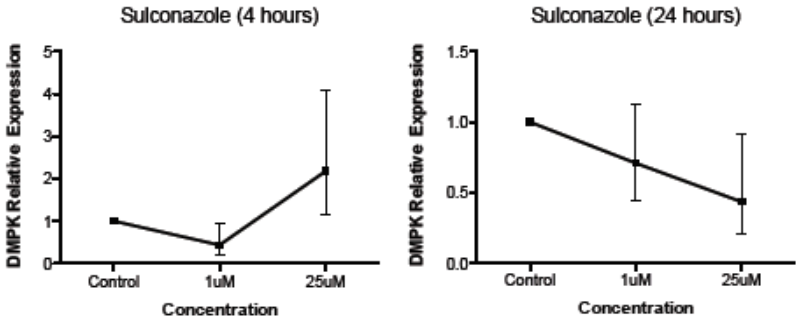

Supplemental Figure 15 - Sulconazole Initial Screen Data.

Relative DMPK RNA levels of C2C12 myoblasts after 4 and 24 hour treatments. Quantification of DMPK mRNA relative to β-2-Microglobulin in C2C12 cells (the ratio of control group set as 1). Mean ± SD (bars) of 3 separate experiments (Treated n= 3).

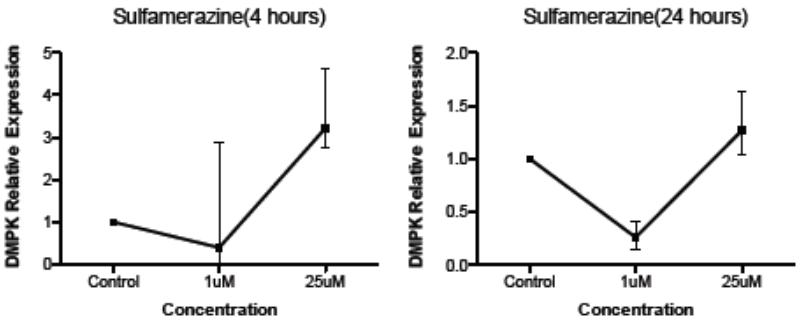

Supplemental Figure 16 - Sulfamerazine Initial Screen Data.

Relative DMPK RNA levels of C2C12 myoblasts after 4 and 24 hour treatments. Quantification of DMPK mRNA relative to β-2-Microglobulin in C2C12 cells (the ratio of control group set as 1). Mean ± SD (bars) of 3 separate experiments (Treated n= 3).

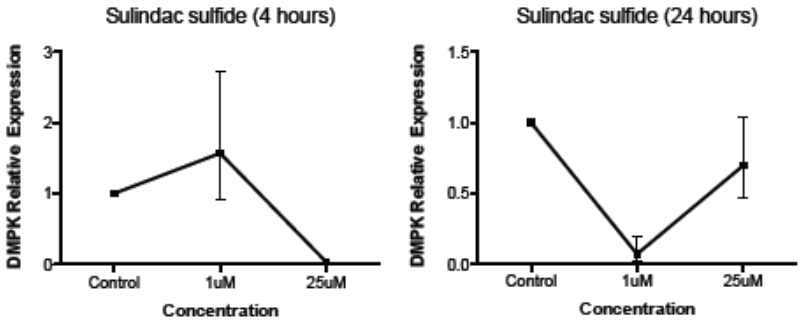

Supplemental Figure 17. Sulindac sulfide Initial Screen Data.

Relative DMPK RNA levels of C2C12 myoblasts after 4 and 24 hour treatments. Quantification of DMPK mRNA relative to β-2-Microglobulin in C2C12 cells (the ratio of control group set as 1). Mean ± SD (bars) of 3 separate experiments (Treated n= 3).

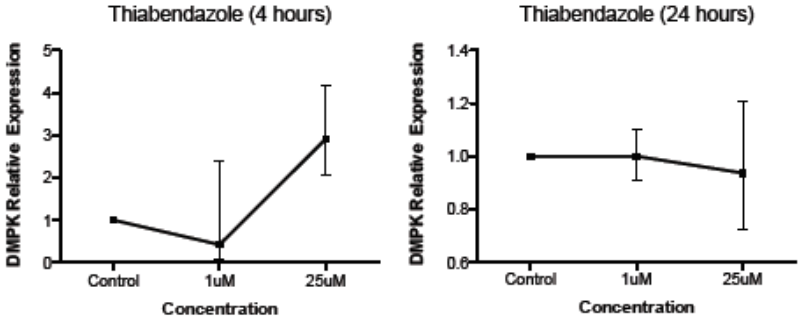

Supplemental Figure 18 - Thiabendazole Initial Screen Data.

Relative DMPK RNA levels of C2C12 myoblasts after 4 and 24 hour treatments. Quantification of DMPK mRNA relative to β-2-Microglobulin in C2C12 cells (the ratio of control group set as 1). Mean ± SD (bars) of 3 separate experiments (Treated n= 3).

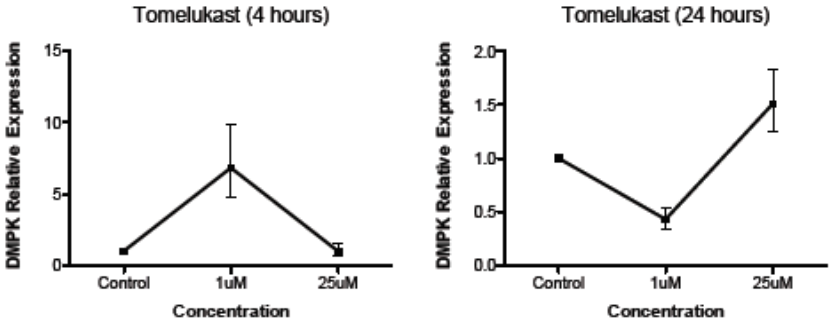

Supplemental Figure 19 - Tomelukast Initial Screen Data.

Relative DMPK RNA levels of C2C12 myoblasts after 4 and 24 hour treatments. Quantification of DMPK mRNA relative to β-2-Microglobulin in C2C12 cells (the ratio of control group set as 1). Mean ± SD (bars) of 3 separate experiments (Treated n= 3).

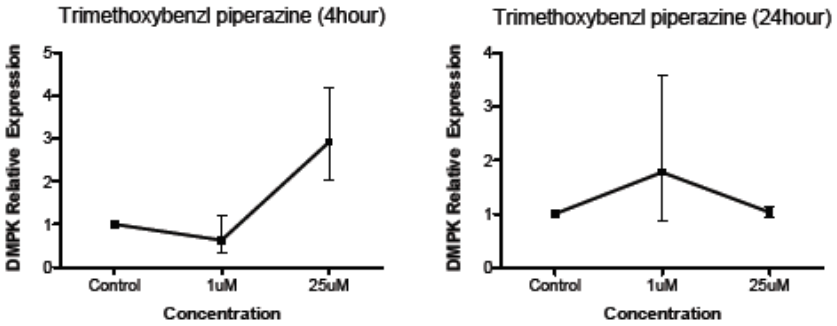

Supplemental Figure 20 - Trimethoxybenzl piperazine Initial Screen Data.

Relative DMPK RNA levels of C2C12 myoblasts after 4 and 24 hour treatments. Quantification of DMPK mRNA relative to β-2-Microglobulin in C2C12 cells (the ratio of control group set as 1). Mean ± SD (bars) of 3 separate experiments (Treated n= 3).

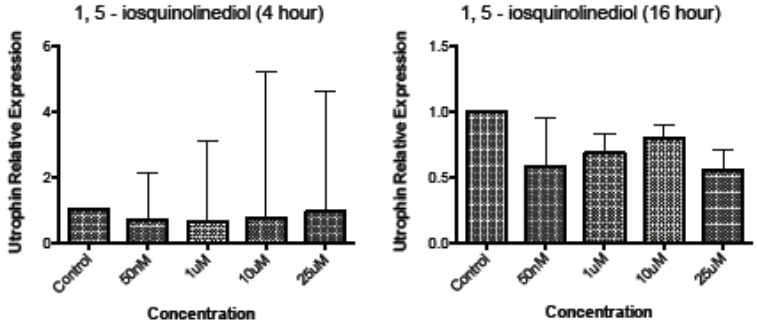

Supplemental Figure 21 - 1, 5 iosquinolinediol Initial Screen Data.

Relative Utrophin RNA levels of C2C12 myoblasts after 4 and 16 hour treatments. Quantification of DMPK mRNA relative to β-2-Microglobulin in C2C12 cells (the ratio of control group set as 1). Mean ± SD (bars) of 3 separate experiments (Treated n= 3).

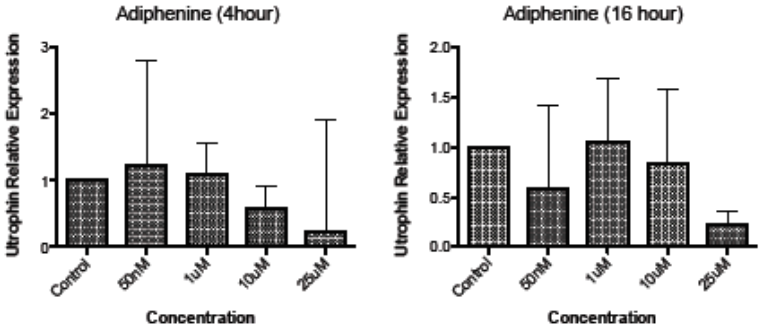

Supplemental Figure 22 – Adiphenine Initial Screen Data

Relative Utrophin RNA levels of C2C12 myoblasts after 4 and 16 hour treatments. Quantification of DMPK mRNA relative to β-2-Microglobulin in C2C12 cells (the ratio of control group set as 1). Mean ± SD (bars) of 3 separate experiments (Treated n= 3).

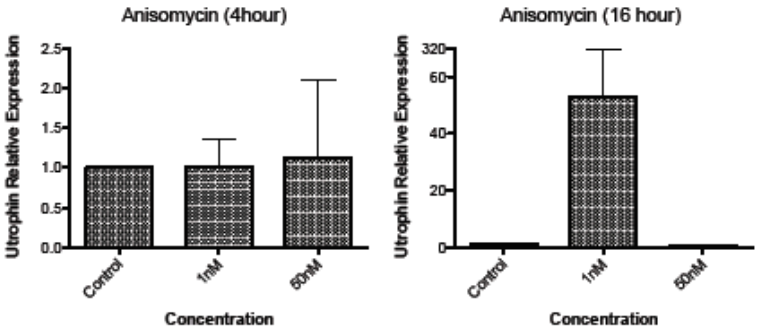

Supplemental Figure 23 – Anisomycin Initial Screen Data.

Relative Utrophin RNA levels of C2C12 myoblasts after 4 and 16 hour treatments. Quantification of DMPK mRNA relative to β-2-Microglobulin in C2C12 cells (the ratio of control group set as 1). Mean ± SD (bars) of 3 separate experiments (Treated n= 3).

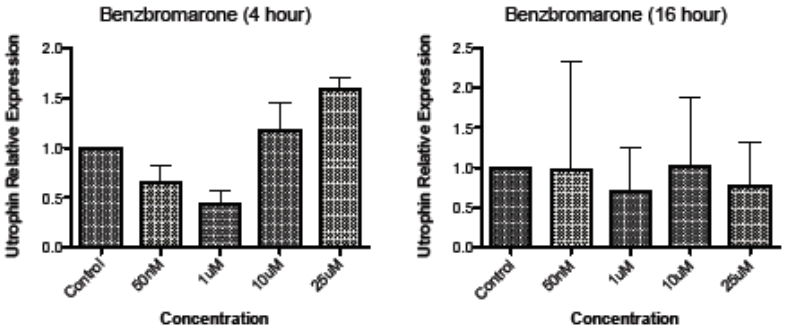

Supplemental Figure 24 – Benzbromarone Initial Screen Data.

Relative Utrophin RNA levels of C2C12 myoblasts after 4 and 16 hour treatments. Quantification of DMPK mRNA relative to β-2-Microglobulin in C2C12 cells (the ratio of control group set as 1). Mean ± SD (bars) of 3 separate experiments (Treated n= 3).

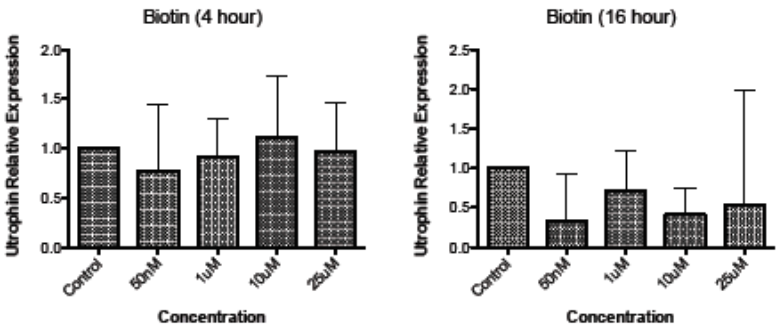

Supplemental Figure 25 – Biotin Initial Screen Data.

Relative Utrophin RNA levels of C2C12 myoblasts after 4 and 16 hour treatments. Quantification of DMPK mRNA relative to β-2-Microglobulin in C2C12 cells (the ratio of control group set as 1). Mean ± SD (bars) of 3 separate experiments (Treated n= 3).

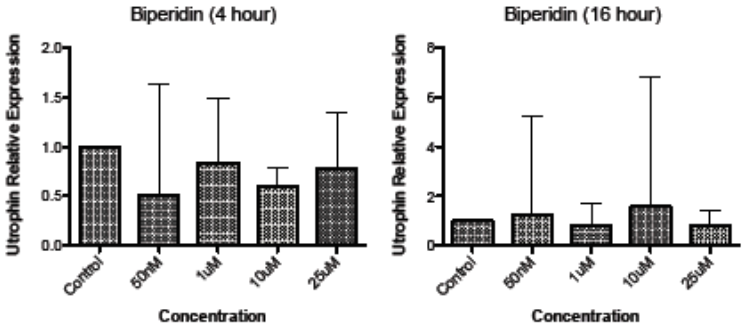

Supplemental Figure 26 – Biperidin Initial Screen Data.

Relative Utrophin RNA levels of C2C12 myoblasts after 4 and 16 hour treatments. Quantification of DMPK mRNA relative to β-2-Microglobulin in C2C12 cells (the ratio of control group set as 1). Mean ± SD (bars) of 3 separate experiments (Treated n= 3).

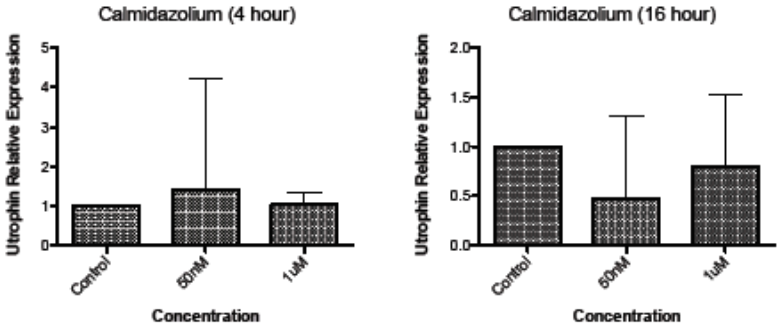

Supplemental Figure 27 – Calmidazolium Initial Screen Data.

Relative Utrophin RNA levels of C2C12 myoblasts after 4 and 16 hour treatments. Quantification of DMPK mRNA relative to β-2-Microglobulin in C2C12 cells (the ratio of control group set as 1). Mean ± SD (bars) of 3 separate experiments (Treated n= 3).

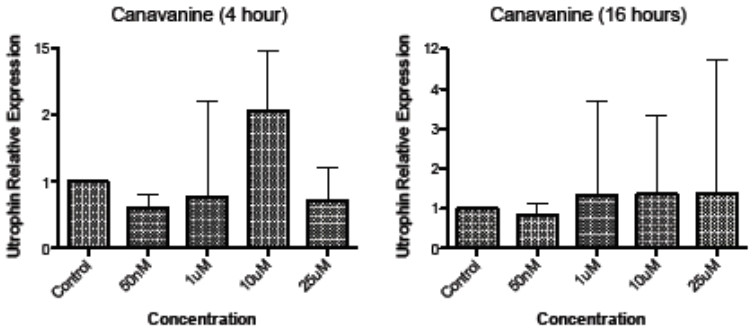

Supplemental Figure 28 – Canavanine Initial Screen Data.

Relative Utrophin RNA levels of C2C12 myoblasts after 4 and 16 hour treatments. Quantification of DMPK mRNA relative to β-2-Microglobulin in C2C12 cells (the ratio of control group set as 1). Mean ± SD (bars) of 3 separate experiments (Treated n= 3).

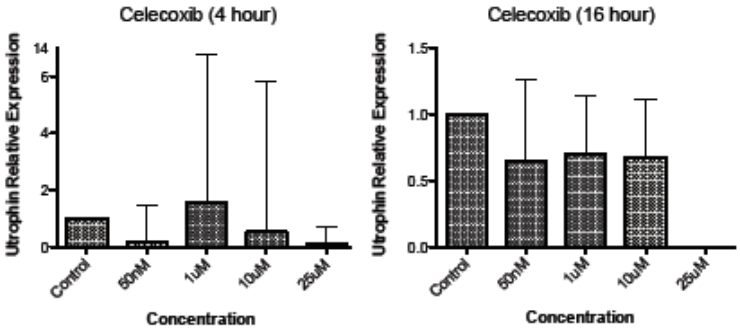

Supplemental Figure 29 – Celexocib Initial Screen Data.

Relative Utrophin RNA levels of C2C12 myoblasts after 4 and 16 hour treatments. Quantification of DMPK mRNA relative to β-2-Microglobulin in C2C12 cells (the ratio of control group set as 1). Mean ± SD (bars) of 3 separate experiments (Treated n= 3).

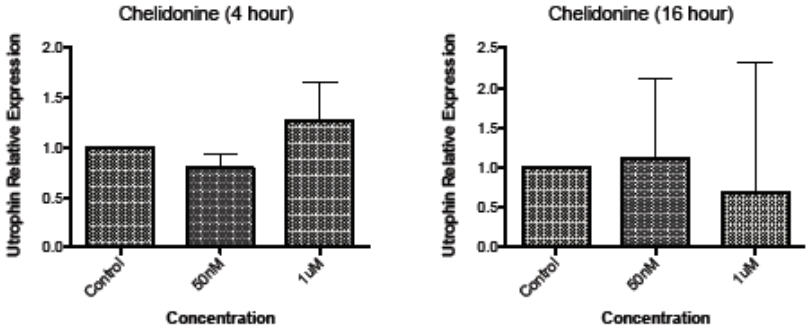

Supplemental Figure 30 – Chelidonine Initial Screen Data.

Relative Utrophin RNA levels of C2C12 myoblasts after 4 and 16 hour treatments. Quantification of DMPK mRNA relative to β-2-Microglobulin in C2C12 cells (the ratio of control group set as 1). Mean ± SD (bars) of 3 separate experiments (Treated n= 3).

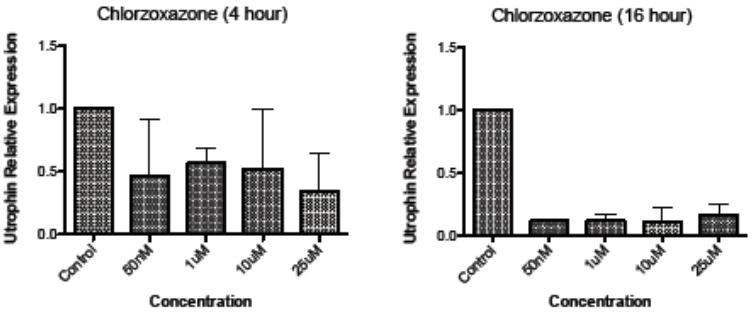

Supplemental Figure 31 – Chlorzoxazone Initital Screen Data.

Relative Utrophin RNA levels of C2C12 myoblasts after 4 and 16 hour treatments. Quantification of DMPK mRNA relative to β-2-Microglobulin in C2C12 cells (the ratio of control group set as 1). Mean ± SD (bars) of 3 separate experiments (Treated n= 3).

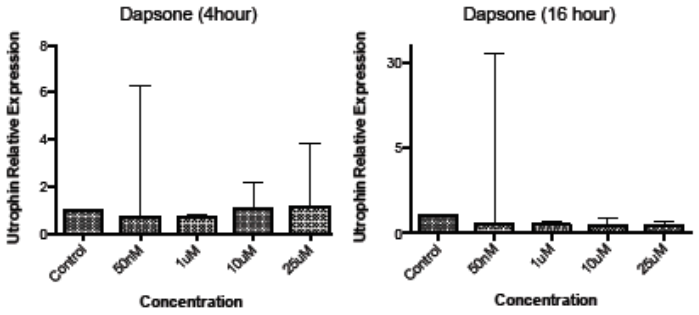

Supplemental Figure 32 – Dapsone Initial Screen Data.

Relative Utrophin RNA levels of C2C12 myoblasts after 4 and 16 hour treatments. Quantification of DMPK mRNA relative to β-2-Microglobulin in C2C12 cells (the ratio of control group set as 1). Mean ± SD (bars) of 3 separate experiments (Treated n= 3).

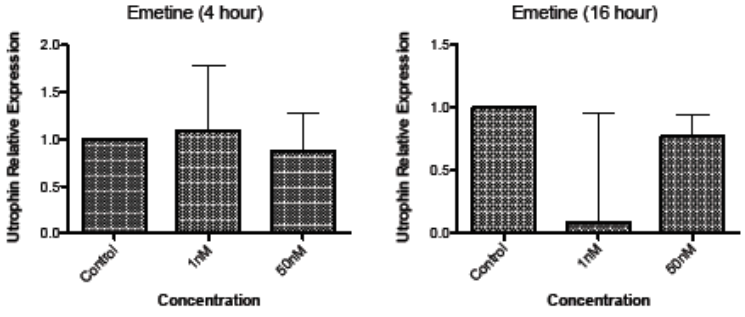

Supplemental Figure 33 – Emetine Initial Screen Data.

Relative Utrophin RNA levels of C2C12 myoblasts after 4 and 16 hour treatments. Quantification of DMPK mRNA relative to β-2-Microglobulin in C2C12 cells (the ratio of control group set as 1). Mean ± SD (bars) of 3 separate experiments (Treated n= 3).

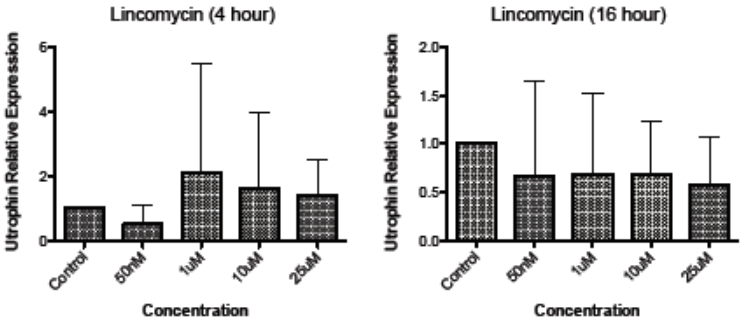

Supplemental Figure 34 – Lincomycin Initial Screen Data.

Relative Utrophin RNA levels of C2C12 myoblasts after 4 and 16 hour treatments. Quantification of DMPK mRNA relative to β-2-Microglobulin in C2C12 cells (the ratio of control group set as 1). Mean ± SD (bars) of 3 separate experiments (Treated n= 3).

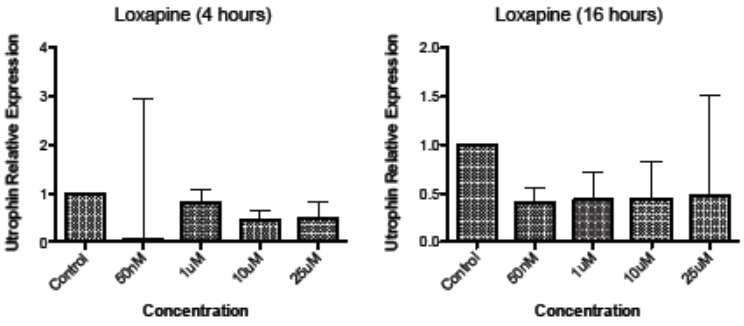

Supplemental Figure 35 – Loxapine Initial Screen Data.

Relative Utrophin RNA levels of C2C12 myoblasts after 4 and 16 hour treatments. Quantification of DMPK mRNA relative to β-2-Microglobulin in C2C12 cells (the ratio of control group set as 1). Mean ± SD (bars) of 3 separate experiments (Treated n= 3).

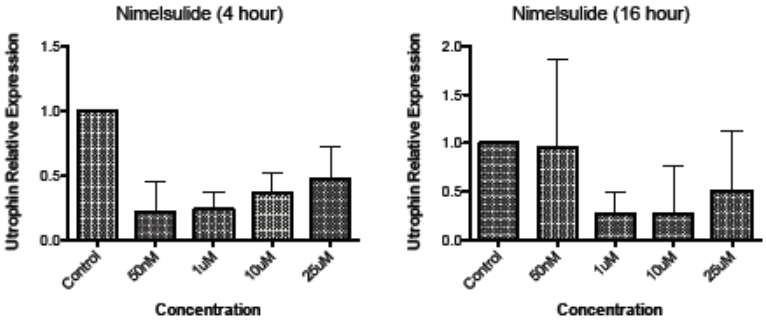

Supplemental Figure 36 – Nimelsulide Initial Screen Data.

Relative Utrophin RNA levels of C2C12 myoblasts after 4 and 16 hour treatments. Quantification of DMPK mRNA relative to β-2-Microglobulin in C2C12 cells (the ratio of control group set as 1). Mean ± SD (bars) of 3 separate experiments (Treated n= 3).

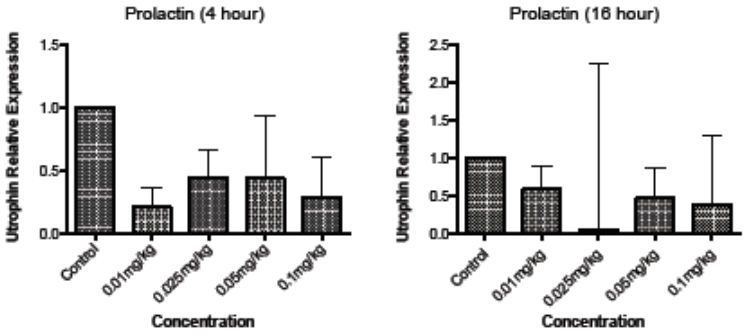

Supplemental Figure 37 – Prolactin Initial Screen Data.

Relative Utrophin RNA levels of C2C12 myoblasts after 4 and 16 hour treatments. Quantification of DMPK mRNA relative to β-2-Microglobulin in C2C12 cells (the ratio of control group set as 1). Mean ± SD (bars) of 3 separate experiments (Treated n= 3).

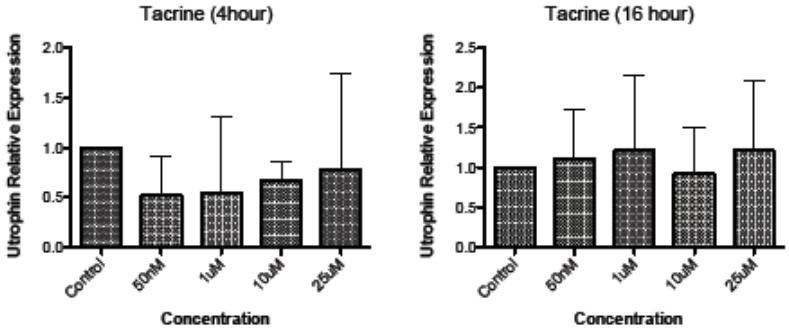

Supplemental Figure 38 – Tacrine Initial Screen Data.

Relative Utrophin RNA levels of C2C12 myoblasts after 4 and 16 hour treatments. Quantification of DMPK mRNA relative to β-2-Microglobulin in C2C12 cells (the ratio of control group set as 1). Mean ± SD (bars) of 3 separate experiments (Treated n= 3).

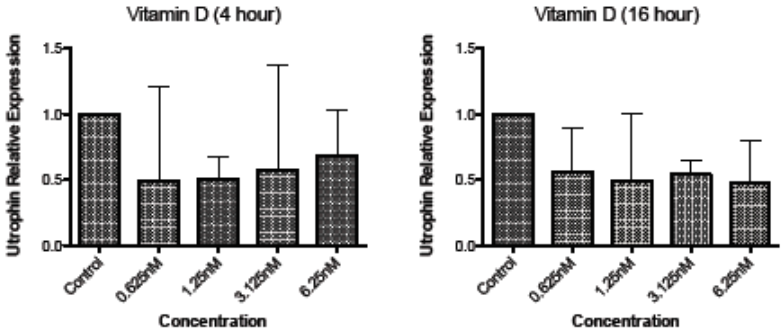

Supplemental Figure 39 – Vitamin D Initial Screen Data.

Relative Utrophin RNA levels of C2C12 myoblasts after 4 and 16 hour treatments. Quantification of DMPK mRNA relative to β-2-Microglobulin in C2C12 cells (the ratio of control group set as 1). Mean ± SD (bars) of 3 separate experiments (Treated n= 3).

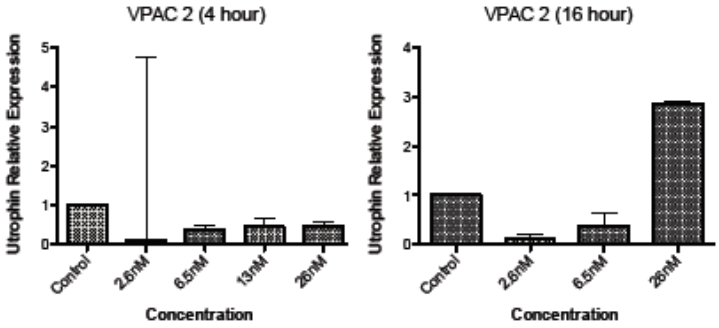

Supplemental Figure 40 – VPAC 2 Initial Screen Data.

Relative Utrophin RNA levels of C2C12 myoblasts after 4 and 16 hour treatments. Quantification of DMPK mRNA relative to β-2-Microglobulin in C2C12 cells (the ratio of control group set as 1). Mean ± SD (bars) of 3 separate experiments (Treated n= 3).